

# 20<sup>ο</sup>

## Πανελλήνιο Φαρμακευτικό Συνέδριο



Η Πολυδιάστατη Επιστήμη της Φαρμακευτικής  
Εθνικό Ίδρυμα Ερευνών - Αθήνα

# 16 - 17 Δεκεμβρίου 2023

## ΒΙΒΛΙΟ ΠΕΡΙΛΗΨΕΩΝ

**Πρόεδρος Συνεδρίου:**

**Σκαλτσά Ελένη, Καθηγήτρια Φαρμακευτικής ΕΚΠΑ**

**Διοργάνωση**



**Με την Υποστήριξη**

**PHARMACY<sup>®</sup>**  
**management**  
www.PharmaManage.gr **ΚΑΙ ΕΠΙΚΟΙΝΩΝΙΑ**



**ΧΑΡΑΜΗ ΑΕ**  
Ενδυναμώνουμε την  
Επικοινωνία Υγείας

**Με την Αιγίδα των:**

ΕΛΛΗΝΙΚΗ ΕΝΩΣΗ MARKET ACCESS • ΕΛΛΗΝΙΚΗ ΕΠΙΣΤΗΜΟΝΙΚΗ ΕΤΑΙΡΕΙΑ ΟΙΚΟΝΟΜΙΑΣ ΚΑΙ ΠΟΛΙΤΙΚΗΣ ΤΗΣ ΥΓΕΙΑΣ  
ΙΝΣΤΙΤΟΥΤΟ ΟΙΚΟΝΟΜΙΚΩΝ ΥΓΕΙΑΣ (i-hecon) • ΠΑΝΕΛΛΗΝΙΑ ΕΝΩΣΗ ΦΑΡΜΑΚΟΒΙΟΜΗΧΑΝΙΑΣ  
ΣΥΛΛΟΓΟΣ ΕΠΙΧΕΙΡΗΜΑΤΙΩΝ ΣΥΜΠΛΗΡΩΜΑΤΩΝ ΔΙΑΤΡΟΦΗΣ • ΣΥΝΔΕΣΜΟΣ ΕΠΙΧΕΙΡΗΣΕΩΝ ΙΑΤΡΙΚΩΝ ΚΑΙ ΒΙΟΤΕΧΝΟΛΟΓΙΚΩΝ ΠΡΟΪΟΝΤΩΝ

## Chemical composition of *Stachys parolinii* extract and its formulation for cutaneous use

Maria Anagnostou<sup>1\*</sup>, Ekaterina-Michaela Tomou<sup>1</sup>, Giulia Vanti<sup>2</sup>, Emmanouela Mylonaki<sup>1,2</sup>, Nikos Krigas<sup>3</sup>, Anastasia Karioti<sup>4</sup>, Anna-Rita Bilia<sup>2</sup>, Helen Skaltsa<sup>1</sup>

<sup>2</sup>Department of Chemistry "Ugo Schiff" (DICUS), University of Florence, Via Ugo Schiff 6, 50019 Sesto Fiorentino, Florence, Italy

<sup>3</sup>Balkan Botanic Garden of Kroussia-Laboratory for the Conservation and Evaluation of Native and Floricultural Species, Institute of Plant Breeding and Genetic Resources, Hellenic Agricultural Organization (HAO)-DEMETER, 57001, Themi, Thessaloniki, Greece

<sup>4</sup>Laboratory of Pharmacognosy, School of Pharmacy, Aristotle University of Thessaloniki, University Campus, 54124, Thessaloniki, Greece

\*Corresponding Author: Maria Anagnostou, E-mail: maanagno@pharm.uoa.gr

### Introduction:

The genus *Stachys* L. contains 365 species and is one of the largest genera of the Lamiaceae family [1]. In Greece, approximately 56 species and subspecies of *Stachys* are found on parts of the mainland and/or insular Greece [2]. In continuation to our research in the genus *Stachys*, we studied *Stachys parolinii* Vis., native in North Peloponnese, Central Greece, and Ionian Islands (Kefalonia and Lefkada). Several *Stachys* plants have been mentioned in various have been mentioned in various traditional medicines to treat diseases such as inflammations, skin and stomach disorder [3,4]. This study focused on the phytochemical analysis of the *S. parolinii* methanol extract and the formulation of an oil-in-water microemulsion for cutaneous use to improve the low aqueous solubility of the extract for achieving optimal cutaneous administration and bioavailability.

### Methodology:

The dried aerial parts of *S. parolinii* (Fig. 1) were extracted with solvents of increasing polarity: dichloromethane and methanol by maceration at room temperature. The chemical fingerprint of the methanol extract was obtained through HPLC-PDA-MS (Fig. 2) and NMR analysis (Fig. 3). The dried methanol extract was subjected to Vacuum Liquid Chromatography over silica gel to yield 9 fractions. The fractions were further fractionated by column chromatography and preparative TLC. The isolated compounds were identified by one-dimensional and two-dimensional NMR spectra. The microemulsion was prepared using Solutol HS 15 (surfactant), Transcutol P (co-surfactant), and Capryol 90 (oil), selected for the high solubility of the extract. According to previous studies, we fixed the surfactant/co-solvent ratio at 1:1, 2:1, and 3:1,

and we constructed the corresponding pseudo-ternary phase diagrams by the titration method to investigate the microemulsion existence regions. The extract solubility in the final microemulsion was evaluated for those with the lowest polydispersity index (around 0.15) by the flask shake method for three hours.



Figure 1: *Stachys parolinii* Vis.

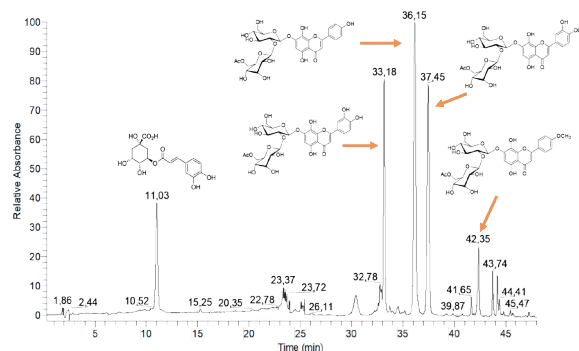


Figure 2: HPLC-PDA-MS chromatogram of the methanol extract.

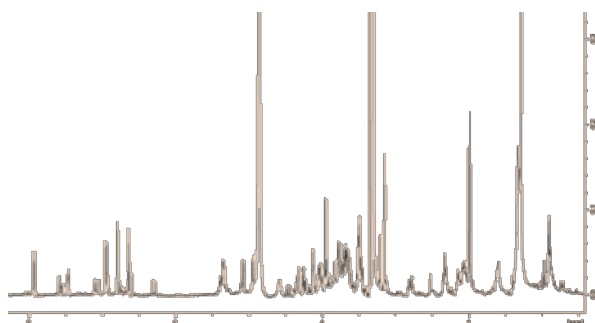


Figure 3: <sup>1</sup>H-NMR spectrum of the methanol extract

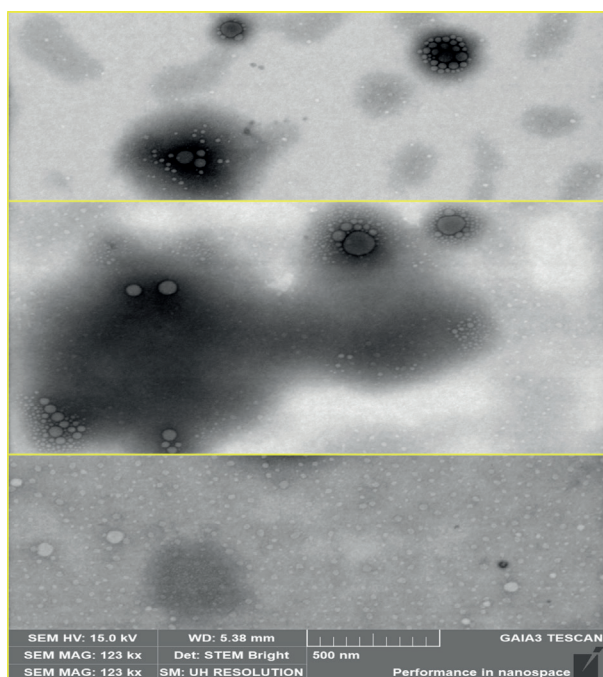


Figure 4: Morphological Analysis: TEM

## Results

Overall, 14 compounds were isolated. Isoscutellarein-7-O-[6''-O-acetyl]-β-D-allopyranosyl-(1→2)-β-D-glucopyranoside and 4'-methyl-hypolaetin-7-O-[6''-O-acetyl]-allopyranosyl-(1→2)-glucopyranoside were the main constituents, as shown in the HPLC-PDA-MS chromatogram (Fig. 2) and the <sup>1</sup>H-NMR spectrum (Fig. 3) of the methanol extract. The microemulsion was prepared using Solutol HS 15 (surfactant, 11 %w/w), Transcutol P (co-surfactant, 3.6 %w/w) and Capryol 90 (oil, 1.7 %w/w), selected for the high solubility of the extract, and water (82.8 %w/w). The extract solubility in the selected microemulsion was 34.33±4.246 mg/mL. Dynamic Light Scattering analysis showed microemulsion droplets with a small average diameter (Size of 23.53±2.206) and high dimensional homogeneity (Pdl of 0.1675±0.0004171). Transmission Electron Microscope gave further information on the spherical shape of the droplets (Fig. 4). The formulation was physically and chemically stable for 1 month at 25°C. A preliminary assay showed a slow release of the main extract component over time.

## References

- [1] <https://powo.science.kew.org/taxon/urn:lsid:ipni.org:names:325931-2>
- [2] <https://portal.cybertaxonomy.org/flora-greece/intro>
- [3] Tomou, EM; Barda, C; Skaltsa H. Genus Stachys: A Review of Traditional Uses, Phytochemistry and Bioactivity. Medicines, 2020, 7, 63.
- [4] Tundis, R.; Peruzzi, L.; Menichini, F. Phytochemical and biological studies of Stachys species in relation to chemotaxonomy: A review. Phytochemistry, 2014, 102, 7-39.

## Extraction optimization of Betulinic acid through different herbal preparations from *Rosmarinus officinalis* L. by <sup>1</sup>H-qNMR

Panagiotis Kallimanis<sup>1</sup>, Prokopios Magiatis<sup>1</sup>, Angeliki Panagiotopoulou<sup>2</sup>, Ioanna Chinou<sup>1</sup>

<sup>1</sup>Department of Pharmacy, National & Kapodistrian University of Athens, 157 71 Zografou, Greece

<sup>2</sup>Institute of Biosciences & Applications, National Centre for Scientific Research "Demokritos", 15310 Agia Paraskevi Attikis, Greece

\*Corresponding Author: Panagiotis Kallimanis, e-mail.: Drpkallimanis@gmail.com

### Introduction

Betulinic acid (BA) belongs to pentacyclic triterpenes and is widely distributed in plants. It has plenty of biological and pharmacological actions, such as antiviral, antitumor, anti-inflammatory, antibacterial, antidiabetic and many others [1]. In previous study we have reported that BA isolated from the leaves of *Rosmarinus officinalis* L. (syn. *Salvia rosmarinus* Spenn.), was able to antagonize *in vitro* the action of the well known pollutant TCDD on AhR by 82.96% in a dose-dependent manner. The discovery of natural agents that act as competitors of AhR seems of great importance as they could be used to prevent or treat established dioxin toxicity [2]. The scope of the current study was to validate and compare different extraction methods and parameters (extraction solvents, drug/solvent ratio etc.) towards the optimization of different betulinic acid extraction of *R. officinalis*.

### Plant Material

Leaves of *R. officinalis* L. were collected in 2019 from J. & A.N. Diomedes Botanic Garden, National and Kapodistrian University of Athens, in the morning during the flowering period of the plants in July and were dried at room temperature.

### Isolation of BA by Rosemary officinalis

BA has been isolated and identified by our team from the dry leaves of *R. officinalis* using chromatographic and NMR methods [2].

### Extraction procedure

Dried leaves of *R. officinalis* were ground in an ultra-centrifugal mill ZM 200 (Retsch, Haan, Germany) using 0.5 mm hole size sieve. Each experiment was repeated in triplicate.

**Aqueous extracts:** The drug: solvent ratio was 2: 150 w/v

- Infusions and decoctions: Were made with maceration: 2, 5, 10 and 15 min
- Turbulent flow extraction: The process of extract preparation was the same as the classic maceration method, with the difference that the drug-water system was placed in a mixer and followed by vortexing for 2 min. We performed two experiments (1) at room temperature and (2) with boiled water.

**Tinctures:** We performed two different experiments:

- 1) drug: solvent ratio 1:10 w/v in 2 different alcoholic degrees, (a) 45o and (b) 70o
- 2) drug: solvent ratio 1:20 w/v with an alcoholic degree of 20°, that is similar to liqueurs and wine.

### Oleolites:

Maceration:

- in room temperature: the drug: olive oil ratio was 5: 100 w/w (5 g of drug in 100 g of oil)
- In heating («Digestion»): two experiments were performed with drug: olive oil ratio, 5:100 and 10:100, keeping the other conditions of the experiment constant.

### Qualitative and quantitative <sup>1</sup>H-qNMR analysis of the extracts

**Aqueous extract** (infusion, decoctions, turbulent-extraction) The aqueous extract was placed into a separatory funnel with an equal volume of CH<sub>2</sub>Cl<sub>2</sub> and the organic phase was collected and concentrated in vacuo (40°C) followed by 1D <sup>1</sup>H-NMR (CDCl<sub>3</sub>).

### Tinctures

- (1) **In case of tinctures of 45o and 70o:** 10 mL of the tincture was concentrated to dryness in vacuo (Rotavapor V-200)

and Büchi heating bath B-490). The dry residue was subjected to 1D 1H-NMR spectroscopy (CDCl<sub>3</sub>).

(2) In case of tinctures of 20o: 20 mL of the tincture was placed in a separatory funnel together with an equal volume of CH<sub>2</sub>Cl<sub>2</sub>. After shaking and allow to stand for 20 minutes, the organic phase was collected and concentrated to dryness followed by 1D 1H-qNMR spectroscopy (CDCl<sub>3</sub>).

### Oleolites

We used the method described before by Karkoula *et al.* (2012) for the analysis of olive oil's polyphenols: 5 g of oleolite was placed in a 50 mL plastic container and 20 mL CH<sub>x</sub> was added. The container was closed and the whole was shaken vigorously for 1 min. 25 mL of acetonitrile (ACN) was then added to the container resulting in phase separation (polar with ACN and non-polar with CH<sub>x</sub> and olive oil). The final system was placed in the centrifuge at 4000 rad for 5 min. 25 mL of ACN solution was concentrated and subjected to 1D 1H-qNMR spectroscopy (CDCl<sub>3</sub>).

### **Quantification of BA**

For the quantitative analysis three independent samples were prepared by weighing of each dry extract, adding 700 μL of chloroform-d, and transferring the mixture to 5 mm NMR tubes. NMR measurements were recorded on a Bruker DRX 500 MHz instrument. For the quantification of BA was taken into account the broad single peak (brs) (H-29a) (LOD=0.04, LOQ=0.01,  $y=0.624+0.001x$ ,  $R^2 = 0.9998$ )

## **Results**

### Aqueous extracts

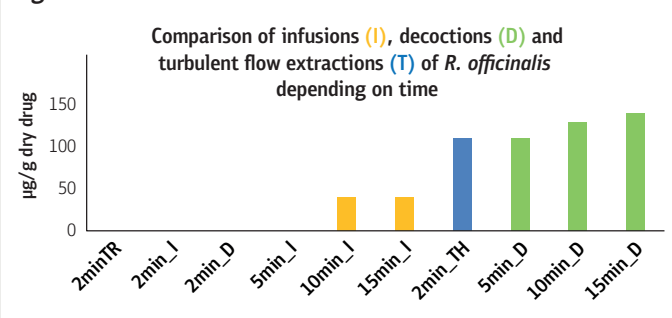
The results of aqueous extracts are presented in Table 1 and in Figure 1.

**Table 1.** Turbulent flow extraction in room temperature (TR) and under heating (TH). Results in mg ±SD/ g dry leaves

Extract	2 min	5 min	10 min	15 min
<b>Infusions</b>	nd	nd	tr	tr
<b>Decoctions</b>	nd	0.11±0.2	0.13±0.03	0.14±0.04
<b>TC</b>	nd	nm	nm	nm
<b>TH</b>	0.11±0.02	nm	nm	nm

*tr:* trace, *nd:* not detected, *nm:* not measured

**Figure 1.**



### Tinctures

The results are presented in Table 2.

**Table 2.**

Tinctures of <i>R. officinalis</i> (mg ± SD in 100 mL of tincture)		
A. 10: 100 w/v, 70% EtOH	B. 10: 100 w/v, 45% EtOH	Γ. 5: 100 w/v, 20% EtOH
17.22±1.31	1.69±0.23	nd

### Oleolites

The results are presented in Tables 3, 4 and in Figure 2.

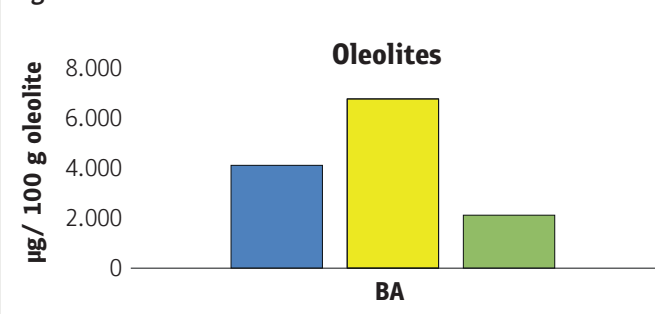
**Table 3.**

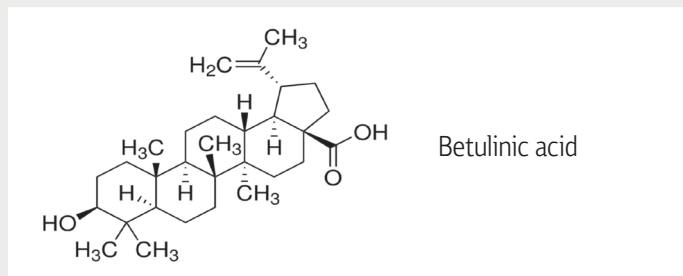
Oleolites of <i>R. officinalis</i> (mg ±SD in 100 g of oleolite)		
A. 5: 100 w/w, 65°C, 6 h	B. 10: 100 w/w, 65°C, 6 h	Γ. 5: 100 w/w, 21 days, room To
4.13±0.32	6.8±0.48	2.13±0.32

**Table 4**

Stability of BA in oleolite during storage (mg ±SD in 100 g of oleolite)	
0 months	2 months
2.13±0.32	2.08±0.41

**Figure 2.**





### Conclusions

Regarding aqueous extracts, decoctions appeared the richer sources of BA, then turbulent flow extraction under heating and finally infusions. The optimum drug-solvent ratio for the preparation of tinctures was 1:10 w/v in 70% EtOH. For the oleolites the maceration of the drug in 1:10 ratio with extra virgin olive oil by heating in 60 oC for 6 h was the most efficient procedure. Olive oil as a solvent was very protective

for BA during the storage of the oleolite. Moreover, the established <sup>1</sup>H-qNMR spectroscopy method offers a fast, simple, reliable and accurate method for the quantitative and qualitative analysis of BA, in complex extracts in a direct way with high precision and without sample deterioration.

### References:

1. Lou H, Li H, Zhang S, *et al.* (2021). A Review on Preparation of Betulinic Acid and Its Biological Activities. *Molecules*; 26(18):5583.
2. Kallimanis P, Chinou I, Panagiotopoulou A, *et al.* (2022). *Rosmarinus officinalis* L. Leaf extracts and their metabolites inhibit the aryl hydrocarbon receptor (AhR) activation *in vitro* and in human keratinocytes: Potential impact on inflammatory skin diseases and skin cancer. *Molecules*; 27(8): 2499.
3. Karkoula E, Skantzari A, Melliou E. *et al.* (2012). Direct measurement of oleocanthal and oleacein levels in olive oil by quantitative (<sup>1</sup>H) NMR. Establishment of a new index for the characterization of extra virgin olive oils. *J Agric Food chem*; 60(47): 11696–11703.

## Onychomycosis due to *Candida albicans* successfully treated topically with an herbal formulation: a case report

Panagiotis Kallimanis<sup>1</sup>, Serafim Prodromidis<sup>2</sup>, Prokopios Magiatis<sup>3</sup>

<sup>1</sup>Pharmacist MSc, PhD; Dr. Kallimanis' Community Pharmacy, Lesvou 57, Athens 11364, Greece

<sup>2</sup>MD Dermatologist; Private Practice, Fedriadon 11, 11364, Athens, Greece

<sup>3</sup>Associate Professor, Division of Pharmacognosy and Chemistry of Natural Products, Department of Pharmacy, National & Kapodistrian University of Athens, Greece

\*Corresponding Author: Dr. Panagiotis Kallimanis, e-mail.: Drpkallimanis@gmail.com

### Introduction

Onychomycosis is a denomination used to describe fungal infection of one or more of the nail units and can be caused by dermatophytes, yeasts or non dermatophyte molds. The term onychomycosis is derived from the Greek word «onyx», a nail and «mykes» a fungus. Onychomycosis affects approximately 5% of the population worldwide. Toenails are about 25 times more likely than fingernails to be infected. *Candida* nail infections are caused by *Candida albicans* in 70%. The remainder cases are due to *C. parapsilosis*, *C. tropicalis*, *C. krusei*. Current treatment agents for onychomycosis include both systemic and topical medications. Oral therapy has the potential for adverse effects, most notably hepatotoxicity. Topical therapies have cure rates lower than those obtained with systemic treatments. Onychomycosis never resolves spontaneously and recurrence after treatment is very common [1, 2]. Fungal melanonychia due to *Candida albicans* is rare and only few cases have been reported in the literature. Melanonychia refers to brown to black pigmentation of the nail unit. We report herein a case of fungal melanonychia due to *Candida albicans* successfully treated topically by a herbal formulation [3].

### Case report

The present case concerns a Caucasian Greek woman, 40 years old, with onychomycosis on the left big toenail. The patient had the first signs of onychomycosis in 2018, but she went to a private dermatologist after 2 years when the situation got worse, namely diffuse melanonychia with intensive dystrophy and hyperkeratosis. At that time a fungal culture from nail clippings showed growth of *Candida* species and she has been treated with terbinafine 250 mg twice a day, per os, and with local application of amorolfine 5% w/v nail lacquer every second night. Both drugs had been used for 6 months. The treatment was ineffective.

Later, in the same year, the patient came to S. Prodromidis, MD Dermatologist, presenting the same clinical picture, that was diffuse, complete black pigmentation, dystrophy and hyperkeratosis of the left big toenail without paronychia or onycholysis (Figure 1.A). The nails of the other toes were unaffected. The patient was otherwise in good health without taking any medication. Routine blood tests were normal. There was no past history of trauma or nail abnormalities. Nail scrapings from the surface of the pigmented nail were collected with a scalpel. Direct examination of nail scrapings with potassium hydroxide showed round yeast cells in the specimen. The samples were cultured and showed growth of *Candida albicans*.

The patient refused to continue with other conventional-synthetic medication because she was unsatisfied and was worried about overuse of orally administering drugs. Hence she asked about other therapeutic approaches like herbal medicine that she considered effective and safe. For this reason a liquid herbal formulation was prescribed, containing a mixture of selected extracts of *Rosmarinus officinalis* L., *Cinnamomum zeylanicum* Blume, *Origanum vulgare* L., *Thymus vulgaris* L. and *Syzygium aromaticum* L., [4], to use topically, twice a day. After a few months an improvement on clinical picture was observed and one year later the maximum result was achieved that was a complete absence of clinical signs. Indeed, no more melanonychia, nail dystrophy and hyperkeratosis were observed as shown in the Figure 1.B. Mycological examination at that moment demonstrated an absence of *C. albicans*. However, we must be aware of the fact that in many cases the recurrence of *C. albicans* infection even after a negative culture can be observed. So, the patient continued the therapy for other 1 month. After 1.5 years from the start the clinical picture was still clear (Figure 1.C). No adverse effects

were observed during the treatment except a reversible yellowish coloration of the nail. The patient was very satisfied with the treatment outcome.

We notice that despite the long period of product use no resistance to remedy was developed. No concurrent therapies have been used

### Discussion

A herbal product might provide an effective and safe alternative or addition to the current options for treating onychomycosis caused by *C. albicans*. The advantages are no or less side effects, topical application, natural synthesis, easy to use it, more desired and acceptable by the patients. Notably

the development of resistance during therapy with a herbal remedy is very difficult, due to the large number of substances which are pharmacologically active. The combination of herbal medications with the conventional per os antifungal therapy in repletion of other drugs of topical application, and the use of a herbal product in cases which appear a matter of resistance to the conventional therapy, will be of interesting in future studies.

### Conclusions

We cannot make a solid conclusion from a case report. Further studies are needed with more patients to get an reliable evaluation on the therapeutic potential of the herbal product



**Figure 1.** Onychomycosis of the left great toenail caused by *Candida albicans*.

- A.** Initially, at the time of patient presentation, were observed a markedly dystrophy and hyperkeratosis with diffuse melanonychia due to the presence of *Candida albicans*
- B.** After 1 year of treatment were achieved a complete absence of melanonychia, nail dystrophy and hyperkeratosis. The culture of nail sample was negative.
- C.** The same clear clinical picture was after 1.5 years



in onychomycosis due to *C. albicans* (or to other *Candida* species) and to dermatophytes and non dermatophyte molds. However, the described herbal remedy in this study might provide an effective and safe alternative as monotherapy or as addition to the current options for treating onychomycosis caused by *C. albicans*, without problems of resistance development or side effects.

#### **Acknowledgement**

We thank G. Kolovos MD Microbiologist for his contribution in this article.

#### **References:**

- [1] R. Kaur, B. Kashyap, P Bhalla. Onychomycosis-epidemiology, diagnosis and management. *Indian J Med Microbiol* 2008; 26 (2), 108-116.
- [2] AK. Gupta, N. Stec, RC. Summerbell, *et al.* Onychomycosis: a review. *J Eur Acad Dermatol Venereol.* 2020 Sep; 34(9): 1972-1990.
- [3] E. Cho, YB. Lee, HJ. Park *et al.* Fungal melanonychia due to *Candida albicans*. *Int J Dermatol* 2013; 52(12): 1598- 1600.
- [4] P. Kallimanis. "Compositions with antibacterial, antifungal and antiparasitic activity for treating infections of the skin, nails and urogenital system". Patent; GR20190100361; 2021.

## Medicinal Properties of Six Balkan Plants Traditionally Used for the Treatment of Skin Diseases: From Ethnobotany to Scientific Evidence

Z. Kardasi<sup>1,3\*</sup>, E. Dina<sup>2</sup>, N. Aligiannis<sup>2</sup>, A. Kourounakis<sup>3</sup>

<sup>1</sup>Department of Pharmaceutical Technology, Faculty of Pharmacy, National and Kapodistrian University of Athens, Greece

<sup>2</sup>Department of Pharmacognosy and Natural Products Chemistry, Faculty of Pharmacy, National and Kapodistrian University of Athens, Greece

<sup>3</sup>Department of Medicinal Chemistry, Faculty of Pharmacy, National and Kapodistrian University of Athens, Greece

\*Panepistimiopolis of Zographou Zographou 157 71, zoikardasi@gmail.com

### Introduction

Traditional medicinal resources, especially plants, have been found to play a major role in managing skin disorders. In spite of the great advances achieved in modern medicine during the past decades, plants still make an important contribution to health care and people are turning to natural remedies more and more. The Balkan region has a great diversity of medicinal flora and people living in this area have traditionally used these ethno-medicines for many skin problems.

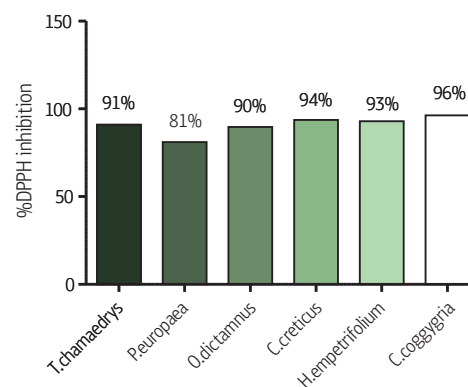
Combining ethnobotanical surveys and scientific studies is a good strategy for new herbal medicines to be discovered and exploited. In this study, a total of six plant species from the Balkan area were selected based on their ethnopharmacological properties and existing scientific evidence in the literature was sought for. Further, the *in vivo* and *in vitro* activities of their methanol and water-methanol (1:1) extracts were studied in our laboratory.

### Methods

**Bibliographical search** was conducted using the databases *Pubmed*, *Google Scholar*, *Science direct* and *Scopus*. ***In vitro* antioxidant activity** evaluation included assays of scavenging the free radical DPPH as well as iron-chelation (ferrozine assay) at a concentration of 200 µg/mL. Also, the total phenolic (TPC) and total flavonoid content (TFC) were evaluated using the Folin-Ciocalteu and the aluminium chloride colorimetric methods, respectively.

**Inhibition of skin enzymes** was evaluated *in vitro*; specifically, anti-tyrosinase and anti-collagenase activities were tested at a concentration of 300 µg/mL and 100 µg/mL, respectively. ***In vivo* anti-inflammatory activity** of the plant extracts was studied via a carrageenan-induced edema protocol in female C57BL/6 mice (at an i.p dose of 3mg/100g BW).

### Results





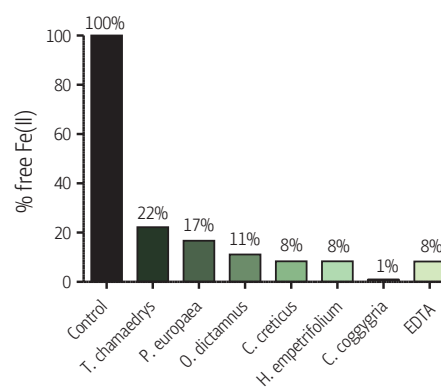




**Figure 1:** DPPH inhibition (%) at 200µg/ml concentration of extracts.



**Figure 2:** Iron chelation of extracts; % free Fe(II) remaining after incubation with 200 µg/ml. concentration

**Table 1:** Medicinal plants from the Balkan region with therapeutic potential.

Plant name	Family	Activities <sup>2,3,4,5</sup>	Traditional use <sup>1</sup>
<b>Teucrium chamaedrys</b> L. (Herba)	Lamiaceae 	<ul style="list-style-type: none"> <li>• Antimicrobial</li> <li>• Antioxidant</li> <li>• Urticaria-Body Itch</li> </ul>	Wound healing, Eczema, Edema, Anti-inflammatory,
<b>Plumbago europaea</b> L. (Roots)	Plumbaginaceae 	<ul style="list-style-type: none"> <li>• Antimicrobial</li> <li>• Antioxidant</li> </ul>	Wound healing, Skin disorders, Eczema, Edema, Anti-inflammatory, Antimicrobial, Urticaria-Body Itch, Moles-Skin tumor, Erythema
<b>Origanum dictamnus</b> L. (Aerial parts)	Lamiaceae 	<ul style="list-style-type: none"> <li>• Antioxidant</li> <li>• Antiaging</li> <li>• Antimicrobial</li> </ul>	Wound healing, Antiinflammatory, Antimicrobial, Acne-Pimples-oily skin, Moles-Skin tumor
<b>Cistus creticus subspecies creticus</b> L. (Aerial parts)	Cistaceae 	<ul style="list-style-type: none"> <li>• Antimicrobial</li> <li>• Anti-inflammatory - Cytotoxic</li> </ul>	Wound healing, Skin diseases-disorders, Antimicrobial
<b>Hypericum empetrifolium</b> Willd. (Aerial parts)	Hypericaceae 	<ul style="list-style-type: none"> <li>• Antimicrobial</li> <li>• Antioxidant</li> <li>• Wound healing</li> <li>• Anti-Elastase, Anti-Tyrosinase, Anti-Collagenase</li> <li>• Anti-Inflammatory</li> </ul>	Wound healing
<b>Cotinus coggygria</b> Scop. (Herba)	Anacardiaceae 	<ul style="list-style-type: none"> <li>• Antimicrobial</li> <li>• Antioxidant</li> <li>• Wound healing</li> <li>• Anti-Elastase, Anti-Tyrosinase, Anti-Collagenase</li> <li>• Anti-inflammatory</li> </ul>	Wound healing, Eczema, Edema, Skin diseases-disorders, Antimicrobial, Moles-Skin tumor

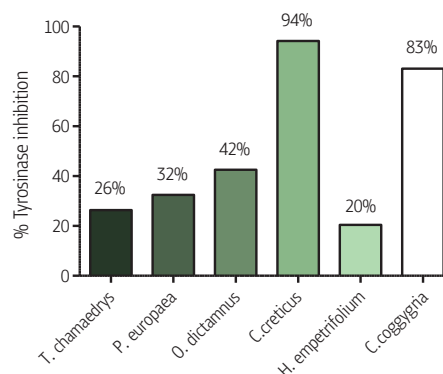


**Figure 3:** Tyrosinase inhibition (%) at 300 µg/ml concentration of extracts.

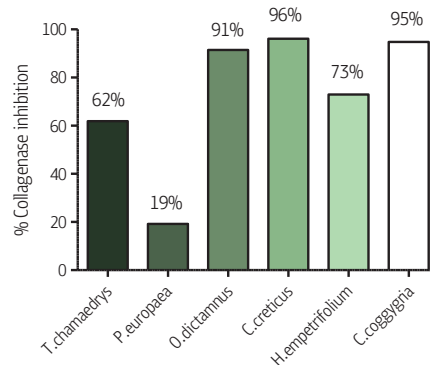


**Figure 4:** Collagenase inhibition (%) at 100 µg/ml of extracts.

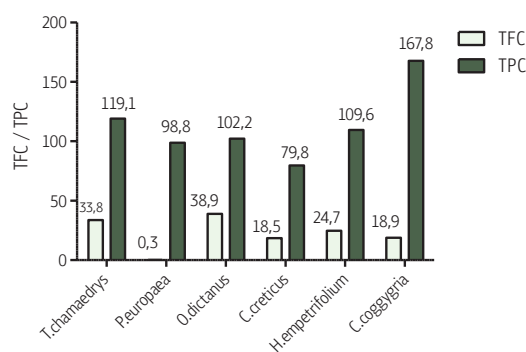


**Figure 5:** TFC (mg QUE/g extract) and TPC (mg GAE/g extract) content of the plant extracts.

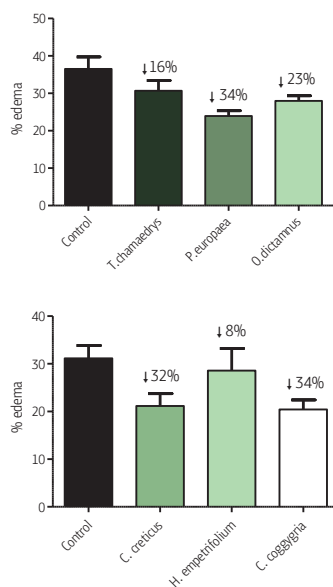


**Figure 6:** *In vivo* anti-inflammatory activity of the medicinal plants studied; % edema and its reduction (n=6).

## Conclusions

- The highest antioxidant activity was found in the extracts

of Cistus Creticus, Cotinus coggygia and Hypericum empetrifolium.

- The highest enzyme inhibition was found in the extracts of Cistus creticus and Cotinus coggygia.
- The highest TPC was found in Cotinus coggygia and TFC in Origanum dictamnus.
- The highest anti-inflammatory activity was found in Cotinus coggygia and Plumbago europaea extracts.

## References

1. Tsioutsou, E. E. *et al.* Medicinal Plants Used Traditionally for Skin Related Problems in the South Balkan and East Mediterranean Region—A Review. *Frontiers in Pharmacology* 13, (2022).
2. Skorić, M. *et al.* Bioactivity-guided identification and isolation of a major antimicrobial compound in Cistus creticus subsp. creticus leaves and resin “ladano”. *Industrial Crops and Products* 184, 114992 (2022).
3. Ertaş, B. *et al.* The effect of Cotinus coggygia L. ethanol extract in the treatment of burn wounds. *jrj* 26(3), 554–564 (2022).
4. Akdeniz, M. *et al.* Essential oil content, *in-vitro* and *in-silico* activities of Hypericum triquetrifolium Turra, H. empetrifolium subsp. empetrifolium Willd., and H. pruinatum Boiss. & Balansa species. *ijp* 53, 177–185 (2023).
5. Marrelli, M. *et al.* Composition, antibacterial, antioxidant and antiproliferative activities of essential oils from three Origanum species growing wild in Lebanon and Greece. *Natural Product Research* 30, 735–739 (2016).

## Τσάι του βουνού: Ανεξάντλητη πηγή βιοδραστικών συστατικών

Αικατερίνα-Μιχαέλα Τόμου\*, Ελένη Σκαλτσά

Τμήμα Φαρμακευτικής, Σχολή Επιστημών Υγείας, Εθνικό και Καποδιστριακό Πανεπιστήμιο Αθηνών, Πανεπιστημιούπολη Ζωγράφου, 15771, Αθήνα

\*Corresponding Author: \*Corresponding Author: Αικατερίνα-Μιχαέλα Τόμου, E-mail: mail: ktomou@pharm.uoa.gr

### Εισαγωγή

Τα είδη του γένους Σιδηρίτη (Τσάι του βουνού), *Sideritis scardica* Griseb., *S. clandestina* (Bory & Chaub.) Hayek, *S. raeseri* Boiss. & Heldr. και *S. syriaca* L. είναι επισήμως αναγνωρισμένα από τον Ευρωπαϊκό Οργανισμό Φαρμάκων (EMA) ως παραδοσιακά φάρμακα για τη θεραπεία έναντι του κοινού κρυολογήματος και των ήπιων γαστρεντερικών διαταραχών<sup>1</sup>. Αξίζει να σημειωθεί ότι το τσάι του βουνού αποτελεί κύριο συστατικό και στην παραδοσιακή Ελληνική Μεσογειακή διατροφή.

### Σκοπός μελέτης

Προσπαθώντας να αναδείξουμε τη μεγάλη σημασία των φυτών με ευεργετικές ιδιότητες και υψηλής εθνοφαρμακολογικής σημασίας, μελετήσαμε διάφορα είδη τσάι του βουνού της Ελλάδας.

### Αποτελέσματα & Συζήτηση

- ***Sideritis euboea* Heldr.:** Μέσω βιοκατευθυνόμενης προσέγγισης πραγματοποιήθηκε ο προσδιορισμός των δευτερογενών μεταβολιτών του και η διερεύνηση της *in vitro* κυτταροξικής δράσης του, καθώς και η πιθανή ανασταλτική δράση έναντι του ενζύμου υαλουρονιδάσης (*in vitro* & *in silico* μελέτες)<sup>2,3</sup>
- ***Sideritis sipylea* Boiss.:** Μελετήθηκαν τα πολικά συστατικά και οι βιολογικές δράσεις του μεθανολικού εκχυλίσματος και του παραδοσιακού εγχύματος του *S. sipylea* από τη Σάμο. Διερευνήθηκε η αντιοξειδωτική και η αντι-χολινεστερασική δράση. Η θεραπευτική αξία του φυτού αναφέρθηκε για πρώτη φορά, αποκαλύπτοντας μια πολλά υποσχόμενη πηγή πρωτεΐνης<sup>4</sup>
- ***Sideritis syriaca* L. subsp. *syriaca* (Μαλοτύρα):** Μελετήθηκε το χημικό προφίλ του άπολου εκχυλίσματος και του αιθέριου ελαίου του *ex situ* πολλαπλασιασμένου και καλλιεργούμενου φυτικού υλικού<sup>5</sup>.

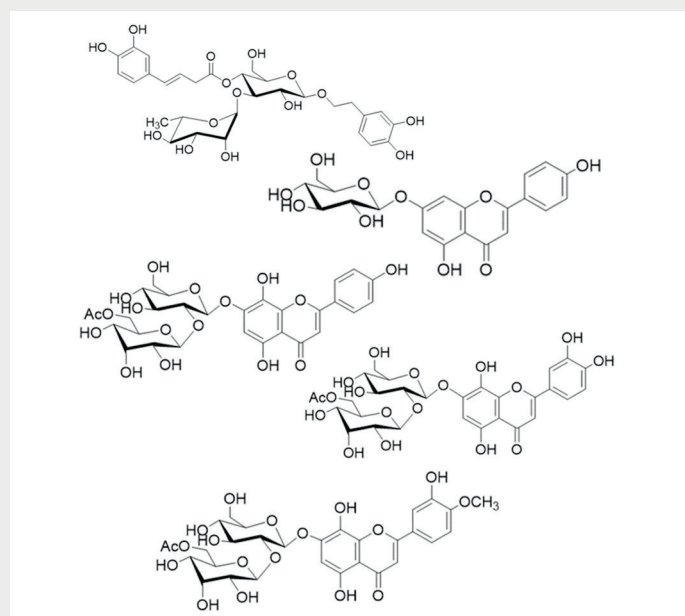
### Συμπεράσματα

Οι παραπάνω μελέτες αναδεικνύουν την παρουσία διαφόρων

βιοδραστικών συστατικών και τις σημαντικές φαρμακολογικές δράσεις των ειδών του γένους Σιδηρίτη, καθώς επίσης αποδεικνύουν ότι η καλλιέργεια των συγκεκριμένων φυτών είναι εφικτή παρέχοντας φυτικά προϊόντα με πλούσιο φυτοχημικό προφίλ και φαρμακολογικές ιδιότητες.

### Βιβλιογραφία

1. EMA/HMPC/39453/2015.
2. Tomou E-M; Papaemmanouil C; Diamantis D.; Kostagianni A; Chatzopoulou P; Mavromoustakos T; Tzakos A; Skaltsa H. Anti-Ageing Potential of *S. euboea* Heldr. Phenolics. *Molecules* 2021, 26, 3151.
3. Tomou E-M; Chatziathanasiadou M; Chatzopoulou P; Tzakos A; Skaltsa H. NMR-Based Chemical Profiling, Isolation and Evaluation of the Cytotoxic Potential of the Diterpenoid Siderol from Cultivated *Sideritis euboea* Heldr. *Molecules* 2020, 25, 2382.
4. Tomou E-M; Lytra K; Chrysargyris A; Christofi MD; Miltiadous P; Corongiu GL; Tziouvelis M; Tzortzakis N; Skaltsa H. Polar constituents, biological effects and nutritional value of *Sideritis sipylea* Boiss. *Nat. Prod. Res.* 2021, 1–5.
5. Kloukina C; Tomou E-M; Krigas N; Sarropoulou V; Madesis P; Maloupa E; Skaltsa H. Non-polar secondary metabolites and essential oil of *ex situ* propagated and cultivated *Sideritis syriaca* L. subsp. *syriaca* (Lamiaceae) with consolidated identity (DNA Barcoding): towards a potential new industrial crop. *Ind. Crops Prod.* 2020, 158, 112957.



## Simulated Dosing Regimens Of Monoclonal Antibodies And Classical Treatments For Migraine

Department of Pharmacy, National and Kapodistrian University of Athens, Greece

**Maria – Ileana Theofili\***, Helen Basdagianni, Vangelis Karalis

Department of Pharmacy, National and Kapodistrian University of Athens, Panepistimioupolis, Zografou, 15784, Athens, Greece

\* Corresponding author: Maria – Ileana Theofili Email: ileanatheofilis@gmail.com

Department of Pharmacy, School of Health Sciences, National and Kapodistrian University of Athens, Panepistimioupolis, Zografou, 15784, Athens, Greece

### Introduction

Pharmacologic treatments for migraine encompass a variety of classes, including nonsteroidal anti-inflammatory drugs (e.g., ibuprofen, aspirin), triptans (e.g., almotriptan, eletriptan), ergot alkaloids, opioids, ditans (e.g., lasmiditan), gepants (e.g., ubrogepant, rimegepant), and more recently, monoclonal antibodies (e.g., erenumab, fremanezumab, galcanezumab, eptinezumab). The pharmacokinetics of all these compounds play a pivotal role in the development of appropriate dosing regimens, aiming to maximize efficacy while minimizing toxicity. This study focuses on investigating the pharmacokinetic behavior of monoclonal antibodies and

other drugs in the context of migraine treatment. Simulations were performed to determine the most suitable dosing regimen.

### Methodology

A literature search was conducted to gather the essential pharmacokinetic information required for the simulations. This encompassed acquiring the structural pharmacokinetic model, parameter estimates, between-subject and within-subject variabilities, the residual error model, and covariates (e.g., age, weight, gender) influencing drug kinetics. Simulations were carried out for representative compounds

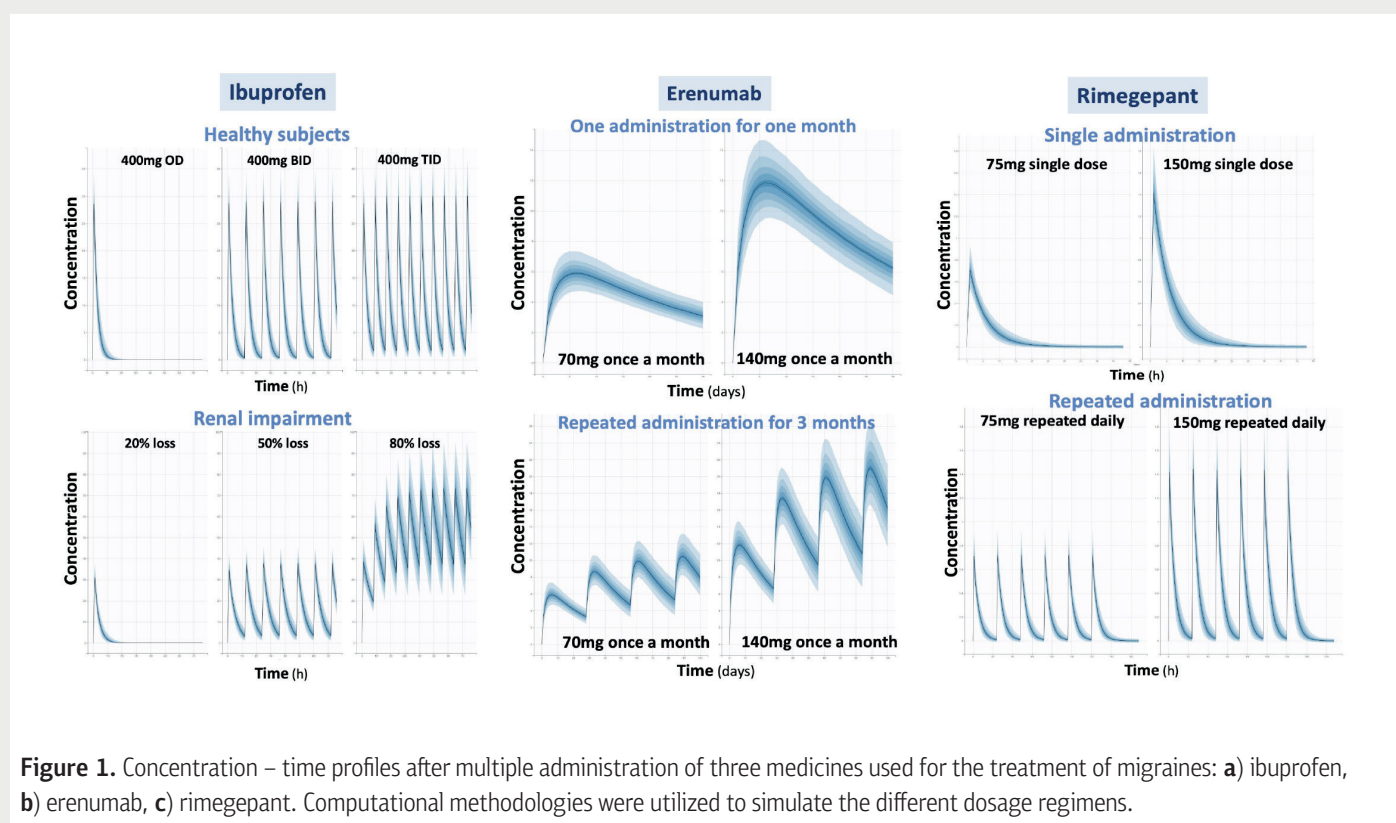


**Figure 1.** Concentration – time profiles after multiple administration of three medicines used for the treatment of migraines: a) ibuprofen, b) erenumab, c) rimegepant. Computational methodologies were utilized to simulate the different dosage regimens.

from each category, specifically ibuprofen, rimegepant, and erenumab. In each scenario, Monte Carlo simulations were employed to generate data for 10,000 simulated patients. The entire computational analysis was executed using Simulx® (Monolix 2021R1®)

### Results

Concentration-time plots describing the pharmacokinetic behavior of ibuprofen, rimegepant, and erenumab were constructed, showing the average performance and the 90% confidence intervals around the mean (Figure 1). The models used were validated by comparing the simulation results with literature results. Several dosage regimens and conditions were simulated referring single administration, repeated administration, and renal impairment. For ibuprofen multiple dosing in healthy subjects does not lead to toxic levels, however, as age increases the derived plasma levels also rise due to the accompanying renal impairment. In the case of rimegepant, the once daily regimen does not lead to accumulation, even after repeated administration. A different be-

havior can be observed for erenumab where accumulation is obvious after multiple dosing and steady state levels are reached the fourth month of administration.

### Discussion

In this study, we utilized population pharmacokinetic models to simulate dosage regimens. This enabled us to explore various dosing scenarios and assess their potential therapeutic outcomes. The simulated dosage regimens facilitated the prediction and optimization of medication administration in a virtual environment, with the latter being selected as the most suitable for use in clinical practice.

### Conclusions

The application of modeling and simulation approaches stands as a valuable tool in the design of optimal dosage regimens. By using sophisticated computational models, researchers and clinicians can gain a comprehensive understanding of how medications interact within the dynamics of the human body.

## A Clinical Study of Allergic Contact Dermatitis in Polysensitized and Monosensitized Patients: Machine Learning and Classic Methods

Aikaterini Kyritsi<sup>a\*</sup>, Anna Tagka<sup>b</sup>, Alexandros Stratigos<sup>b</sup>, Vangelis Karalis<sup>a\*</sup>

<sup>a</sup>Department of Pharmacy School of Health Sciences, National and Kapodistrian University of Athens Panepistimioupolis, Zografou, 15784, Athens, Greece

<sup>b</sup>First Department of Dermatology and Venereology, "Andreas Syggros" Hospital, National and Kapodistrian University of Athens, Ionos Dragoumi 5, 11621, Athens, Greece

\* Corresponding authors: Aikaterini Kyritsi, [akyrits@pharm.uoa.gr](mailto:akyrits@pharm.uoa.gr), Vangelis Karalis, [vkalis@pharm.uoa.gr](mailto:vkalis@pharm.uoa.gr)

### Introduction

The sensitization process is a result of the interplay between genetic and environmental factors [1,2]. Sensitized patients to one hapten have been shown to be at high risk of developing multiple contact allergies [1-3]. This study aims to investigate the sensitization patterns in order to understand the association among allergic contact dermatitis (ACD) - related factors, patient characteristics, polysensitization, and individual susceptibility.

### Methodology

Patch test data from 400 patients (200 polysensitized and 200 monosensitized patients) were collected at the Laboratory for Patch Testing, «Andreas Syggros» Hospital in

Athens, Greece. The detection of sensitization comprised at least one positive reaction to thimerosal 0.1% and patients were divided into two groups: patients with thimerosal contact allergies and patients with concomitant thimerosal and other contact allergies; information was also collected for an extended MOAHLFA (Male Occupational Atopic Hand Leg Face Age) index [4].

To assess the relationship between patient characteristics and ACD-related parameters, the chi-square test for independence was utilized. To uncover the underlying relationships in the data, multiple correspondence analysis (MCA), which is a machine learning approach, was applied [5]. The entire statistical analysis was implemented in IBM SPSS v.26.

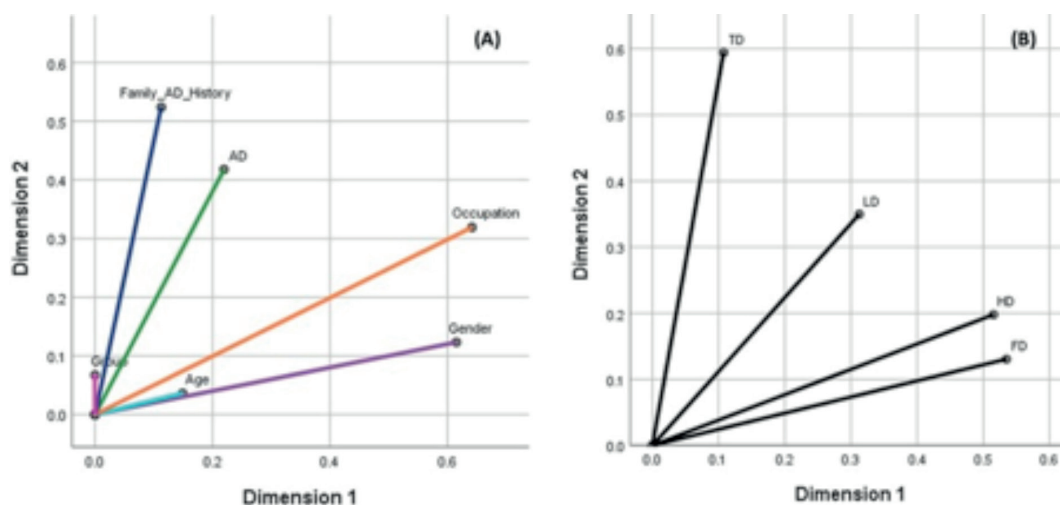


**Figure 1.** Multiple correspondence analysis of the patients' characteristics (A) and anatomical regions (B) of allergic contact dermatitis. The analysis was performed for the following patients' features: patient group (polysensitized and monosensitized patients), atopic dermatitis (AD), family atopic dermatitis (AD) history, occupation class (health workers, hairdressers, cleaners, bakers, cooks, builders, engineers, householders, office workers, nail technicians, make-up artists, technicians, metal workers), age group ( $\leq 40$ ,  $> 40$ ), gender. Also, for the anatomic region of dermatitis: face dermatitis (FD), hand dermatitis (HD), leg dermatitis (LD), and trunk dermatitis (TD).



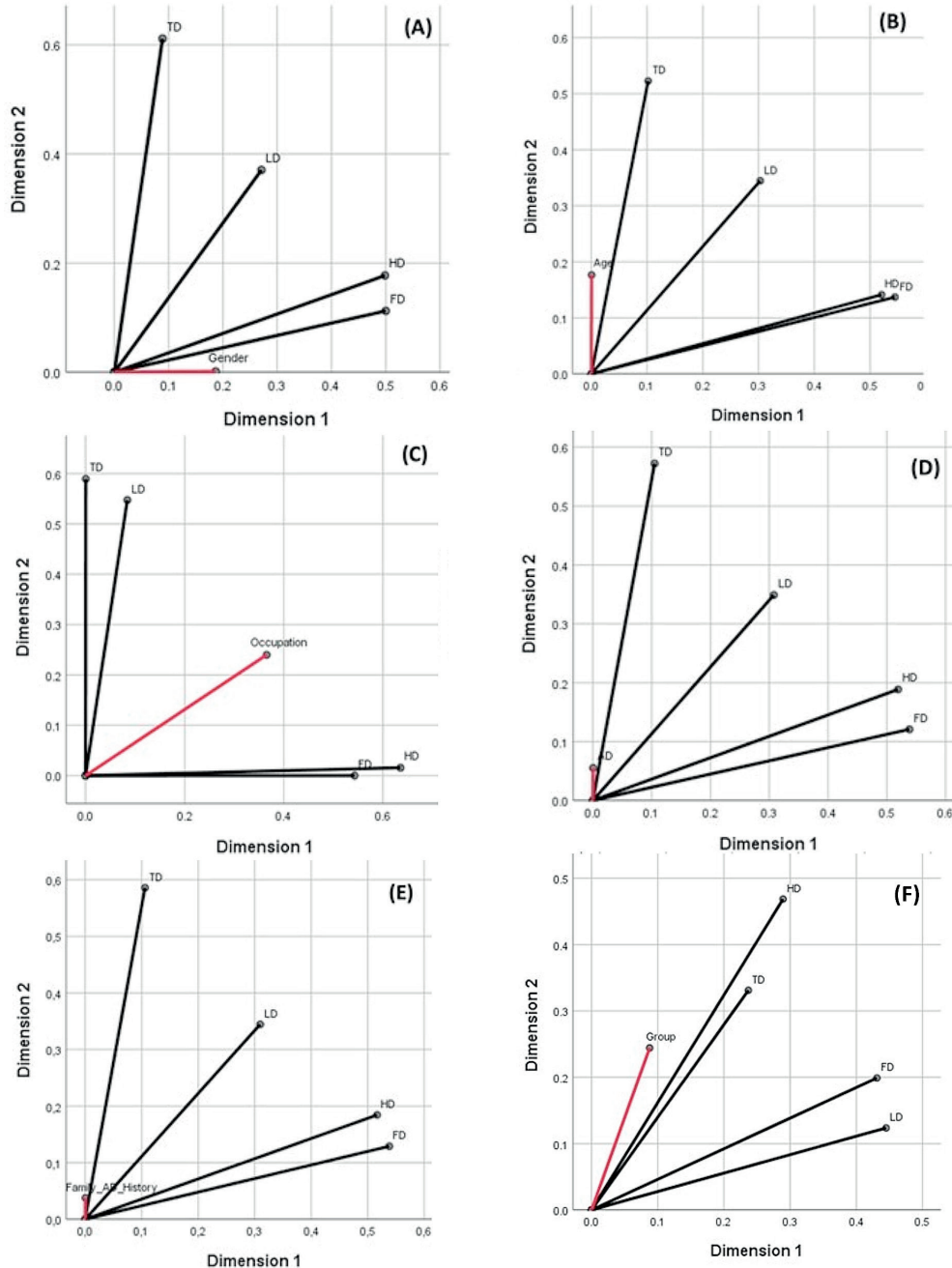


**Figure 2.** Multiple correspondence analysis of the anatomical regions of allergic contact dermatitis in relation to each patient characteristics. The analysis was performed for: **A)** gender, **B)** age group ( $\leq 40$ ,  $>40$ ), **C)** occupation class (health workers, hairdressers, cleaners, bakers, cooks, builders, engineers, householders, office workers, nail technicians, make-up artists, technicians, metal workers), **D)** atopic dermatitis (AD), **E)** family atopic dermatitis (AD) history, and **F)** patient group. In all cases, the anatomic sites referred to hand dermatitis (HD), face dermatitis (FD), leg dermatitis (LD), and trunk dermatitis (TD).

## Results

A total of 400 medical records were examined. The average age was 34.5 years, with equal contributions from both sexes. Half of the patients (were polysensitized, while

the remaining were monosensitized. Office employees accounted for 160 (40.0%) of all occupations, followed by technicians/metal workers (64.0%), health workers (45.2%), cleaners/householders (31.7%), nail technicians

and make-up artists (30.5%), bakers/cooks (29.3%), engineers/builders (29.3%), and hairdressers (12.0%). 162 (40.5%) of the patients had a positive personal history of atopic dermatitis, whereas 98 (24.5%) had a positive family history. According to the MOAHLFA index, hand dermatitis was the most prevalent type of dermatitis in 285 cases (71.3%), with facial dermatitis coming in second with 136 cases (34.0%), trunk dermatitis coming in third with 96 cases (24.4%), and leg dermatitis coming in fourth with 85 cases (21.3%).

Chi-square analysis revealed statistically significant relationships between hand dermatitis and patient group ( $p$ -value = 0.005). In particular, the percentage of monosensitized patients was higher than the percentage of polysensitized patients (monosensitization > polysensitization). None of the groups, however, were shown to be associated with the other dermatitis kinds (FD/Face Dermatitis, LD/Leg Dermatitis, TD/Trunk Dermatitis, and AD/Atopic Dermatitis). Also, both polysensitized ( $p$ -value = 0.003) and monosensitized ( $p$ -value = 0.000) individuals had significant relationships between

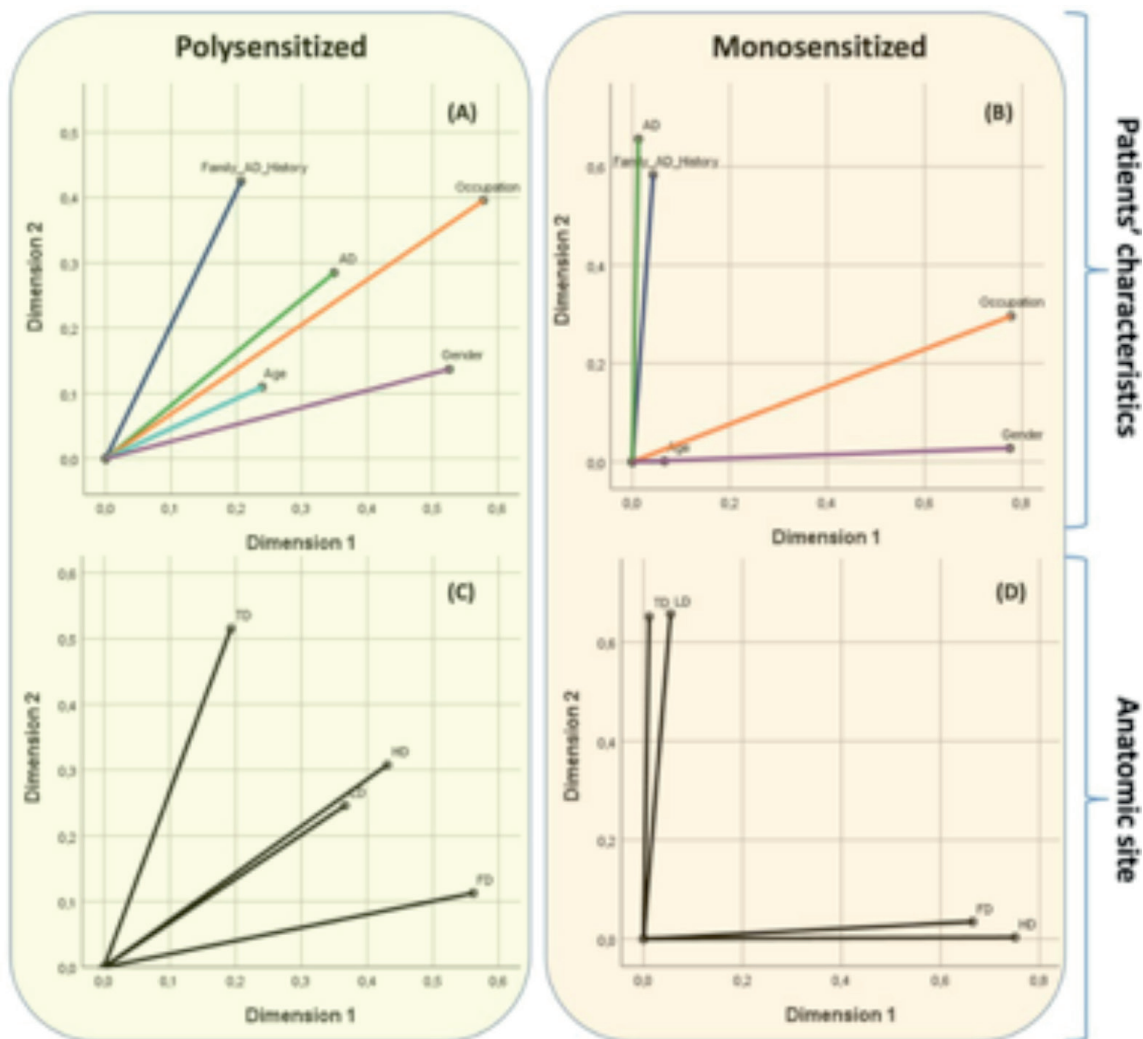


**Figure 3.** Separate multiple correspondence analysis for the polysensitized (A, C) and monosensitized (B, D) patients. Key: AD, atopic dermatitis history, occupation class (health workers, hairdressers, cleaners, bakers, cooks, builders, engineers, householders, office workers, nail technicians, make-up artists, technicians, metal workers), age group ( $\leq 40$ ,  $> 40$ ); gender; HD, hand dermatitis; LD, leg dermatitis; FD, face dermatitis; TD, trunk dermatitis.

hand dermatitis and occupation class. Only in the monosensitized patients' group were significant relationships between hand dermatitis and gender revealed ( $p$ -value = 0.025), with males outnumbering females (number of males > number of females).

MCA analysis revealed interesting relationships among several patients' characteristics. Indeed, occupation showed a strong association with gender and age, while AD was related to familial AD history (Figure 1A). Interestingly, patient groups were found not to be related to occupation, age, or gender, while the total patient cohort was associated with AD and family AD history (Fig. 1A).

Additional relationships were found among the anatomical regions of ACD. Specifically, HD was shown to be most associated with FD, then with LD, and less with TD (Fig. 1B).

In terms of anatomical regions, gender was most strongly linked with FD and HD, then LD, and finally TD (Fig. 2A). Age, on the other hand, was significantly related to TD, followed by LD, but not to HD or FD (Fig. 2B). Occupation was most closely associated with HD and FD, then LD, and less correlated with TD (Fig. 2C). Furthermore, both AD and family AD history were most strongly associated with TD, followed by LD, HD, and less so with FD (Fig. 2D, Fig. 2E). Additional correlations were found between patient groups and the anatomical regions of ACD in the following descending order: HD > TD > FD > LD (Fig. 2F).

In the group of polysensitized patients, similar positive correlations, as in the total patient cohort, were identified for the following variables: Occupation manifested a positive correlation with gender and age, as well as AD with family AD history (Fig.

3A). In the group of monosensitized patients, occupation also manifested a positive correlation with gender and age, as well as AD with family AD history. On the contrary, AD and family AD history were found to be independent of age and gender (Fig. 3B).

In the group of polysensitized patients, HD, in contrast to the total patient cohort (Fig. 1B), was found to be most correlated to LD, then to FD and TD (Fig. 3C). In the group of monosensitized patients, HD, as in the total patient cohort, was found to be most correlated to FD. On the contrary, LD was found to be most correlated with TD and independent of HD and FD (Fig. 3D).

## Conclusions

Hand dermatitis was associated with patient group, occupation, and gender (only in monosensitized patients). Demographics, MOAHLFA index, and allergy category were linked by MCA. Application of machine learning can reveal demographic-clinical relationships.

## References

1. Carlsen CB, Andersen EK, Menne T, Johansen DJ. Patients with multiple contact allergies: a review. *Contact Dermatitis* 2008;58:1-8.
2. Schnuch A, Brasch J, Uter W. Polysensitization and increased susceptibility in contact allergy: a review. *Allergy* 2008;63:156-167.
3. Gosnell LA, Schmotzer B, Nedorost TS. Polysensitization and Individual Susceptibility to Allergic Contact Dermatitis. *Contact Dermatitis* 2015;26(3):133-135.
4. Oosterhaven J, Uter W, Aberer W *et al.* European Surveillance System on Contact Allergies (ESSCA): Contact allergies in relation to body sites in patients with allergic contact dermatitis. *Contact Dermatitis* 2019;80(5):263-272.
5. Greenacre M, Blasius J. Multiple Correspondence Analysis and Related Methods. 2006, 1st ed. Chapman and Hall/CRC, New York.

## Contact Allergy to Preservatives in a Patient Cohort with Occupational Contact Dermatitis: Machine Learning Analysis of Patch Test Data

Aikaterini Kyritsi<sup>a\*</sup>, Anna Tagka<sup>b</sup>, Alexandros Stratigos<sup>b</sup>, and Vangelis Karalis<sup>a\*</sup>

<sup>a</sup>Department of Pharmacy School of Health Sciences, National and Kapodistrian University of Athens Panepistimioupolis, Zografou, 15784, Athens, Greece

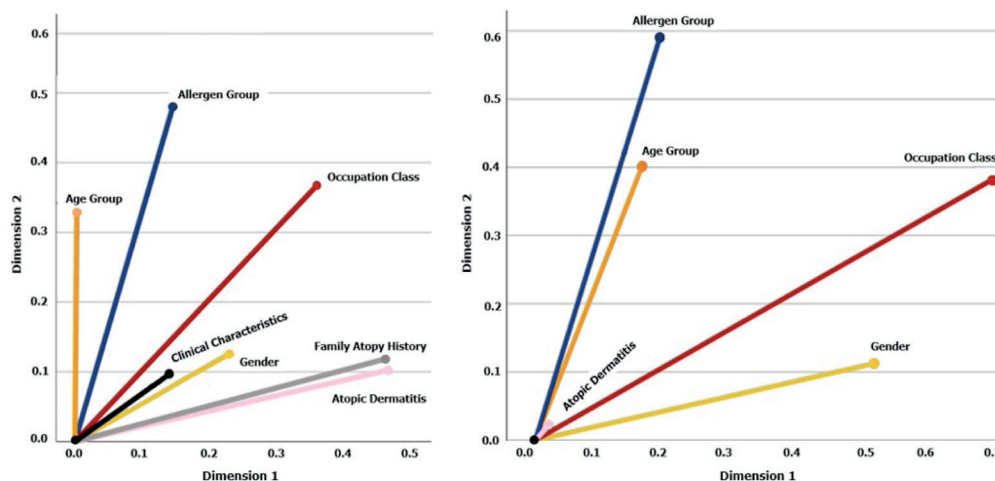
<sup>b</sup>First Department of Dermatology and Venereology, "Andreas Syggros" Hospital, National and Kapodistrian University of Athens, Ionos Dragoumi 5, 11621, Athens, Greece

\*Corresponding authors: Aikaterini Kyritsi, [akyrits@pharm.uoa.gr](mailto:akyrits@pharm.uoa.gr), Vangelis Karalis, [vkalis@pharm.uoa.gr](mailto:vkalis@pharm.uoa.gr)

### Introduction

Occupational dermatoses have a major socioeconomic burden [1]. Occupational-related allergic contact dermatitis (ACD) is common in healthcare workers, cleaning service, beauty industry and industry workers[1,2]. Among risk factors,

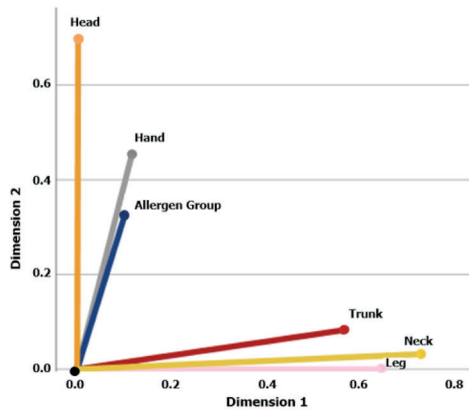
the exposure to preservatives is frequent, since they are extensively added in products for occupational use [3]. The purpose of this analysis was two-fold: a) to identify the linkage among hypersensitivity to preservatives, occupational profiles, patients' clinical and demographic characteristics,



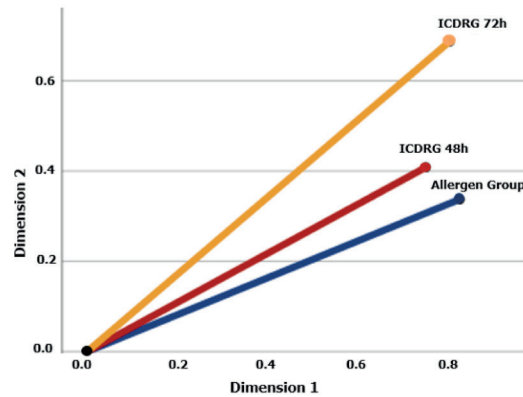
Variables	Dimension 1	Dimension 2
Allergen Group	0.145	0.481
Gender	0.228	0.126
Occupation Class	0.358	0.367
Atopic Dermatitis	0.463	0.102
Family Atopy History	0.460	0.119
Age Group	0.003	0.329
Clinical Characteristics	0.140	0.097

Variables	Dimension 1	Dimension 2
Allergen Group	0.193	0.590
Gender	0.524	0.112
Occupation Class	0.707	0.382
Atopic Dermatitis	0.021	0.021
Age group	0.165	0.401

**Figure 1.** Multiple correspondence analysis of the patients' characteristics in the total patient cohort (N=800) (A) and its simplified version (B). The analysis was performed for the following patients' features: allergen group (Formaldehyde 2%, KATHON 0.02%, Thimerosal 0.1%, MDBGN 0.5%), gender, occupation class (cleaning service, healthcare workers, industry workers, beauty industry), atopic dermatitis, family atopy history (positive, negative), age group ( $\leq 42$ ,  $> 42$ ) and clinical characteristics (erythema, edema, papules, coalescing vesicles, weeping, cracked skin, itching, scaling). Each table below the graph describes the component loads with a sequential color scale that goes from bright to dark blue. That indicates the correlation between the categorical variables and each of the two dimensions, whose value is expressed by the coordinates at the end of each vector line. The cosine of the angle between two vector lines represents the association between the corresponding variables. If two vector lines are close together, it suggests that the categories they represent are similar or positively associated. Conversely, if they are far apart, it indicates dissimilarity or a negative association. A 90° angle indicates that the variables are not related.



Variables	Dimension 1	Dimension 2
Allergen Group	0.100	0.325
Hand	0.116	0.454
Leg	0.644	0.000
Trunk	0.564	0.083
Head	0.002	0.698
Neck	0.728	0.032



Variables	Dimension 1	Dimension 2
Allergen Group	0.827	0.337
ICDRG 48h	0.751	0.408
ICDRG 72h	0.804	0.687

**Figure 2.** Multiple correspondence analysis in the total patient cohort (N=800) of the allergic contact dermatitis by anatomical regions (A) and the allergic reaction severity (B). The analysis was performed for the following patients' features: allergen group (Formaldehyde 2%, KATHON 0.02%, Thimerosal 0.1%, MDBGN 0.5%), anatomical regions (hand dermatitis, leg dermatitis, trunk dermatitis, head dermatitis, neck dermatitis), and the ICDRG evaluation (negative reaction, weak positive reaction (+), strong positive reaction (++), and extreme positive reaction (+++)). Each table below the graph describes the component loads with a sequential color scale that goes from bright to dark blue. That indicates the correlation between the categorical variables and each of the two dimensions, whose value is expressed by the coordinates at the end of each vector line. The cosine of the angle between two vector lines represents the association between the corresponding variables. If two vector lines are close together, it suggests that the categories they represent are similar or positively associated. Conversely, if they are far apart, it indicates dissimilarity or a negative association. A 90° angle indicates that the variables are not related.

and b) to compare the four allergen groups: Formaldehyde 2%, KATHON 0.02%, Thimerosal 0.1%, and methylidibromo-glutaronitrile (MDBGN) 0.5%.

### Methodology

A number of 800 ACD patients' patch test results from «Andreas Syggros» Hospital in Athens, Greece, were collected. The selected monosensitized patients were divided into four groups of contact allergens: Formaldehyde 2%, KATHON 0.02%, thimerosal 0.1%, and MDBGN 0.5%; information was also collected for an extended MOAHLFA (Male- Occupational-Atopic-Hand-Leg-Face-Age) index [4]. To investigate the relationship between the allergen group and occupational-related ACD characteristics, the multiple correspondence analysis (MCA) and the categorical principal components

analysis (CATPCA) were applied, which are machine learning approaches [5]. The entire statistical analysis was implemented in IBM SPSS v.28.

### Results

MCA analysis revealed interesting relationships among several patients' characteristics. Strong associations were found among allergen group - age group, atopic dermatitis - family atopy history, and occupation class - gender- clinical characteristics (Fig. 1A). The first dimension was mainly explained by atopic dermatitis (0.463) and family atopy history (0.460), followed by occupation class (0.358). In the second dimension, the variable with the greatest contribution was the allergen group (0.481). Overall, the model explains 68.831% of the total variability (first dimension: 35.679%,

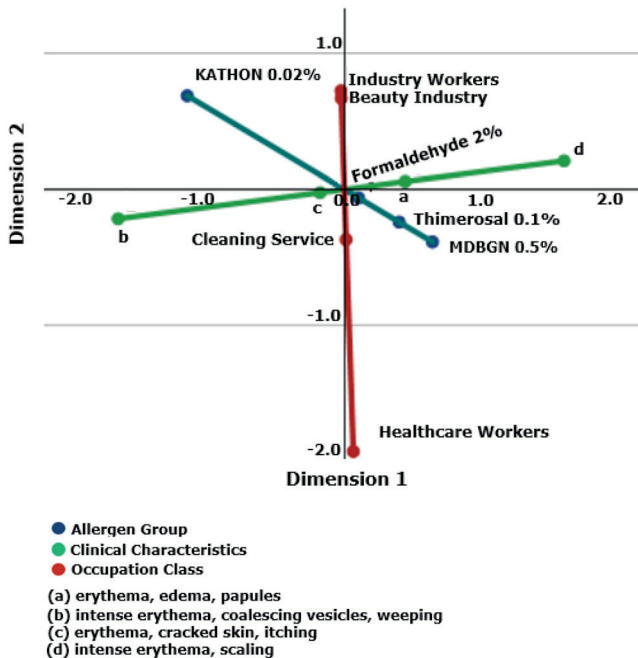


**Figure 3.** Categorical principal components analysis of the patients' characteristics in the total patient cohort (N=800). The analysis was performed for the following patients' features: allergen group (Formaldehyde 2%, KATHON 0.02%, Thimerosal 0.1%, MDBGN 0.5%), occupation class (cleaning service, healthcare workers, industry workers, beauty industry) and clinical characteristics (erythema, edema, papules, coalescing vesicles, weeping, cracked skin, itching, scaling). The cosine of the angle between two vector lines represents the correlation coefficient between the categorical variables. An angle close to zero indicates a high correlation between the variables, while a 180° angle indicates an inverse relationship. A 90° angle indicates that the variables are not related. The proximity between points (centroids) represents the association between the categories of the variables.

second dimension: 33.152%). In the model simplified version (Fig. 1B), atopic dermatitis was found to be positively related to occupation class, age group, and allergen group. In this case, the first dimension was principally explained by occupation class (0.707), followed by gender (0.524), while the second dimension, as previous, by the allergen group (0.590). Overall, the model explains 72.346% of the total variability (first dimension: 37.192%, second dimension: 35.154%).

Additional correlations were found between allergen groups and the affected body sites attributed to occupational-related ACD in the following descending order: hand > head > trunk > neck > leg (Fig. 2A). Strong

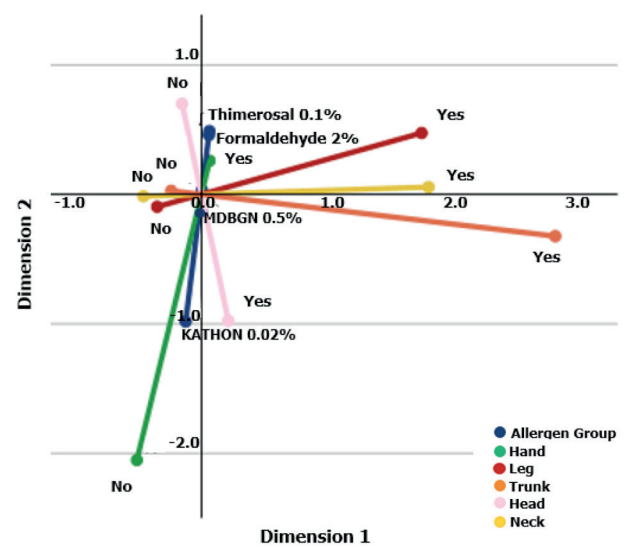


**Figure 4.** Categorical principal components analysis of the allergic contact dermatitis by anatomical regions in the total patient cohort (N=800). The analysis was performed for the following patients' features: allergen group (Formaldehyde 2%, KATHON 0.02%, Thimerosal 0.1%, MDBGN 0.5%) and anatomical regions (hand dermatitis, leg dermatitis, trunk dermatitis, head dermatitis, neck dermatitis). The cosine of the angle between two vector lines represents the correlation coefficient between the categorical variables. An angle close to zero indicates a high correlation between the variables, while a 180° angle indicates an inverse relationship. A 90° angle indicates that the variables are not related. The proximity between points (centroids) represents the association between the categories of the variables.

associations were found among hand - head, trunk - neck - leg, while leg was found to be independent of head dermatitis. Overall, the model explains 62.423% of the total variability (first dimension: 35.905%, second dimension: 26.518%). In terms of ICDRG clinical evaluation, the allergen group was most strongly linked with ICDRG 48h and then with ICDRG 72h (Fig. 2B). The first dimension was explained by allergen group (0.827), followed by ICDRG 72h (0.804) and ICDRG 48h (0.751), while the second dimension principally by ICDRG 72h (0.687). Overall, the model explains 87.163% of the total variability (first dimension: 59.399%, second dimension: 27.764%).

Joint representations of CATPCA revealed interesting correlations among patients' characteristics. In the first CATPCA model (Fig. 3), strong associations were found between allergen group - occupation class and allergen group - clinical

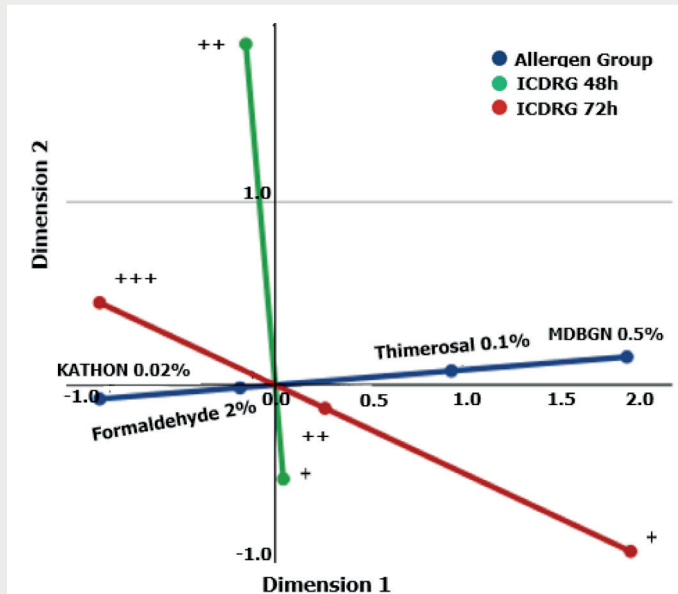


**Figure 5.** Categorical principal components analysis of allergic reaction severity in the total patient cohort (N=800). The clinical evaluation was based on the International Contact Dermatitis Research Group (ICDRG) criteria at 48h and 72h. The analysis was performed for the following patients' features: allergen group (Formaldehyde 2%, KATHON 0.02%, Thimerosal 0.1%, MDBGN 0.5%) and ICDRG evaluation (negative reaction, weak positive reaction (+), strong positive reaction (++) and extreme positive reaction (+++)). The cosine of the angle between two vector lines represents the correlation coefficient between the categorical variables. An angle close to zero indicates a high correlation between the variables, while a 180° angle indicates an inverse relationship. A 90° angle indicates that the variables are not related. The proximity between points (centroids) represents the association between the categories of the variables.

characteristics. Conversely, occupation class and clinical characteristics were not found to be strongly related. Industry and beauty industry workers were found to follow similar sensitization patterns and be primarily sensitized to formaldehyde 2%, followed by KATHON 0.02%, thimerosal 0.1%, and MDBGN 0.5%. Cleaning service and healthcare workers were found to be reversely sensitized to formaldehyde 2%, thimerosal 0.1%, and MDBGN 0.5%, with a stronger linkage to formaldehyde 2% and MDBGN 0.5%, respectively. Moreover, intense erythema/coalescing vesicles/weeping were observed mainly in KATHON patients, erythema/cracked skin/itching in formaldehyde patients, as well as erythema/edema/papules in thimerosal and MDBGN patients. This model explains 78.120% of the total variability (first dimension: 41.827%, second dimension: 36.293%).

Additional correlations were found between allergen group and the anatomical regions in the following descending order: hand > head > leg > neck > trunk (Fig. 4). Strong associations were found among hand - head, and trunk - neck - leg, while leg was found to be independent of head dermatitis. Thimerosal and formaldehyde patients seemed to develop occupational-related ACD primarily in hand, followed by head, leg, neck, and trunk, while MDBGN patients in hand, followed by head, neck and leg. Only in KATHON patients the most frequent affected body site is head, followed by hand. This model explains 71.852% of the total variability (first dimension: 39.782%, second dimension: 32.070%).

Regarding ICDRG clinical evaluation, allergen group was found to be positively correlated with ICDRG 72h, but not related to ICDRG 48h (Fig. 5). Scores of ICDRG 72h clinical evaluation, following a pattern of increasing allergic reaction severity, found to be significantly higher in patients monosensitized to KATHON 0.02% and formaldehyde 2% than thimerosal 0.1% and MDBGN 0.5%. This model explains 89.393% of the total variability (first dimension: 52.259%, second dimension: 37.134%).

## Conclusions

Significant relationships were identified between the allergen group and various manifestations of dermatitis. The utilization of machine learning techniques facilitated the discernment of meaningful patterns in the data.

## References

- Bauer A, Pesonen M, Brans R, Caroppo F, *et al.* Occupational contact allergy: The European perspective—Analysis of patch test data from ESSCA between 2011 and 2020. *Contact Dermatitis* 2023;88(4):263–74. doi: 10.1111/cod.14280
- Schwensen FJ, Friis FU, Menné T, Flyvholm M, Johansen DJ. Contact allergy to preservatives in patients with occupational contact dermatitis and exposure analysis of preservatives in registered chemical products for occupational use. *Int Arch Occup Environ Health* 2017;90(4):319–33. doi: 10.1007/s00420-017-1203-5. Sasseville D.
- Hypersensitivity to preservatives. *Dermatol Ther* 2004;17(3):251–63. doi: 10.1111/j.1396 0296.2004.04028.x.
- Frosch JP, Kugler K. In: Johansen DJ, Frosch JP, Lepoittevin PJ, eds. *Contact Dermatitis*. 5th ed. New York, CT: Springer; 2010:831–840.
- Shai S, Shai BD. *Understanding Machine Learning: From Theory to Algorithms*. 1st ed. New York, CT: Cambridge University Press; 2014.

## Prolonged Infusion of Antibiotics in Critically Ill Patients: Dosage Regimens Based on Simulations for Meropenem and Tobramycin

Kelly Papadaki, Vangelis D. Karalis

Department of Pharmacy School of Health Sciences, National and Kapodistrian University of Athens Panepistimiopolis, Zografou, 15784, Athens, Greece

\*Corresponding author: Vangelis D. Karalis, vkaralis@pharm.uoa.gr

### Introduction

Prolonged infusion antibiotics involve administering antibiotics over an extended period, typically several hours, in contrast to traditional bolus dosing [1,2]. The latter method allows for the maintenance of more consistent drug levels in the blood and sustained therapeutic concentrations of antibiotics. The need for prolonged infusion of certain drugs, including antibiotics like meropenem, is based on pharmacokinetic and pharmacodynamic considerations. Prolonged infusion can optimize the therapeutic effects of the medication in certain difficult clinical situations. The objective of this study was to investigate prolonged infusion dosage regimens for two commonly used antibiotics in critically ill patients: meropenem and tobramycin.

### Methodology

The population pharmacokinetic models, along with the parameter estimates and significant covariates such as creatinine clearance for meropenem and tobramycin, were obtained from literature-validated models [3,4]. In the simulation studies, various levels of variabilities and covariate values, such as renal deficiency, were explored. Simulations were performed in Simulx® (Monolix 2023R1TM, Simulation Plus). The conditions of prolonged infusion were simulated and compared with the official recommendations quoted in the summary of product characteristics for each drug. For meropenem, this refers to a 5-minute infusion, while for tobramycin, the infusion time is set at 1 hour. The simulated prolonged infusion profiles for meropenem were set at 30 minutes and 3 hours, while for tobramycin, an infusion regimen of 3 hours was considered. For meropenem, the administered dosage regimens explored were 500 mg TID and 1000 mg TID. In the case of tobramycin, the dosage scheme was 80 mg TID. Two patient populations were generated; the first refers to patients with normal renal function (mean GFR

100 ml/min, with standard deviation of 12.5 ml/min, assuming normal distribution). The patient renal function was taken from a critically ill pool of patients [5].

### Results

For meropenem, the patient population exhibited a volume of distribution of 54.95 L, with clearance initiating at 3.27 L/hour, including a positive contribution from glomerular filtration rate. Accurate dosing regimens for meropenem were determined which were found suitable for patients with moderate to severe renal impairment. To characterize the kinetics of tobramycin, an one-compartment model was used with a linear relationship between drug clearance and creatinine clearance (with a proportionality constant of 0.059 mL/min), and a linear relationship between the volume of distribution and body weight. The volume of distribution and clearance estimates were 30 L and 80 ml/min, respectively.

Figure 1 illustrates the administration of meropenem (500 mg 1x3) under the conventional administration scheme (5 min infusion) and the two prolonged infusion scenarios (30 min and 3 h)

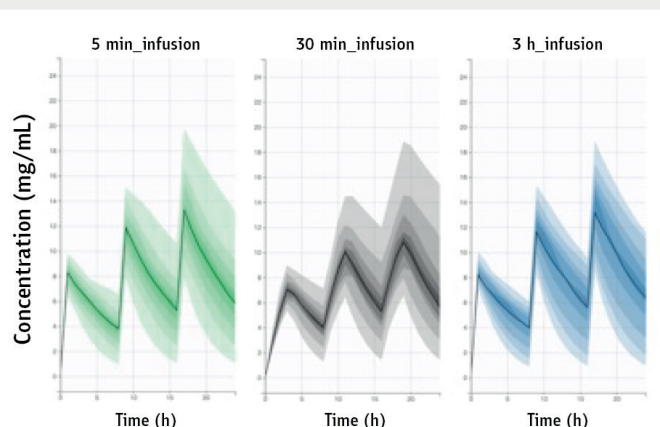
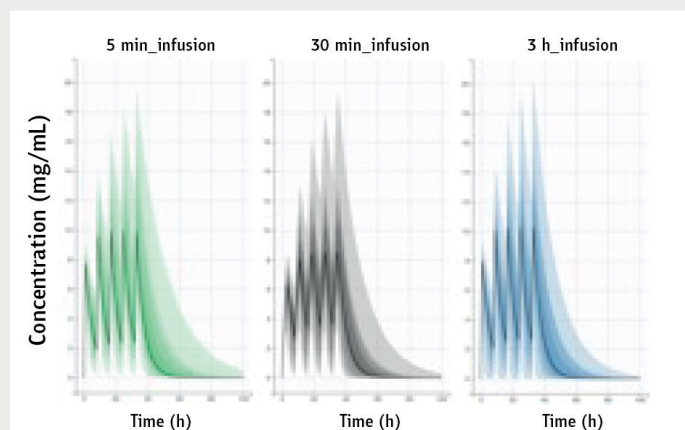


Figure 1. Meropenem levels under the three simulated scenarios of IV infusion (500 mg TID): 5 min, 30 min, 3 h.



Similar simulations were performed for the meropenem administration of 1000 mg TID, in patients with normal renal function (Figure 2).



**Figure 2.** Meropenem levels, in patients with normal renal function, under the three simulated scenarios of IV infusion (1000 mg TID): 5 min, 30 min, 3 h.

The conditions of renally impaired, critically ill patients in an ICU are depicted in Figure 3. The administration schedule assumed a dosage of 1000 mg TID.

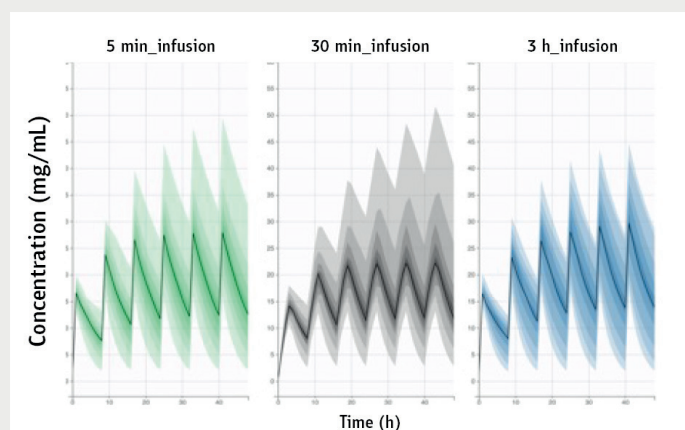


**Figure 3.** Meropenem levels, in critically ill patients, under the three simulated scenarios of IV infusion (1000 mg TID): 5 min, 30 min, 3 h.

Figure 4 illustrates the difference in the plasma levels, between conventional and prolonged infusion of tobramycin. The latter involves an administration schedule of 80 mg TID for critically ill patients, either through a 1-hour or 3-hour infusion. The administration schedule for tobramycin refers to 80 mg TID.

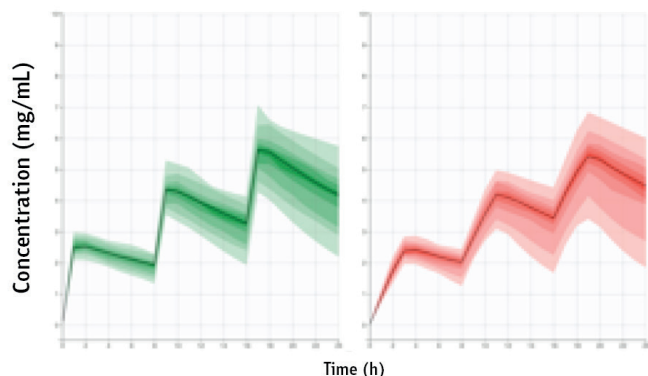


**Figure 4.** Tobramycin levels, in critically ill patients: 1h infusion (left panel), 3 h infusion (right panel).

## Conclusions

The administration of both drugs, meropenem and tobramycin, through continuous infusion has been shown to significantly increase the likelihood of achieving the pharmacokinetic target compared to the standard administration schedule. Prolonged infusion of certain medications, like antibiotics, offers advantages such as optimized pharmacokinetics, enhanced antibacterial activity (especially for time-dependent killing antibiotics), reduced development of bacterial resistance, improved tissue penetration, potentially lower toxicity, and better patient tolerance. The decision to use prolonged infusion depends on factors like the specific medication, infection type, and patient characteristics.

## References

- Gatti M, Pea F. Continuous versus intermittent infusion of antibiotics in Gram-negative multidrug-resistant infections. *Curr Opin Infect Dis.* 2021 Dec 1;34(6):737-747. doi: 10.1097/QCO.0000000000000755.
- Campion M, Scully G. Antibiotic. *J Intensive Care Med.* 2018;33(12):647-655.
- Murínová I, Švidrnoch M, Gucký T, Řezáč D, Hlaváč J, Slanař O, Šíma M. Meropenem population pharmacokinetics and model-based dosing optimisation in patients with serious bacterial infection. *Eur J Hosp Pharm.* 2022 Oct 28;ejhpharm-2022-003535. doi: 10.1136/ejhpharm-2022-003535.
- Aarons L, Vozeh S, Wenk M, Weiss P, Follath F. Population pharmacokinetics of tobramycin. *Br J Clin Pharmacol.* 1989 Sep;28(3):305-14. doi: 10.1111/j.1365-2125.1989.tb05431.x.
- Markantonis SL, Markou N, Karagkounis A, Koutrafouris D, Stefanatou H, Kousovista R, Karalis V. The Pharmacokinetics of Levetiracetam in Critically Ill Adult Patients: An Intensive Care Unit Clinical Study. *Appl. Sci. (Basel)* 2022, 12 (3), 1208. <https://doi.org/10.3390/app12031208>

## Machine Learning and Modeling Approaches for the Analysis of Antiepileptic Plasma Levels

Anastasia Tsyplakova<sup>1</sup>, Ivana Damnjanović<sup>2</sup>, Nikola Stefanović<sup>2</sup>, Tatjana Tošić<sup>3</sup>, Aleksandra Catić-Đorđević<sup>2</sup>, Vangelis Karalis<sup>1</sup>

<sup>1</sup>Department of Pharmacy, National and Kapodistrian University of Athens, 15784, Athens, Greece

<sup>2</sup>Department of Pharmacy, Faculty of Medicine, University of Nis, Nis, Serbia

<sup>3</sup>Clinic of Pediatric Internal Medicine, Department of Pediatric Neurology, University Clinical Center of Nis, Nis, Serbia

Presenter: Anastasia Tsyplakova (nastia31@windowslive.com)

Corresponding author: Vangelis D. Karalis. (Department of Pharmacy, School of Health Sciences, National and Kapodistrian University of Athens, 15784 Athens, Greece, vkaralis@pharm.uoa.gr)

### Introduction

The aim of this study is to describe the pharmacokinetics of valproic acid (VA), lamotrigine (LTG), and levetiracetam (LEV) in a pediatric population through the application of non-linear mixed effects modeling (PopPK). In addition, machine learning algorithms (ML) were employed to uncover potential relationships between the plasma concentrations of the three drugs and patient characteristics. Furthermore, the ML algorithms were utilized to construct a predictive model for the occurrence of seizures.

### Methods

The study comprised 71 pediatric patients of both sexes, aged 2-18 years, undergoing combined antiepileptic treatment with one of the following combinations: VA/LTG, VA/LEV, and LTG/LEV. Separate PopPK models were developed for VA, LTG, and LEV. Three ML approaches were applied based on estimated pharmacokinetic parameters and patient characteristics: mainstream component analysis, mixed data analysis, and random forest analysis.

### Results

The results from PopPK modeling have shown that the pharmacokinetics of Lev, LTG and VA are best described by an one-compartment model with first-order absorption and elim-

ination. According to PopPK analysis and analysis by ML methods, children's weight appeared to be negatively related to LTG, LEV and VA levels. Co - administration of LTG and VA has shown to lead to an increase in LTG levels, while the increase in the daily dose of VA was found to increase the purification of the drug. The predictive performance and robustness of the model were confirmed by the relevant predicted versus observed concentration plot (Figure 1) and the individual model predictions overlaid with the observations (Figure 2).

As for the predictive model of seizures, it appeared to have high prediction capacity and it has been observed that the appearance of crises contributes more to the levels of antiepileptic drugs followed by age and body weight.

### Conclusions

The application of population pharmacokinetics and machine learning models represents crucial tools for enhancing pharmacotherapy in pediatric epilepsy.

### References

- Lebedev G, Fartushnyi E, Fartushnyi I, *et al.* Technology of Supporting Medical Decision Making Using Evidence-Based Medicine and Artificial Intelligence. *Procedia Comput Sci* 2020; 176: 1703-1712.
- Oliva CF, Gangi G, Marino S, *et al.* Single and in combination antiepileptic drug therapy in children with epilepsy: how to use it. *AIMS Medical Science* 2021; 8: 138-146

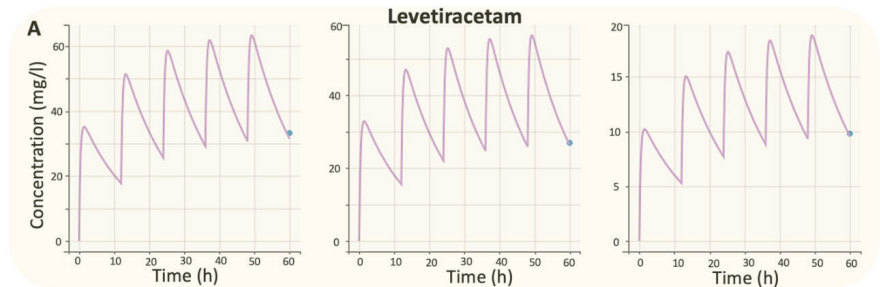
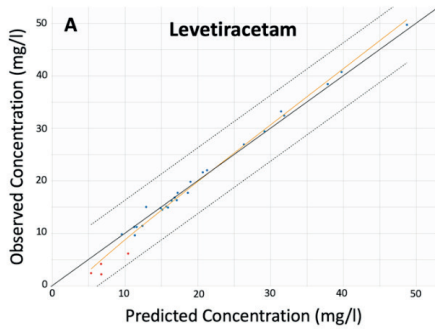
### A. LEVETIRACETAM

#### Population PK analysis

- $V/F = 25.01 \cdot \exp(BW/26.7) \cdot \exp(n_V)$
- $Cl/F = 1.51 \cdot \exp(0.75 \cdot (BW/26.7)) \cdot \exp(n_{Cl})$

#### Pop PK and Principal component analysis (PCA)

BW ↑ ↑ V, Cl ↔ BW ↓ LEV conc.



### B. LAMOTRIGINE

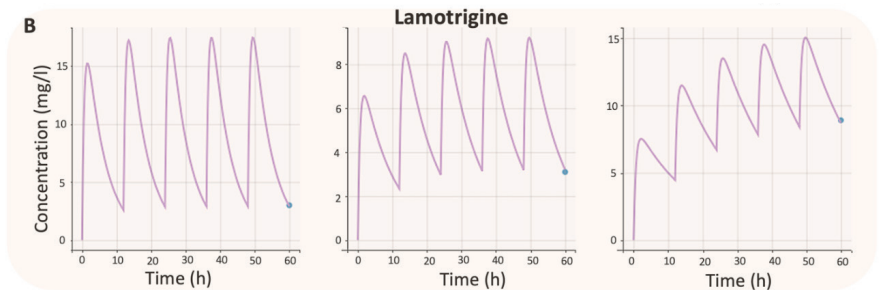
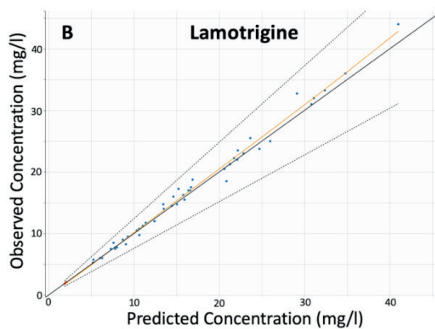
#### Population PK analysis

- $V/F = 5.15 \cdot \exp(2.83 \cdot BW/39.5) \cdot \exp(n_V)$
- $Cl/F = 0.15 \cdot \exp(0.0056 \cdot \text{daily dose}) \cdot \exp[(-0.61) \cdot 1_{\text{comed. with VA}}] \cdot \exp(n_{Cl})$

#### Pop PK and Principal component analysis (PCA)

1. BW ↑ ↑ V ↔ BW ↓ LG conc.

2. comed.VA & LG ↑ ↓ Cl ↔ LG conc. ↑ ↑ VA και LG conc. ↓ ↓ LEV conc.



### C. VALPROIC ACID

#### Population PK analysis

- $V/F = 15.61 \cdot \exp(BW/32) \cdot \exp(0.07 \cdot \text{age}) \cdot \exp(n_V)$
- $Cl/F = 0.12 \cdot \exp(0.0012 \cdot \text{daily dose}) \cdot \exp(n_{Cl})$

#### Pop PK and Principal component analysis (PCA)

BW, age ↑ ↑ V ↔ BW, age ↓ VA συγκέντρωση

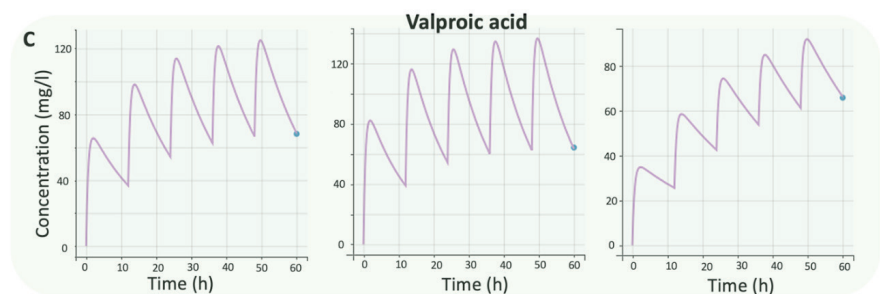
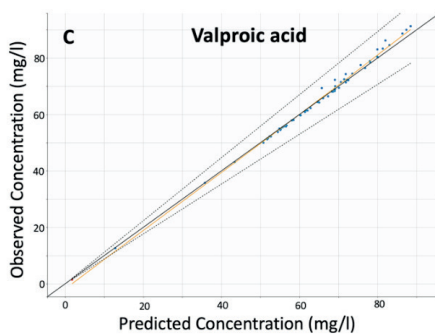


**Figure 1.** Individual predicted versus observed concentration data for the models of the three drugs: (A) levetiracetam, (B) lamotrigine, and (C) valproic acid.

**Figure 2.** Individual fittings to the experimental concentration–time data of the three drugs: (A) levetiracetam, (B) lamotrigine, and (C) valproic acid. Due to space limitations, three random subjects were chosen for each drug.

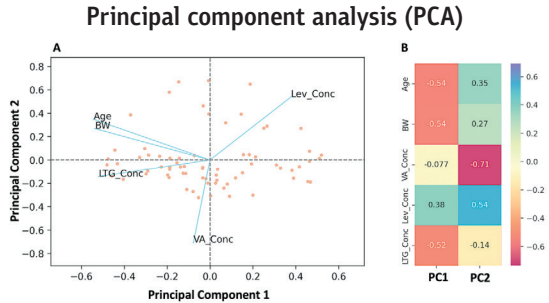


**Figure 3.** PCA of the plasma levels of the three antiepileptic drugs, age, and BW. **(A)** Biplot of the two PC showing the individual scores and the loadings (blue lines) of the pharmacokinetic parameters. **(B)** Loading values for the two initial PCs. Lev\_Conc, levetiracetam concentration; LTG\_Conc, lamotrigine concentration; PC, principal components; PCA, principal component analysis; VA\_Conc, valproic acid concentration.

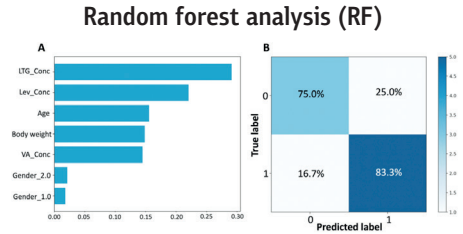


**Figure 4.** Variable importance scores **(A)** and confusion matrix **(B)**, from the RF analysis, predicting the existence or not of epileptic activity. The features parameters were levetiracetam concentration (Lev\_Conc), valproic acid concentration (VA\_Conc), lamotrigine concentration (LTG\_Conc), gender (1.0 for boys, 2.0 or girls), and BW.

## ΠΡΟΣΔΙΟΡΙΣΜΟΣ ΤΟΥ ΜΕΓΕΘΟΥΣ ΤΩΝ ΣΩΜΑΤΙΔΙΩΝ ΤΩΝ ΔΡΑΣΤΙΚΩΝ ΟΥΣΙΩΝ ΣΤΗΝ ΚΡΕΜΑ TRAVOCORT® ΜΕ ΤΗ ΧΡΗΣΗ ΦΑΣΜΑΤΟΣΚΟΠΙΑΣ MICRO-RAMAN

Μιχαήλ Λυκούρας<sup>1</sup>, Μαλβίνα Όρκουλα<sup>2</sup>, Χρίστος Κοντογιάννης<sup>1,2\*</sup>

<sup>1</sup>Ινστιτούτο Επιστημών Χημικής Μηχανικής, ΙΤΕ, Πάτρα, Ελλάδα

<sup>2</sup>Τμήμα Φαρμακευτικής, Πανεπιστήμιο Πατρών, Πάτρα, Ελλάδα

\*Υπεύθυνος Συγγραφέας: Χρίστος Κοντογιάννης, +30 2610 962328, kontoyan@upatras.gr

Η κρέμα Travocort® περιέχει τις δραστικές ουσίες Νιτρική Ισοκοναζόλη και Βαλερική Διφθοριοκορτολόνη σε συγκεντρώσεις 1% w/w και 0.1% w/w, αντίστοιχα και χρησιμοποιείται τοπικά για την αντιμετώπιση εκζεματικών και φλεγμονωδών παθήσεων του δέρματος [1]. Αποτελεί ένα γαλάκτωμα ο/w, στο οποίο και οι δύο δραστικές ουσίες είναι διεσπαρμένες εντός σταγονιδίων που σχηματίζονται στην ελαιώδη φάση. Ο προσδιορισμός του μεγέθους των σωματιδίων των δραστικών ουσιών κατά την ανάπτυξη των κρεμών είναι μείζονος σημασίας, καθώς οι διαφορές στο μέγεθός τους είναι πιθανόν να επηρεάσουν το ρυθμό απορρόφησης και τη διαπερατότητα τους από το δέρμα. Οποιαδήποτε μεταβολή αυτών των παραμέτρων μπορεί να επιφέρει σημαντικές αλλαγές στην αποτελεσματικότητα και στην ασφάλεια των κρεμών [2]. Για τη μέτρηση του μεγέθους των σωματιδίων των δραστικών ουσιών έχουν αναπτυχθεί διάφορες τεχνικές, όπως η οπτική μικροσκοπία φωτεινού πεδίου (Bright-Field Optical Microscopy), η οπτική μικροσκοπία πολωμένου φωτός (Polarized Light Optical Microscopy), η δυναμική σκέδαση φωτός (Dynamic Light Scattering) και η σκέδαση δέσμης laser (Laser Diffraction) [3, 4]. Παρόλα αυτά, είναι πιθανό να προκύψουν πολλές προκλήσεις κατά την ανίχνευση των σωματιδίων των δραστικών ουσιών σε κρέμες με τη χρήση των τεχνικών αυτών.

### Στόχος

Στόχος της μελέτης αποτέλεσε η ανάπτυξη κατάλληλης μεθοδολογίας για τη διάκριση μεταξύ των σωματιδίων των δραστικών ουσιών Νιτρικής Ισοκοναζόλης και Βαλερικής Διφθοριοκορτολόνης στη φαρμακευτική κρέμα Travocort® και ο προσδιορισμός της κατανομής του μεγέθους των σωματιδίων κάθε δραστικής ουσίας ξεχωριστά.

### Μεθοδολογία

Για τη μέτρηση του μεγέθους των σωματιδίων των δραστικών ουσιών πραγματοποιήθηκε εφάπλωση μικρής ποσότητας των

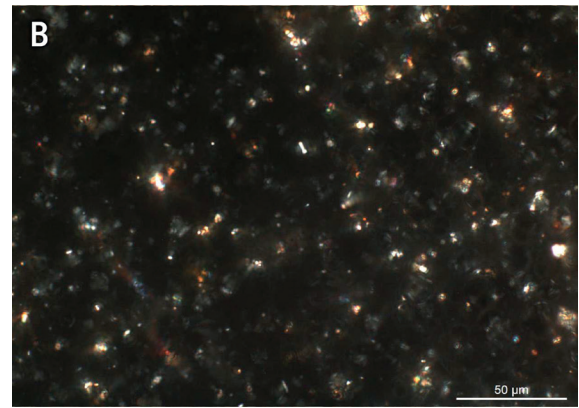
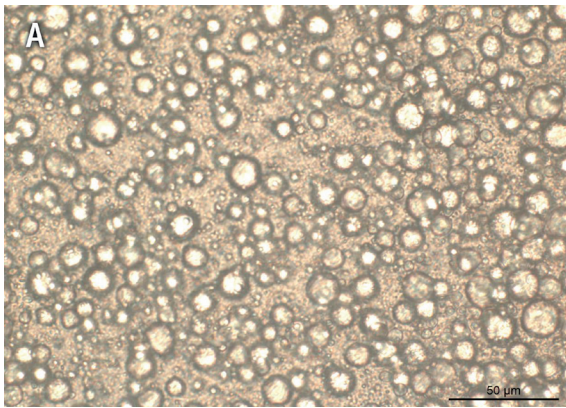
φαρμακευτικών κρεμών πάνω σε αντικειμενοφόρο πλάκα, χωρίς τη χρήση καλυπτρίδας. Χρησιμοποιήθηκε αρχικά οπτικό μικροσκόπιο (Leica DM 2500M) εξοπλισμένο με βιντεοκάμερα (Leica DFC420 C) και έγινε χρήση αντικειμενικού φακού 40x. Οι φωτογραφίες λήφθηκαν με λειτουργία διαπερατότητας, ενώ η εναλλαγή από τη λειτουργία φωτεινού πεδίου σε πολωμένου φωτός βοήθησε στη μελέτη των δραστικών ουσιών.

Για τον προσδιορισμό του μεγέθους των σωματιδίων κάθε δραστικής ουσίας ξεχωριστά, χρησιμοποιήθηκε η φασματοσκοπία micro-Raman (LabRam HR Evolution, Horiba Scientific). Επιλέχθηκε αντικειμενικός φακός 50x, ενώ εφαρμόστηκε μικροσκοπία πολωμένου φωτός. Για τη λήψη των φασμάτων Raman επιλέχθηκε πηγή ακτινοβολίας laser 532 nm με ονομαστική ισχύ 100 mW, η έντασή του οποίου ρυθμίστηκε στο 25% της ισχύος και το οπτικό φράγμα στα 600 gratings/mm (500 nm). Τα φάσματα καταγράφηκαν στην περιοχή 1500-1700  $\text{cm}^{-1}$ , με χρόνο έκθεσης τα 10 s, ενώ ήταν το αποτέλεσμα 1 επανάληψης. Ως υπόστρωμα χρησιμοποιήθηκε επιχρυσωμένο πλακίδιο υψηλής ανακλαστικότητας.

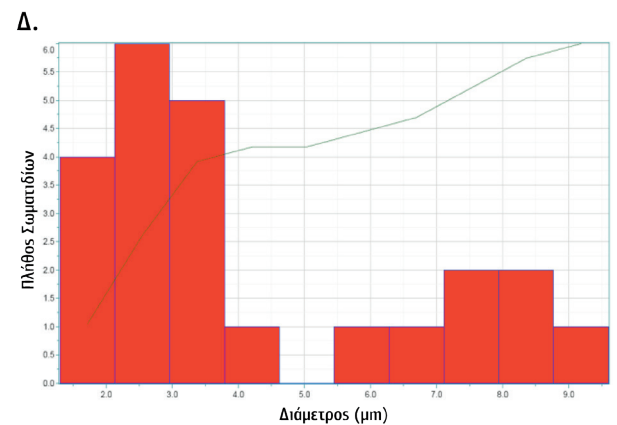
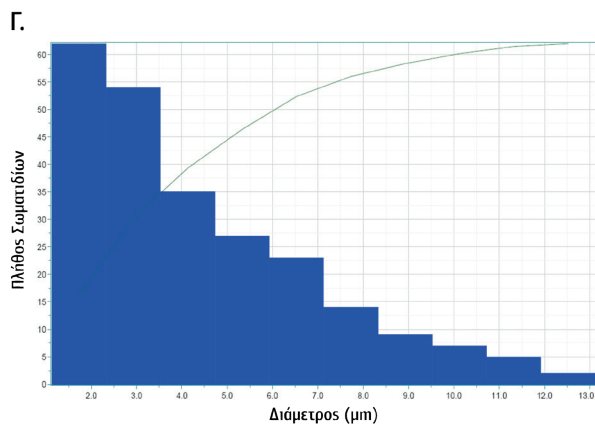
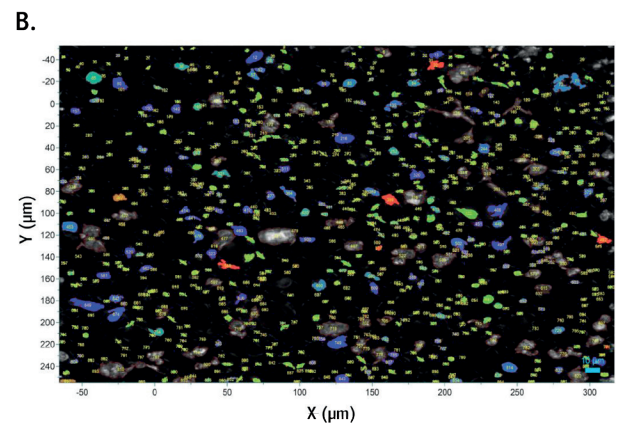
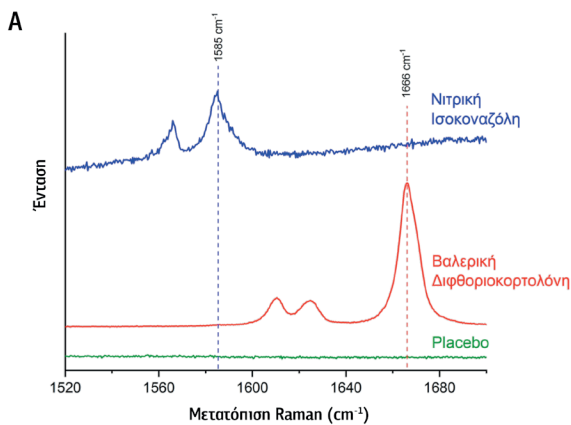
### Αποτελέσματα και Συζήτηση

Η ανίχνευση των σωματιδίων των δραστικών ουσιών σε κρέμα Travocort® δεν κατέστη εφικτή με την απλή οπτική μικροσκοπία φωτεινού πεδίου, καθώς παρατηρούνταν μόνο ελαιώδη σταγονίδια (Εικόνα 1A). Οι δραστικές ουσίες ήταν εγκλωβισμένες εντός των ελαιωδών σταγονιδίων και η παρατήρηση των κρυστάλλων των σωματιδίων τους πραγματοποιήθηκε με την εφαρμογή οπτικής μικροσκοπίας πολωμένου φωτός (Εικόνα 1B). Παρόλα αυτά, η χρήση της οπτικής μικροσκοπίας δεν ήταν σε θέση να διακρίνει μεταξύ των σωματιδίων των δύο δραστικών ουσιών.

Για το λόγο αυτό χρησιμοποιήθηκε η φασματοσκοπία micro-Raman, μέσω της οποίας οι δύο δραστικές ουσίες μπορούσαν να διακριθούν από τα φάσματα Raman τους. Πιο συγκεκριμένα, οι χαρακτηριστικές κορυφές της Νιτρικής



Εικόνα 1. Φωτογραφία του ίδιου πεδίου κρέμας Travocort® με (Α) οπτική μικροσκοπία φωτεινού πεδίου και (Β) οπτική μικροσκοπία πολωμένου φωτός.



Εικόνα 2. (Α) Φάσματα Raman των δύο δραστικών ουσιών και placebo, (Β) φωτογραφία των σωματιδίων με οπτική μικροσκοπία πολωμένου φωτός και ταυτοποίησή τους με φασματοσκοπία micro-Raman (μπλε σωματίδια: Νιτρική Ισοκυαναζόλη, κόκκινα σωματίδια: Βαλερική Διφθοριοκορτολόνη, πράσινα σωματίδια: placebo/θόρυβος), (Γ) ιστόγραμμα κατανομής μεγέθους σωματιδίων Νιτρικής Ισοκυαναζόλης και (Δ) ιστόγραμμα κατανομής μεγέθους σωματιδίων Βαλερικής Διφθοριοκορτολόνης

Ισοκοναζόλης ( $1585\text{ cm}^{-1}$ ) και της Βαλερικής Διφθοριοκορτολόνης ( $1666\text{ cm}^{-1}$ ) διαφοροποιούνταν επαρκώς μεταξύ τους, ενώ το Placebo δε διέθετε χαρακτηριστική κορυφή στη συγκεκριμένη φασματική περιοχή (Εικόνα 2Α). Ακολούθησε η αναγνώριση, με τη χρήση μικροσκοπίας πολωμένου φωτός, 864 σωματιδίων σε ένα σύνολο πεδίων της κρέμας Travocort®, των οποίων τα φάσματα Raman καταγράφηκαν και αναγνωρίστηκαν ως Νιτρική Ισοκοναζόλη (μπλε σωματίδια), Βαλερική Διφθοριοκορτολόνη (κόκκινα σωματίδια) ή ως Placebo/θόρυβος (πράσινα σωματίδια) (Εικόνα 2Β).

Στη συνέχεια με τη χρήση του λογισμικού ParticleFinder® (Horiba Scientific) [5] υπολογίστηκε το μέγεθος των σωματιδίων κάθε δραστικής ουσίας που αναγνωρίστηκαν και προσδιορίστηκαν οι κατανομές μεγέθους σωματιδίων των δύο δραστικών ουσιών (Εικόνα 2Γ και Εικόνα 2Δ). Ειδικότερα, το μέσο μέγεθος των σωματιδίων της δραστικής ουσίας Νιτρικής Ισοκοναζόλης βρέθηκε ίσο με  $4.3\ \mu\text{m}$  με τυπική απόκλιση  $2.6\ \mu\text{m}$ ,  $D_{10} = 1.5\ \mu\text{m}$ ,  $D_{50} = 3.6\ \mu\text{m}$ ,  $D_{90} = 8.4\ \mu\text{m}$  και μέγιστο μέγεθος ίσο με  $13.1\ \mu\text{m}$ , ενώ παρόμοια μεγέθη προσδιορίστηκαν και για τα σωματίδια της Βαλερικής Διφθοριοκορτολόνης (μέσο μέγεθος  $4.2\ \mu\text{m}$ , τυπική απόκλιση  $2.6\ \mu\text{m}$ ,  $D_{10} = 1.8\ \mu\text{m}$ ,  $D_{50} = 3.6\ \mu\text{m}$ ,  $D_{90} = 8.6\ \mu\text{m}$  και μέγιστο μέγεθος  $9.6\ \mu\text{m}$ ) (Πίνακας 1).

### Συμπεράσματα

Ο συνδυασμός της οπτικής μικροσκοπίας πολωμένου φωτός, της φασματοσκοπίας micro-Raman και του λογισμικού ParticleFinder™ οδήγησε στην ανάπτυξη κατάλληλης μεθοδολογίας για τον ταυτόχρονο προσδιορισμό των κατανομών των μεγεθών των σωματιδίων δύο δραστικών ουσιών σε φαρμακευτικές κρέμες.

**Πίνακας 1.** Προσδιορισμός κατανομών μεγέθους σωματιδίων Νιτρικής Ισοκοναζόλης και Βαλερικής Διφθοριοκορτολόνης σε κρέμα Travocort® με φασματοσκοπία micro-Raman και το λογισμικό ParticleFinder™

	Νιτρική Ισοκοναζόλη	Βαλερική Διφθοριοκορτολόνη
<b>Πλήθος Σωματιδίων που Μετρήθηκαν</b>	238	23
<b>Μέσο Μέγεθος (<math>\mu\text{m}</math>)</b>	4.3	4.2
<b>Τυπική Απόκλιση (<math>\mu\text{m}</math>)</b>	2.6	2.6
<b>Μέγιστο Μέγεθος (<math>\mu\text{m}</math>)</b>	13.1	9.6
<b>D10 (<math>\mu\text{m}</math>)</b>	1.5	1.8
<b>D50 (<math>\mu\text{m}</math>)</b>	3.6	3.6
<b>D90 (<math>\mu\text{m}</math>)</b>	8.4	8.6

### Βιβλιογραφικές Αναφορές

- [1] Havlickova, B.; Friedrich, M. The advantages of topical combination therapy in the treatment of inflammatory dermatomycoses. *Mycoses* 2008, 51(Suppl. 4), 16-26.
- [2] Bułaj, L.; Szulc-Musioł, B.; Siemiradzka, W.; Dolińska, B. Influence of Technological Parameters on the Size of Benzocaine Particles in Ointments Formulated on Selected Bases. *Appl. Sci.* 2023, 13(4), 2052.
- [3] Shekunov, B.Y.; Chattopadhyay, P.; Tong, H.H.Y.; Chow, A.H.L. Particle size analysis in pharmaceuticals: principles, methods and applications. *Pharm Res* 2007, 24(2), 203-227.
- [4] Osborne, D.W.; Dahl, K.; Parikh, H. Determination of Particle Size and Microstructure in Topical Pharmaceuticals. In Langley, N.; Michniak-Kohn, B.; Osborne, D.W. (Eds.). *The Role of Microstructure in Topical Drug Product Development*. AAPS Advances in the Pharmaceutical Sciences Series book series (AAPS, volume 36). Springer. 2019, pp. 89-106.
- [5] Horiba Scientific. Available online: [https://static.horiba.com/fileadmin/Horiba/Products/Scientific/Molecular\\_and\\_Microanalysis/SW\\_Particle\\_Finder/Particle\\_Finder\\_Brochure.pdf](https://static.horiba.com/fileadmin/Horiba/Products/Scientific/Molecular_and_Microanalysis/SW_Particle_Finder/Particle_Finder_Brochure.pdf)

## Development of novel plga nanospheres co-loaded with paclitaxel and losartan for the treatment of highly desmoplastic tumors

Andreas Mouikis<sup>a</sup>, Ioanna Aspioti<sup>a</sup>, Ligeri Papaioannou<sup>a</sup>, Maria Gazouli<sup>b</sup>, Konstantinos Dimas<sup>c</sup>,  
Konstantinos Avgoustakis<sup>a\*</sup>

<sup>a</sup>Department of Pharmacy, University of Patras, Patras GR-26504, Greece

<sup>b</sup>Laboratory of Biology, Medical School, National and Kapodistrian University of Athens, Athens GR-11527, Greece

<sup>c</sup>Laboratory of Pharmacology, Faculty of Medicine, University of Thessaly, Larissa GR-41500, Greece

\*Corresponding Author: Konstantinos Avgoustakis, 2610-962317, avgoust@upatras.gr

### Introduction

The nanomedicines in order to be effective in the case of solid tumors must be capable of penetrating the tumors, however, this is limited by the heterogeneous, hypovascular, and desmoplastic tumor microenvironment of many types of solid cancers. This structure significantly reduces the fraction of nanomedicines that reaches cancerous cells and represents a major reason for the failure of nanomedicines to improve therapeutic outcomes compared to conventional chemotherapy as well as for the low clinical translation rate of nanomedicines. For desmoplastic cancer tumors, anti-stromal strategies have been proposed aiming to enhance the penetration of medicines to the tumor parenchyma [1]. In this context, the long-term aim of this work is the synthesis and evaluation of a biomimetic and bioresponsive nanomedicine, integrating an anticancer agent (e.g., paclitaxel, PCT) and an agent that will reduce extracellular matrix and the associated physical barriers that normally hinder drug delivery (e.g., losartan LOS), for a more effective treatment of pancreatic cancer. Losartan, an antihypertensive agent that blocks angiotensin II receptor type 1, has shown promise for TME remodeling [2] and is currently under clinical investigation in combination with established chemotherapies for PDAC treatment [3]. In this communication, the results from formulation studies on nanospheres (NS) made of poly(lactide) (PLA) and poly(lactide-co-glycolide) (85:15) (PLGA) loaded with PCT and LOS are presented.

### Methodology

The NS were prepared through an emulsification and solvent evaporation process [4] and were characterized with regard to their morphology and size with transmission electron microscopy (TEM), their hydrodynamic diameter and ζ-potential

with dynamic light scattering (DLS) and their drug loading properties with HPLC. The colloidal stability of the NS was evaluated in the presence of electrolyte (NaCl) and in biorelevant media (cell culture media and human blood plasma). Drug release properties were determined in phosphate buffer pH 7.4, 37°C.

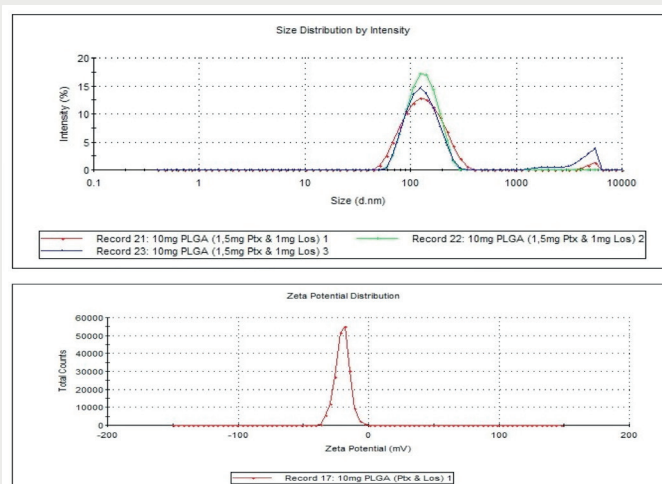


**Figure 1.** Hydrodynamic diameter and ζ-potential of PLGA-PCT-LOS nanospheres.

### Results

The hydrodynamic diameter and ζ-potential of PLGA-PCT NS were determined to be  $119 \pm 1.5$  nm and  $-42.8$  mV, respectively. Following LOS entrapment, the hydrodynamic diameter and ζ-potential of PLGA-PCT-LOS NS became  $156.9 \pm 3.4$  nm and  $-20.2$  mV, respectively (Figure 1). PLA-PCT NS exhibited a hydrodynamic diameter and a ζ-potential of  $107.3 \pm 1.5$  nm and  $-35.8$  mV, respectively, whereas PLA-PCT-LOS NS exhibited a hydrodynamic diameter and a ζ-potential of  $147.2 \pm 2.1$  nm and  $-19.8$  mV, respectively. PCT and LOS entrapment in the NS initially increased but then decreased



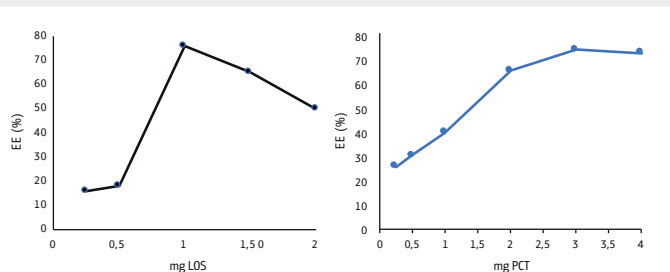


**Figure 2.** Entrapment efficiency (EE%) of LOS and PCT in the nanospheres as a function of drug feed.

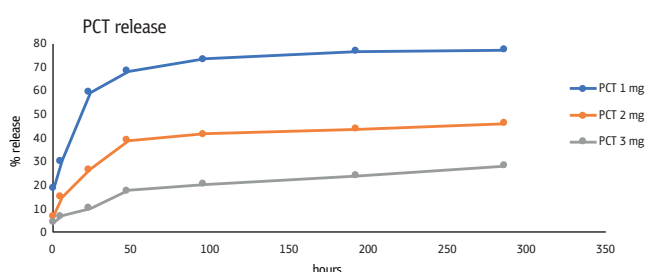


**Figure 3.** PCT release from PLGA nanospheres as a function of PCT loading.

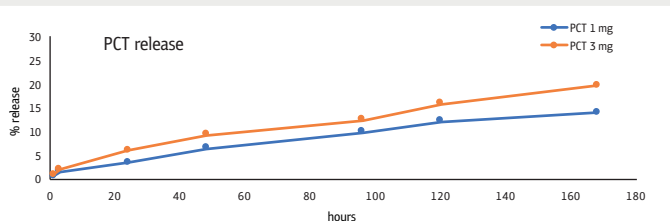


**Figure 4.** LOS release from PLGA nanospheres as a function of PCT loading.

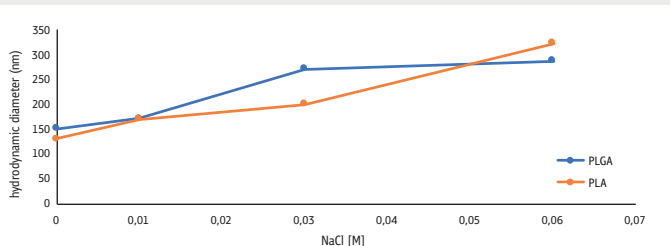


**Figure 5.** Hydrodynamic diameter of PLGA and PLA nanospheres change with increasing NaCl concentrations.

with an increase in drug feed (initial amount of drug added in the preparation), reaching a maximum at 3 mg/mL and 1 mg/mL feed, respectively (Figure 2). The amount of PCT loaded in the NS did not affect the efficiency of LOS entrapment in the NS. PCT release from the NS was sustained, with the rate of release decreasing as the PCT loading increased (Figure 3). Biphasic PCT release kinetics were observed with an initial phase of a relatively fast release, lasting up to 48 hours, followed by a second phase of very slow release (Figure 3). LOS release from the NS was very low, with less than 10% release at 48 hours (Figure 4), with the rate of release increasing as the PCT loading increased (Figure 4). The NS exhibited satisfactory stability in the presence of physiological concentrations of electrolyte (NaCl) but tended to aggregate at high electrolyte concentrations (Figure 5), and a similar behavior was observed in biorelevant media (cells culture media and blood plasma), indicating the need for protective surface functionalization of the nanospheres.

## Conclusion

The obtained results indicate that the synthesized NS have suitable in vitro properties for the intended application. Functionalization of the NS with membranes from pancreatic cancer cells is in progress.

## References

1. Minchinton, A. I. and Tannock, I. F. Drug penetration in solid tumours, *Nature Reviews Cancer*, 2006, 6, 583–592.
2. V. P. Chauhan *et al.*, Angiotensin inhibition enhances drug delivery and potentiates chemotherapy by decompressing tumour blood vessels, *Nat. Commun.*, 4, 2013.
3. J. E. Murphy *et al.*, Total Neoadjuvant Therapy With FOLFIRINOX in Combination With Losartan Followed by Chemoradiotherapy for Locally Advanced Pancreatic Cancer A Phase 2 Clinical Trial, *JAMA Oncol.*, 2019, 5, 1020–1027.
4. Mu, L. and Feng, S.S. A novel controlled release formulation for the anticancer drug paclitaxel (Taxol®): PLGA nanoparticles containing vitamin E TPGS, *J. Control Release*, 2003, 86, 33–48.

## Data mining in the design and development of liposomal anticancer drugs

Anastasios Nikolopoulos<sup>a</sup>, Nefeli Lagopati<sup>a\*</sup>, Natassa Pippa<sup>b</sup>, Vangelis D. Karalis<sup>b†</sup>

<sup>a</sup>Medical School, School of Health Sciences, National and Kapodistrian University of Athens, 11527, Athens, Greece

<sup>b</sup>Department of Pharmacy, School of Health Sciences, National and Kapodistrian University of Athens, 15701, Greece

### Introduction

Liposomes hold a pivotal role in nanomedicine, because of the presence of two different compartments; the aqueous and the lipidic, which allow for the trapping of both hydrophilic and hydrophobic molecules. This structure gives liposomes the advantage of improved pharmacokinetic qualities of the medicine they are encapsulating, decreased systemic toxicity, longer circulation durations, and targeted drug delivery in tumor areas. Meanwhile in the digital era, machine learning (ML) algorithms have played a critical role in improving predictions of biological, physical, chemical, and toxicological impacts, by uncovering patterns within datasets.

### Objective

This study aims to identify relationships and correlations among the physicochemical parameters of the liposomes, with a particular focus on size, zeta potential, polydispersity index (PDI), and encapsulation efficiency (EE). By collecting quantitative and qualitative data from PubMed between 2022 and 2023, analyzing them, and finally, extracting valuable information, this study seeks to uncover relationships and correlations among these parameters.

### Methodology

- The articles were collected from PubMed using the keywords: liposomes and cancer. The initial number of papers was 603, but after the exclusion criteria [e.g. not about an active pharmaceutical ingredient (API)] the number was finalized to 130, with 313 formulations. The data from the papers were categorized into qualitative (i.e. Liposome preparation technique) and quantitative [i.e. Mean Size (nm)].
- Python was chosen as the programming language for data analysis. Among the libraries that were implemented were: pandas, numpy, seaborn and sklearn, for data manipulation, numerical computations, data visualizations and ML algorithm implementation, respectively.

- The data files were transformed into python dataframes and data cleaning was followed. Each column was examined separately for their missing or NaN values. For the quantitative data, the NaN values were replaced with the mean of the column, after using descriptive statistics to examine the data. Then, a univariate and a bivariate analysis was conducted, as well as a correlation analysis and a hypothesis testing. Both qualitative and quantitative data were explored for hidden patterns using visualizations.
- The three ML techniques that were employed next were: the k-means clustering method, the agglomerative hierarchical clustering method, and the Principal Component Analysis (PCA) technique. For the first two, the results were evaluated with the silhouette score, while for the PCA the reconstruction error was computed.

### Results

- K-means clustering exhibited a higher evaluation score than the agglomerative clustering. The clustering suggests that the larger the mean size, the higher the PDI will be.
- Also, the EE decreases as the mean size increases (p-value<0.01). On the other hand, the EE appears to be rather high with mean sizes around 500–600 nm.
- The mean PDI, out of the four parameters of the quantitative data, shows a weaker correlation with the other three, according to the PCA.
- The biplot (Figure 1) also indicates a positive association between the EE and the zeta potential.
- Research is focused on breast cancer, with doxorubicin being the primary active substance, followed by docetaxel.
- The thin-film hydration process is the most often utilized method for producing liposome formulations and the ethanol injection method is second.
- In certain studies, the ethanol injection method outperformed the thin film hydration method in terms of EE (breast cancer, liver cancer, colorectal cancer, brain cancer, lung cancer, cervical cancer) (Figure 2).

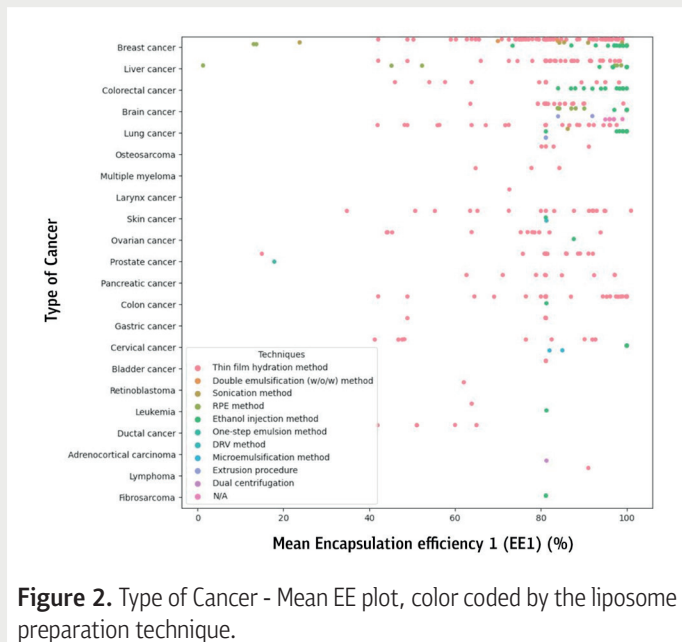


**Figure 2.** Type of Cancer - Mean EE plot, color coded by the liposome preparation technique.

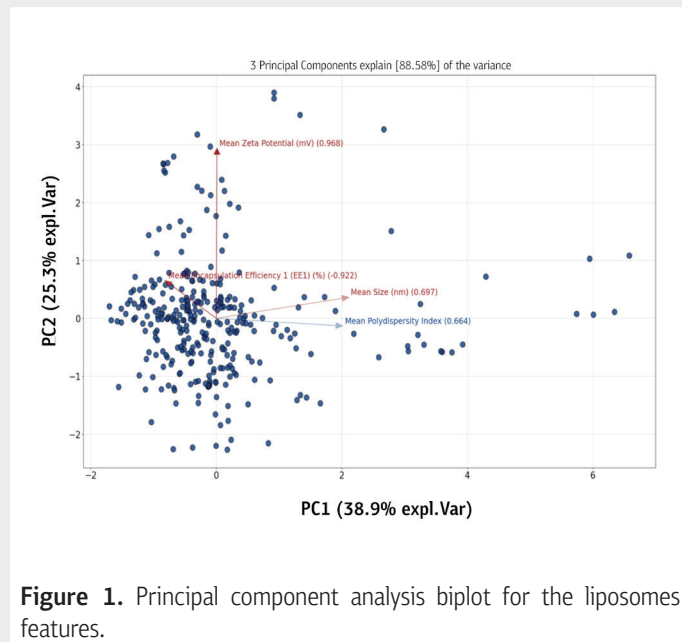


**Figure 1.** Principal component analysis biplot for the liposomes features.

## Conclusion

- This research represents a step toward a time when liposome-based medicines will be essential in the fight against cancer.
- With this information in hand, the formulation scientists can design and develop a liposomal nanomedicine with the desired physicochemical characteristics and added value to the therapeutic outcome.

- Given the findings and the significance of research in cancer therapy, studies should concentrate more on the physicochemical properties of liposomes.
- Considering the large number of APIs studied, it may be inferred that improving how the liposomes reach their goal with the encapsulated API is less important than focusing on a substance real therapeutic effects.

## Nose-to-Brain delivery of donepezil nasal films

Paraskevi Papakyriakopoulou<sup>1</sup>, Evangelos Balafas<sup>2</sup>, Gaia Colombo<sup>3</sup>, Dimitrios M. Rekkas<sup>4</sup>, Nikolaos Kostomitsopoulos<sup>2</sup>, Georgia Valsami<sup>1</sup>

<sup>1</sup>Department of Pharmacy, School of Health Sciences, NKUA, 15784, Greece

<sup>2</sup>Laboratory Animal Facility, Centre of Clinical, Experimental Surgery and Translational Research, BRFAA, 11527, Athens, Greece

<sup>3</sup>Department of Life Sciences and Biotechnology, University of Ferrara, 44121, Italy

CONTACT INFO: ppapakyri@pharm.uoa.gr, valsami@pharm.uoa.gr

### Introduction

Nasal administration has been demonstrated as an effective alternative for drug delivery to central nervous system (CNS). Donepezil Hydrochloride (DH) is a widely used acetylcholinesterase inhibitor for the management of Alzheimer's disease, able to cross the blood brain barrier after oral

administration. However, DH undergoes extensive first-pass metabolism, a fact that limits the amount of drug reaching the CNS. The purpose of the present study was the nose-to-brain delivery *in vivo* of DH, formulated in the recently developed HPMC-Me- $\beta$ -CD-PEG400 based polymeric nasal film characterized *in vitro/ex vivo*.

### Methodology

Eight-week-old mice were randomly divided in two groups, PO and IN, and each one received different treatment as described in Table 1:

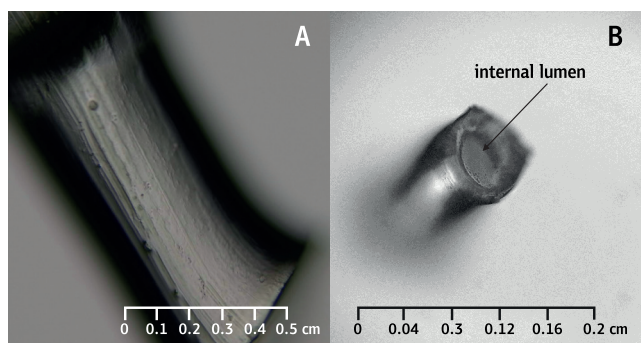
**Table 1.** Protocol of PK study

Mode of administration	Dose (mg/kg)	Time points (min)
Per os DH solution	10	15, 30, 45, 60, 120, 240, 360
Intranasal DH film	4	5, 10, 15, 30, 45, 60, 120

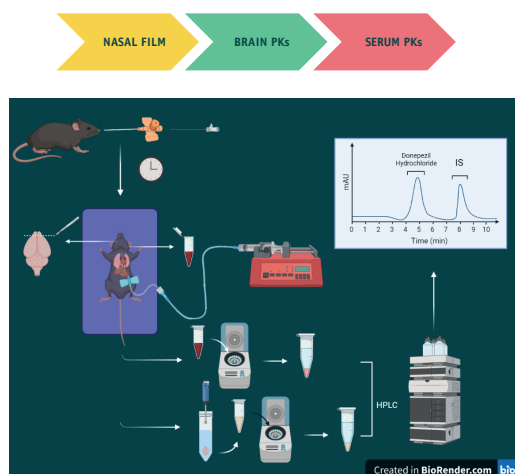
The intranasal dose was **2.5-times lower** than PO one, expecting to achieve satisfying drug levels taking advantage of NTB delivery [1-2]. **Sparse sampling non-compartmental analysis (NCA)** was performed for all *in vivo* data using Phoenix<sup>®</sup> 8.3 (Certara, Princeton, NJ, USA), to determine serum and brain PK parameters ( $AUC_{0-t}$ ,  $C_{max}$ ,  $AUC_{inf}$ ,  $t_{1/2}$ ). The relative IN bioavailability ( $F_{rel}$ ), as well as the Drug Targeting Efficiency Percentage (**DTE**) and NTB Direct Transport Percentage (**DTP**) indexes were calculated to evaluate the effectiveness of nasal delivery, assuming a linear PK of DH [3].

### Results

The NF administration resulted in **high DH brain levels**, even if a lower dose was given (Figure 2).  $C_{max}$  was achieved within **15 min** after NF positioning into the nasal cavity. Accordingly, DH serum profile demonstrated a faster and more extended systemic absorption after the nasal delivery of the



**Figure 1.** A) Lateral, B) upper top view of the cylindrical polymeric film. The black arrow indicates the internal lumen of the film shaped as a hollow cylinder (tube-shaped). The images were captured at 10x magnification, scale bar 1:15 (A), 1:50 (B).



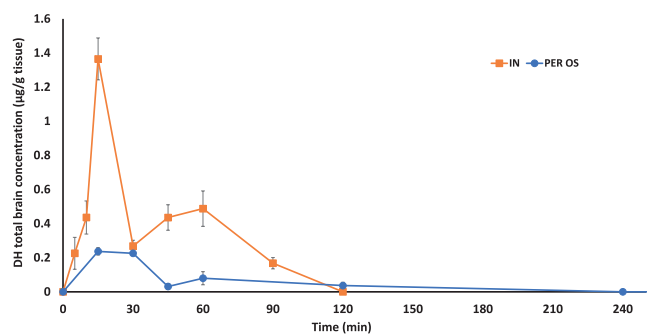


**Figure 2.** Total brain concentration-time profiles of DH administered intranasally, as nasal film (■) and orally, via gavage method (●). The data are presented as mean ± SE, n=3-7 for IN group, n=4-5 for PO group.

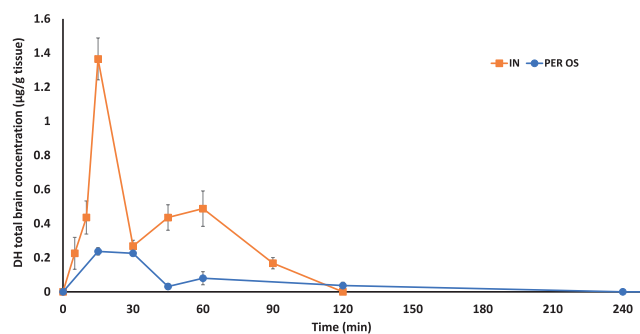


**Figure 3.** Serum concentration-time profiles of DH administered intranasally, as nasal film (■) and orally, via gavage method (●). The data are presented as mean ± SE, n=3-7 for IN group, n=5-6 for PO group.

drug (Figure 3). The  $F_{rel}$  in brain and serum prove the improvement of DH distribution either in brain or bloodstream. Furthermore, the DTE was higher than 100, equal to 184% identifying a more efficient brain targeting via nasal route. The value of DTP, equal to 45% indicates that a significant fraction of IN dose entered the brain directly via NTB, in addition to the amount reaches the tissue through the systematic circulation (Table 2).

**Table 2.** Comparative PK Results

	Brain	Serum
$C_{max}$ IN/ $C_{max}$ PO	5.6	3.9
$AUC_{0-t}$ IN/ $AUC_{0-t}$ PO	2.8	1.5
$F_{rel}$	7.55	3.95

## Conclusions

The PK parameters estimated by NCA sparse data methodology illustrated the effectiveness of IN administration ei-

ther in brain targeting or to reach the bloodstream. Higher drug levels were achieved at both sites, compared to those after oral delivery. Thus, nasal films manage to increase the relative bioavailability in brain and serum after the administration of 2.5 times lower dose, taking advantage of the NTB delivery and the avoidance of first-pass effect.

**Acknowledgments:** P.P. would like to acknowledge the Hellenic Foundation for Research & Innovation (H.F.R.I.), for the funding of the research under the 3rd Call for HFRI PhD Fellowships (Fellowship Number: 5353).

## References

1. Dhuria, S.V., *et al.* (2010) Intranasal delivery to the central nervous system: mechanisms and experimental considerations. *J Pharm Sci*, 99(4):1654-73.
2. Laffleur, F., & Bauer, B. (2021) Progress in nasal drug delivery systems. *Int. J. Pharm.*, 607, 120994.
3. Szpunar, G.J., *et al.* (1987) Pharmacokinetics of flurbiprofen in man. I. Area/dose relationships. *Biopharm. Drug Dispos.* 8, 273-283.

## A modified solvent processed feed HME process for the preparation of drug/amino acid CAMS

**Ioannis Partheniadis, Ioannis Nikolakakis**

Laboratory of Pharmaceutical Technology, School of Pharmacy, Faculty of Health Sciences, Aristotle University of Thessaloniki, 54124 Greece.

Email: ioanpart@pharm.auth.gr (I.P.) and yannikos@pharm.auth.gr (I.N.)

### Introduction

Oral administration is preferred for solid pharmaceuticals. However, most of the new synthetic drugs are poorly soluble categorized as BCS Class II or IV. To address this, researchers investigate new methods like CAMS fabricated by different methods. Amino acids (AAs) are preferred as co-formers for CAMS due to their low-molecular weight, thus enabling high drug loadings. In this work a modified hot-melt (HME) extrusion method was applied to develop co-amorphous Griseofulvin/L-leucine solid dispersions with vastly improved solubility and drug release performance compared to crystalline drug, and which during dissolution testing sustained supersaturation levels for at least 24 h. The modified method bypasses the problems of thermal instability of the drug and AA [1] by making feasible extrusion at temperatures well below their decomposition temperature. The following steps were followed for the preparation of stable CAMS: i) wet mixing of the drug/AA powder blend with suitable solvent to give a thick slurry, ii) drying and sieving to produce agglomerates, (iii) feeding into extruder.

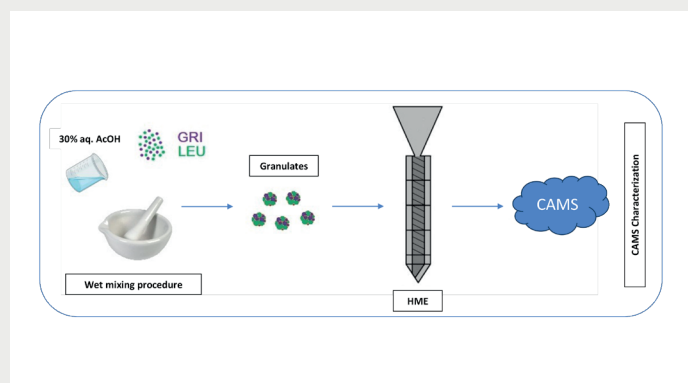
888 ATO (COM) and Kolliphor® P407 Geismar (KOL) 75/25 blend was the plasticizer. Deionized water or 30% w/w aqueous acetic acid (AcOH) were the feed processing solvents.

Compositions: GRI/LEU weight ratio 2:1 (corresponding to 1.3:1.7 molar) was used. Due to GRI's cohesiveness this was the highest ratio enabling feeding into extruder.

Processing of extrusion feeds: A wet mixing/drying/sieving process of GRI/LEU powder blend with or without plasticizer was employed. The GRI/LEU powder mixture was first blended with either deionized H<sub>2</sub>O (dissolves LEU) or 30% w/w AcOH aqueous solution (dissolves both drug and AA) to give a paste. For the required consistency, 9–12 mL solvent per g was needed. The wet mass was dried at 100 °C for 3 h, sieved (850 μm) and the resulting granules were fed into the extruder.

HME Conditions: A bench-type vertical single-screw extruder (Model RCP-0250 Microtruder) fitted with a 2 mm orifice die at 20 rpm screw speed was used. For the H<sub>2</sub>O processed feeds the extrusion temperatures were between 145 and 185 °C, and 30% w/w plasticizer had to be added for extrusion. For the AcOH processed feeds the extrusion temperatures were 145 and 175 °C and there was no need for plasticizer. However, for comparison, blends of AcOH processed feeds containing plasticizer were also tested.

Characterization of HME products: pXRD (Bruker D8, Bruker) was used to estimate the crystalline content, ATR-FTIR (FTIR Prestige 21, Shimadzu) to examine molecular interactions and DSC (DSC204 F1 Phoenix, NETZSCH) for thermal characterization. Dissolution tests were conducted in a USP II apparatus (Pharma Test PTW 2) at 37±0.5 °C and 50 rpm. Non-sink conditions were selected based on the Sink-Index (SI) choosing a value of 0.0115. To test the CAMS stability samples were placed in desiccators at 45 °C/75% RH and analyzed for solid-state changes after 0, 30 and 90 days.



### Methodology

Materials: Griseofulvin (GRI; Mw = 352.76 g/mol) was the poorly water-soluble high dose model drug and L-leucine (LEU; Mw = 131.17 g/mol), the AA co-former. Compritol®

## Results

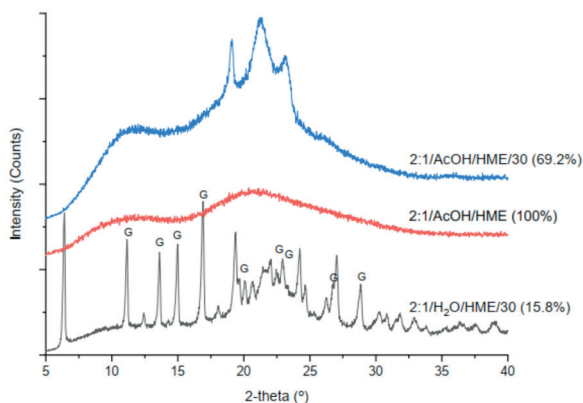


**Figure 1.** pXRD patterns of extrudates with or without 30% w/w plasticizer (% amorphous content in parenthesis).

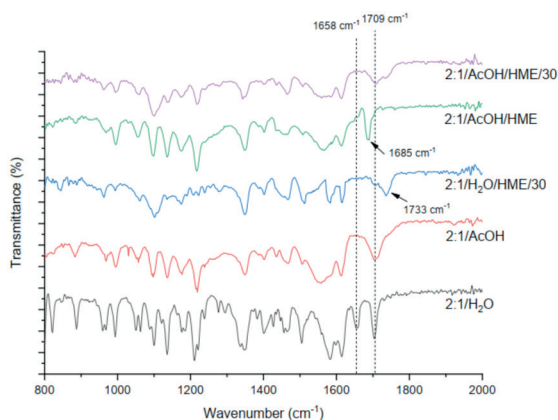


**Figure 2.** ATR-FTIR spectra pre-processed feeds and corresponding extrudates with or without 30% w/w plasticizer.

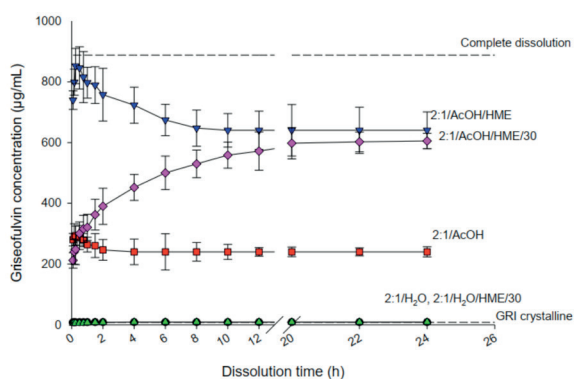


**Figure 3.** Non-sink dissolution profiles of extrudates with or without 30% w/w plasticizer.

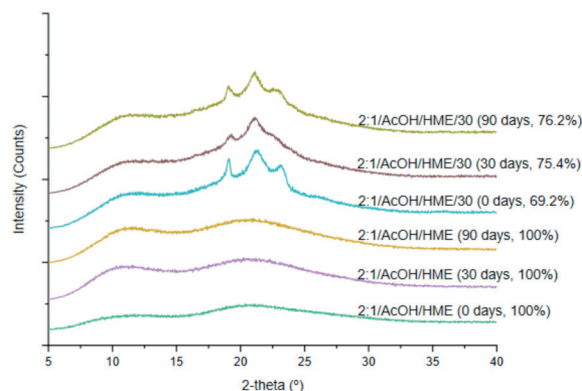


**Figure 4.** pXRDs of the extrudates at the beginning of stability test and after 30 and 90 days at 40°C and 75% RH (% amorphous content in parenthesis).

## Discussion

AcOH processing resulted in complete amorphization of both GRI and LEU indicating CAMS formation (Fig. 1). Wet mixing with AcOH dissolves both GRI and LEU allowing their molecules to come close and interact resulting in amorphization. This does not happen during H<sub>2</sub>O processing.

GRI's peak at 1658 cm<sup>-1</sup> (Fig. 2) is not seen in the extrudates and also in the non-extruded AcOH processed feed, possibly due to shifting and overlapping with peaks in the 1500–1600 cm<sup>-1</sup> region. This signifies H-bonding between GRI's cyclohexanone ring carbonyl with the -OH or -NH of LEU. For the 2:1/AcOH/HME extrudate the carbonyl 1709 cm<sup>-1</sup> peak is shifted to 1685 cm<sup>-1</sup> implying further H-bonding between the benzofuranone ring carbonyl of GRI with the -OH or -NH of LEU.

The 2:1/AcOH feed with 55.4% amorphous drug gave significantly higher concentration than crystalline GRI (293.3 µg/mL vs 7.8 µg/mL) which dropped to 240.0 µg/mL at plateau (Fig. 3). However, the most impressive increase of GRI concentration is exhibited by the 2:1/AcOH/HME extrudate, reaching 852.1 µg/mL in 15 min, before dropping to 640.5 µg/mL at plateau (x80 times higher than the crystalline drug).

The good stability (Fig. 4) of the 2:1/AcOH/HME is due to the strong interaction between GRI and LEU by two H-bonds formed by two -OH of GRI (Fig. 2). It is interesting that although the T<sub>g</sub> of 2:1/AcOH/HME (73.1 °C) is not far from the storage temperature (40 °C), CAMS remained stable.

**Table 1.** Composition of extrusion feeds and % drug recovered from extrudates (mean values  $\pm$ SD, n=3).

Extrudate code	Nominal composition (% w/w)				Drug content (% w/w)
	Griseofulvin	L-leucine	Compritol® ATO 888	Kolliphor® P407	
2:1/H <sub>2</sub> O/HME/30	46.7	23.3	22.5	7.5	98.7 $\pm$ 0.6
2:1/AcOH/HME	66.7	33.3	0.0	0.0	99.2 $\pm$ 0.8
2:1/AcOH/HME/30	46.7	23.3	22.5	7.5	99.3 $\pm$ 0.1

**Table 2.** Composition of extrusion feeds and % drug recovered from extrudates (mean values  $\pm$ SD, n=3).

Code	LOD% in GRI/LEU before processing*	LOD% of extrudates	Solvent residue (%)
2:1/H <sub>2</sub> O	0.27	1.79 $\pm$ 0.24	1.52
2:1/AcOH 0.27	3.81 $\pm$ 0.47	3.54	
2:1/H <sub>2</sub> O/HME/30 *SD < 0.01	0.35	0.71 $\pm$ 0.02	0.36
2:1/AcOH/HME	0.27	0.56 $\pm$ 0.03	0.29
2:1/AcOH/HME/30	0.35	0.69 $\pm$ 0.02	0.34

## Conclusions

- CAMS of the poorly water-soluble high dose drug GRI with LEU was developed.

- The obstacle of chemical degradation during amorphization of the AA by direct HME processing was overcome by a modified HME (Table 1).
- AcOH residues (Table 2) acted as a plasticizer and perhaps formed an acidic microenvironment during *in-vitro* dissolution further stabilizing GRI's release over time.
- The findings validate and encourage application of drug/AA CAMS, particularly for high-dose drugs for which polymers are not suitable.

## References

1. Lenz E, Löbmann K, Rades T, Knop K, Kleinebudde P. Hot Melt Extrusion and Spray Drying of Co-amorphous Indomethacin-Arginine With Polymers. *J Pharm Sci.* 2017; 106(1): 302-312.



## Peppermint Oil Spray Dried Powders - Encapsulating Wall Composition, Particulate Characteristics and Powder Cohesiveness

Ioannis Partheniadis, Alexandra Athanasiou, Ioannis Nikolakakis

Laboratory of Pharmaceutical Technology, School of Pharmacy, Faculty of Health Sciences, Aristotle University of Thessaloniki, 54124 Greece.

Email: ioanpart@pharm.auth.gr (I.P.), aathanasio@pharm.auth.gr (A.A.) and yannikos@pharm.auth.gr (I.N.)

### Introduction

Peppermint essential oil (EO), featuring menthol as its main bioactive constituent, displays antispasmodic effects in the GI, suggesting potential for treating disorders like irritable bowel syndrome (IBS)[1]. In this work, two batches of micro-encapsulated EO spray-dried powders (SDPs) were prepared with polysaccharide (PSC) wall composition using surface active (SOS) or non-surface active (ADA) starch grade. Two additional batches, incorporating enteric methacrylate polymer (Eudragit® L100) (PLM) at a ratio 20:80 with PSC (SOS or ADA) were also prepared. Since the fine particle size of SDPs (<20 μm) does not allow application of conventional methods for the characterization of flowability and processability[2], the prepared SDP batches were characterized by

direct measurement of tensile strength ( $\sigma_f$ ) over the 60 to 65% powder bed porosity range ( $\epsilon\%$ ) using a split-cell type apparatus (Fig. 1). Furthermore, the packing ability of powder products was evaluated by tapping tests and application of light weights.

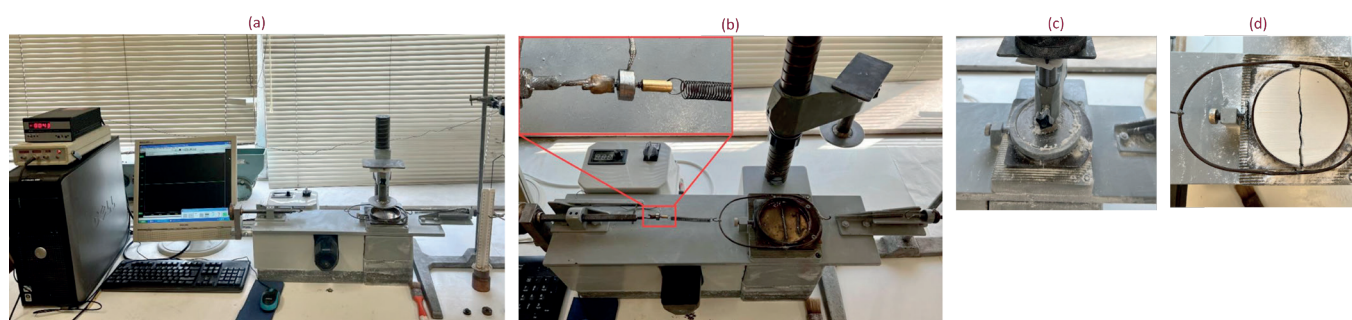
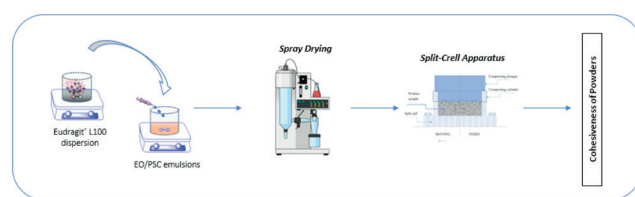


**Figure 1.** (a) Experimental set-up consisting of load cell, signal conditioner and transducer connected to PC for recording force/time profiles. (b) Set-up of split-cell apparatus itself. (c) Compression of powder bed inside the split-cell. (d) Diametral fracture of powder bed (end of test).

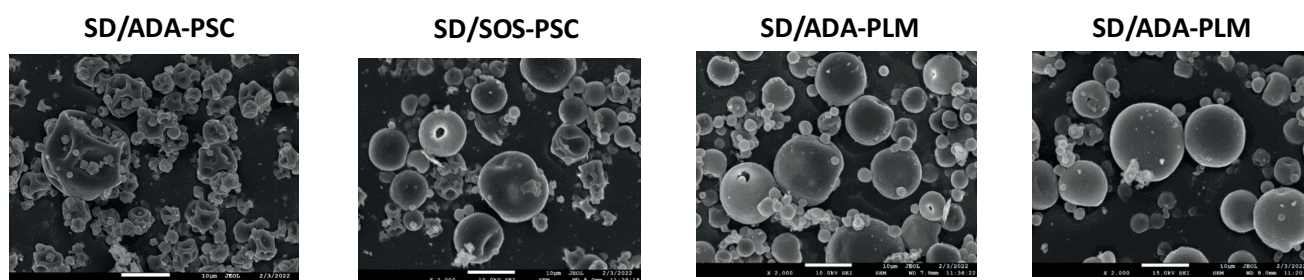


**Figure 2.** SEM images of SD powder products.

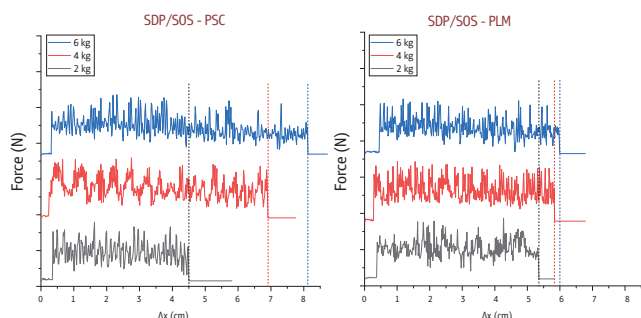


**Figure 3.** Recordings of force (N) with spring elongation (cm) during tensile test

## Methodology

**Materials:** Peppermint essential oil (EO) was from Dioscurides, Greece, Arabic gum (AG) from Nexira, France, and maltodextrin (MD, Glucidex 21), modified food grade starches (Clearam<sup>®</sup> CH 2020, acetylate di-starch adipate; ADA and Cleargum<sup>®</sup>, sodium octenyl succinate starch; SOS) were gifts from Roquette Italy. Eudragit<sup>®</sup> L100 (PLM) was gift from Evonik (Darmstadt, Germany).

**Spray-drying:** EO emulsions were prepared using either polysaccharides AG, MD and MS (ADA or SOS) only, (collectively abbreviated as PSC) or 20% PSC and 80% PLM. The PLM was added to PSC emulsion from a 30% aqueous Eudragit<sup>®</sup> L100 dispersion. The emulsions were spray-dried using a bench-top spray dryer (B-191, Büchi, Switzerland) at 145 °C and 1.4 mL/min flow rate with 600 mL/min airflow. The surface morphology of the SD particles is shown in the SEM images in Fig. 2.

**Tapping test:** Erweka SVM 101, USP1, Heusenstamm, Germany tester - 25 mL glass volumetric cylinder, 14 mm vertical drop height, 300 taps.

**Split-cell apparatus test:** In-house constructed split-cell type apparatus (Fig. 1). SDPs were placed in the split-cell and compressed by using weights up to 6 kg. Tensile strength was estimated from the force required to split the bed over the orthogonal split area (1cm x 10cm). The force was estimated from the total spring extension read from force-time (f/d) recordings after converting the pulling time (25 mm/min) to displacement. Force was monitored

using a cylindrical mini-load cell (2.0 MV/V, Sensotec Columbus, Ohio, USA) to accurately determine the fracture point. The load cell was bolted to the moving motor shaft. A spring of suitable stiffness was mounted at one end to the load cell and at the other to the movable half of the cell. The cohesiveness of the samples was compared from  $\sigma_F$  values at fixed  $p_F$ . Recordings of force with spring elongation during tensile testing are depicted in Fig. 3.

## Discussion

• SD products with PLM wall show markedly lower values of tapping indices (Table 1) compared to PSC products. This is also the case when consolidation is done by application of weights (2 to 6 kg) to the 10 cm circular flat surface of the powder (Fig. 4).

**Table 1.** Particle size and packing properties of the experimental spray-dried powders (mean values  $\pm$ SD, n=3).

Batch	d50 ( $\mu$ m)	$\rho_b^{\#}$ (g/cc)	$\rho_t^{\#}$ (g/cc)	Carr's Index (%)	Hausner Ratio (-)
SDP/ADA	8.00	0.29	0.54	46.3 $\pm$ 2.1	1.86 $\pm$ 0.13
SDP/SOS	10.5	0.31	0.52	40.4 $\pm$ 1.6	1.68 $\pm$ 0.54
SDP/ADA-PLM	9.5	0.39	0.60	35.0 $\pm$ 1.3	1.54 $\pm$ 0.32
SDP/SOS-PLM	10.5	0.45	0.62	27.4 $\pm$ 1.4	1.38 $\pm$ 0.28

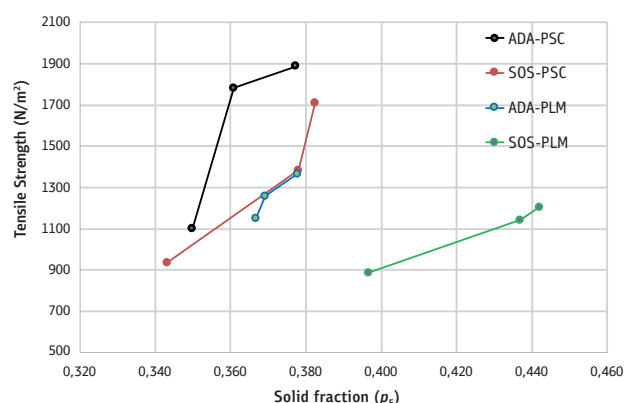


**Figure 4.** Tensile strength against solid fraction  $p_F$  for the spray dried EO powders

• The easier packing of the PLM products is a consequence of their spherical shape and smooth surface (Fig. 2) resulting from a favorable arrangement of Eudragit<sup>®</sup> L100 in the wall.

**Table 2.** Results of the split-cell test (mean values  $\pm$ SD, n=3).

Batch	Packing fraction ( $\rho_F$ )	Time at break ( $t_{br}$ , (s))	Spring elongation ( $\Delta x$ , (cm))	Breaking force ( $F_{br}$ , (N))
SDP/ADA-PSC	0.36 $\pm$ 0.006	39.1 $\pm$ 1.2	7.6 $\pm$ 0.2	1.24 $\pm$ 0.06
	0.37 $\pm$ 0.004	42.3 $\pm$ 1.0	8.2 $\pm$ 0.2	2.01 $\pm$ 0.05
	0.39 $\pm$ 0.001	44.9 $\pm$ 0.9	8.7 $\pm$ 0.1	2.13 $\pm$ 0.04
SDP/SOS-PSC	0.35 $\pm$ 0.003	22.4 $\pm$ 1.5	4.3 $\pm$ 0.2	1.06 $\pm$ 0.07
	0.39 $\pm$ 0.001	32.8 $\pm$ 2.7	6.4 $\pm$ 0.5	1.56 $\pm$ 0.13
	0.40 $\pm$ 0.001	40.6 $\pm$ 2.4	7.9 $\pm$ 0.4	1.93 $\pm$ 0.12
SDP/SOS-PLM	0.37 $\pm$ 0.004	27.4 $\pm$ 1.4	4.9 $\pm$ 0.1	1.30 $\pm$ 0.06
	0.38 $\pm$ 0.002	29.9 $\pm$ 1.8	5.3 $\pm$ 0.2	1.42 $\pm$ 0.08
	0.39 $\pm$ 0.001	32.5 $\pm$ 1.4	5.6 $\pm$ 0.1	1.54 $\pm$ 0.06
SDP/ADA-PLM	0.39 $\pm$ 0.001	25.4 $\pm$ 0.4	5.3 $\pm$ 0.2	1.20 $\pm$ 0.02
	0.40 $\pm$ 0.001	27.3 $\pm$ 1.0	5.8 $\pm$ 0.3	1.29 $\pm$ 0.06
	0.40 $\pm$ 0.001	28.7 $\pm$ 0.8	6.3 $\pm$ 0.2	1.36 $\pm$ 0.07

- The pulling force during measurement remained constant indicating uniform force application at constant rate of 25 mm/min. This enabled conversion of pulling time to spring displacement and total force applied at the point of powder bed split.
- From Fig. 4 it appears that for a fixed solid fraction value SD powders with PSC wall show greater tensile strength than SD powders with PLM due to the stronger bonding of the known binder ability of polysaccharides compared to that of the polymer.

### Conclusions

- An instrumented split-cell (Warren spring) apparatus was used to characterize the cohesiveness of spray dried powders with particles below 20  $\mu$ m which present cascade flow not allowing direct estimation of flowability.
- The modified starch with surface active ability gave product

(SDP/SOS) with spherical smooth surface particles enabling more effective packing and compressibility.

- The PLM spray dried products were less cohesive than products with PSC wall which allows easier handling during transportation and filling into capsules.
- The processing advantages of the PLM products contribute greatly to their use as enteric release formulations based on the solubility of Eudragit® L100 above pH 5.5

### References

1. Alammari N, Wang L, Saberi B, *et al.* The impact of peppermint oil on the irritable bowel syndrome: a meta-analysis of the pooled clinical data. *BMC Complement Altern Med*, 2019; 19(1): 21.
2. Partheniadis I, Zarafidou E, Litinas KE, Nikolakakis I. Enteric Release Essential Oil Prepared by Co-Spray Drying Methacrylate/Polysaccharides-Influence of Starch Type. *Pharmaceutics*. 2020; 12(6): 571.

## Static and Dynamic Vapor Sorption of Hydrophobic Starch Ester Powders and Corresponding Tablets

Ioannis Partheniadis, Georgios Stathakis, Ioannis Nikolakakis

Laboratory of Pharmaceutical Technology, School of Pharmacy, Faculty of Health Sciences, Aristotle University of Thessaloniki, 54124 Greece.

Email: ioanpart@pharm.auth.gr (I.P.), georgioss@pharm.auth.gr (G.S.) and yannikos@pharm.auth.gr (I.N.)

### Introduction

Hydrophobic starch esters have demonstrated high potential as matrix formers in controlled release solid oral dosage forms<sup>[1]</sup>. They can form controlled-release tablets by depressing swelling and enzymatic degradation. Differences in the mechanical properties and tableting performance of native starch (SN), starch acetate (SA) and starch propionate (SP) have been highlighted previously<sup>[2]</sup>. The aim of the present work was to quantify the effects of relative humidity (RH) on the moisture sorption, dimensional changes and mechanical characteristics of the tablets of different starch esters, under static (SVS) or dynamic vapour sorption (DVS).



### Methodology

**Materials:** Native maize starch (SN) was from Colorcon, USA. Starch acetate (SA) and propionate (SP) were synthesized by reacting hydroxyl starch groups with acetic acid or propionic acid anhydride<sup>[1]</sup>.

**ATR-FTIR spectra:** FTIR-Prestige-21 (Shimadzu, Japan) attached to a horizontal Golden Gate MKII single-reflection ATR (Specac, UK) equipped with a Diamond/ZnSe crystal.

**Particle density ( $\rho_s$ ):** Helium pycnometry (Ultrapycnometer 1000, Quantachrome Instruments, USA). The mean values were SN: 1.58 g/cc, SA: 1.39 g/cc and SP: 1.42 g/cc.

**Compression:** Tablet press (Model GTP-1, Gamlen Tableting Ltd, UK); tablet weight 100 mg, 6-mm flat-faced punches, 10 mm/min compression rate and 120 or 174 MPa pressure. Heckel model was used to assess the compression behavior:  $\ln[1/(1-p_f)] = A + KP$ , ( $P$  is compression pressure,  $p_f$  solid fraction,  $1/K$  = yield pressure ( $P_y$ ),  $A$  is related to volume reduction due to die filling and particle rearrangement<sup>[2]</sup>).

**Air permeametry:** Blaine type instrument (PharmaTest, type PTPD, Hainburg, Germany).

**Moisture sorption:** Changes in tablet weight and axial expansion with RH were measured under static (desiccators with saturated salt solutions, equilibrium time 2 days) and DVS (step time 2 h) using a novel in-house developed system in our lab in collaboration with HDK Solutions Ltd., UK). It is comprised of controlled moisture generator, balance, dry air supply and computer with software for system control<sup>[3]</sup>.

**Tablet morphology:** Scanning Electron Microscopy (15 kV, JEOL JSM- 6390LV, Jeol, Japan), EDS and Oxford INCA micro-analysis system.

### Results

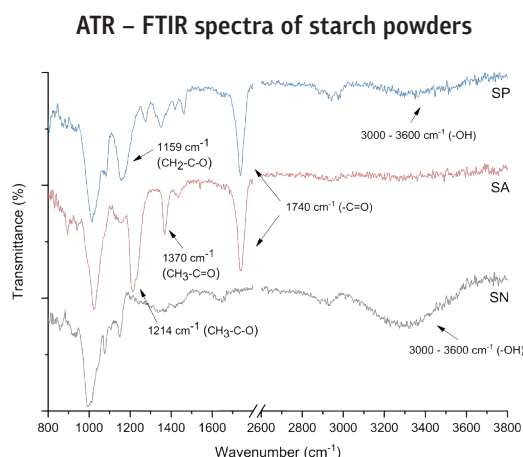


**Figure 1.** ATR – FTIR spectra of native starch (SN), starch acetate (SA) and starch propionate (SP).

### Conclusions

- ATR-FTIR spectra (Fig. 1) show that there are more free -OH groups in SP than SA, thus providing more interaction sites with water vapour.
- Measurements under static conditions (SVS) showed that for both forms of starches, powders and tablets, moisture is sorbed in the order SN >> SP > SA (Fig. 2a-c).

Static and dynamic moisture sorption of starch powders & tablets

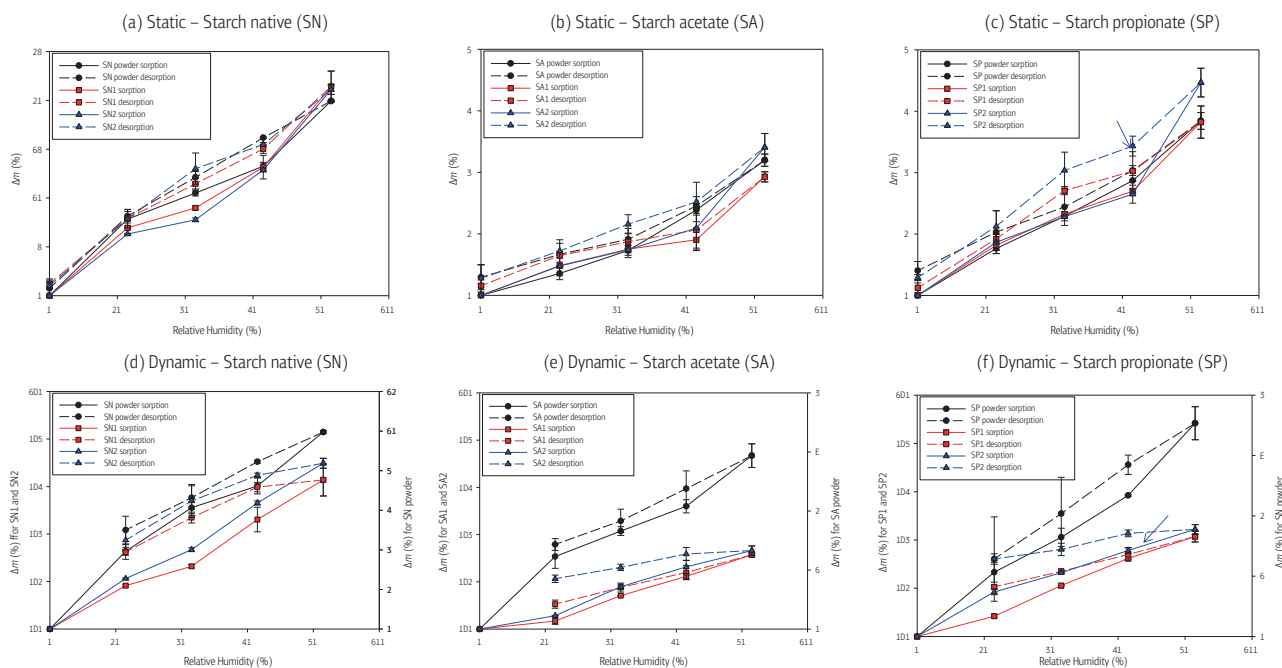


**Figure 2.** Static (a-c) and dynamic (d-f) vapor sorption of native starch (SN) starch acetate (SA) and starch propionate (SP) powders (SN, SA, SP) and corresponding tablets compressed at 120 (SN1, SA1, SP1) and at 174 MPa (SN2, SA2, SP2).

Tablet characteristics & Compression behavior of starch powder

**Table 1.** Compression behavior of native starch (SN), starch acetate (SA) and starch propionate (SP) powders (mean values  $\pm$ SD, n=3). (mean values  $\pm$ SD, n=3).

Tablet code	Compression Pressure (MPa)	Work of compaction, $W_c$ (J)	Solid fraction, $p_f$ (-)	Yield pressure, $P_y$ (MPa)	Air permeametry (sec)
SN1	120	1.80 $\pm$ 0.03	0.755 $\pm$ 0.003	77.6 $\pm$ 3.0	96.5 $\pm$ 6.4
SN2	174	2.46 $\pm$ 0.02	0.789 $\pm$ 0.004		120.0 $\pm$ 4.2
SA1	120	1.86 $\pm$ 0.05	0.781 $\pm$ 0.007	76.6 $\pm$ 2.1	105.5 $\pm$ 4.9
SA2	174	2.37 $\pm$ 0.05	0.824 $\pm$ 0.012		373.5 $\pm$ 13.4
SP1	120	2.17 $\pm$ 0.02	0.792 $\pm$ 0.005	56.7 $\pm$ 2.5	572.5 $\pm$ 61.5
SP2	174	2.56 $\pm$ 0.02	0.844 $\pm$ 0.013		1896.5 $\pm$ 280.7

**Table 2.** Tensile strength (TS) values of starch tablets exposed to different relative humidities (RH) under SVS conditions (mean values  $\pm$ SD, n=3) (LSD<sub>0.05</sub>: least significant difference at 95% confidence level).

Tablet code	TS at 23% RH for 2 days (MPa)	TS at 43% RH for 2 days (MPa)	TS at 63% RH for 2 days (MPa)	TS at 83% RH for 2 days (MPa)	LSD <sub>0.05</sub>
SN1	0.68 $\pm$ 0.03	0.65 $\pm$ 0.07	0.62 $\pm$ 0.04	0.58 $\pm$ 0.02	0.06
SN2	0.87 $\pm$ 0.07	0.84 $\pm$ 0.11	0.80 $\pm$ 0.06	0.74 $\pm$ 0.09	0.08
SA1	0.69 $\pm$ 0.05	0.68 $\pm$ 0.02	0.67 $\pm$ 0.03	0.66 $\pm$ 0.04	0.03
SA2	1.03 $\pm$ 0.08	1.03 $\pm$ 0.08	1.02 $\pm$ 0.04	0.99 $\pm$ 0.07	0.04
SP1	1.39 $\pm$ 0.04	1.35 $\pm$ 0.02	1.29 $\pm$ 0.05	1.24 $\pm$ 0.06	0.14
SP2	2.05 $\pm$ 0.12	2.00 $\pm$ 0.08	1.83 $\pm$ 0.04	1.81 $\pm$ 0.03	0.22

Axial & Diametral tablet expansion (SVS)

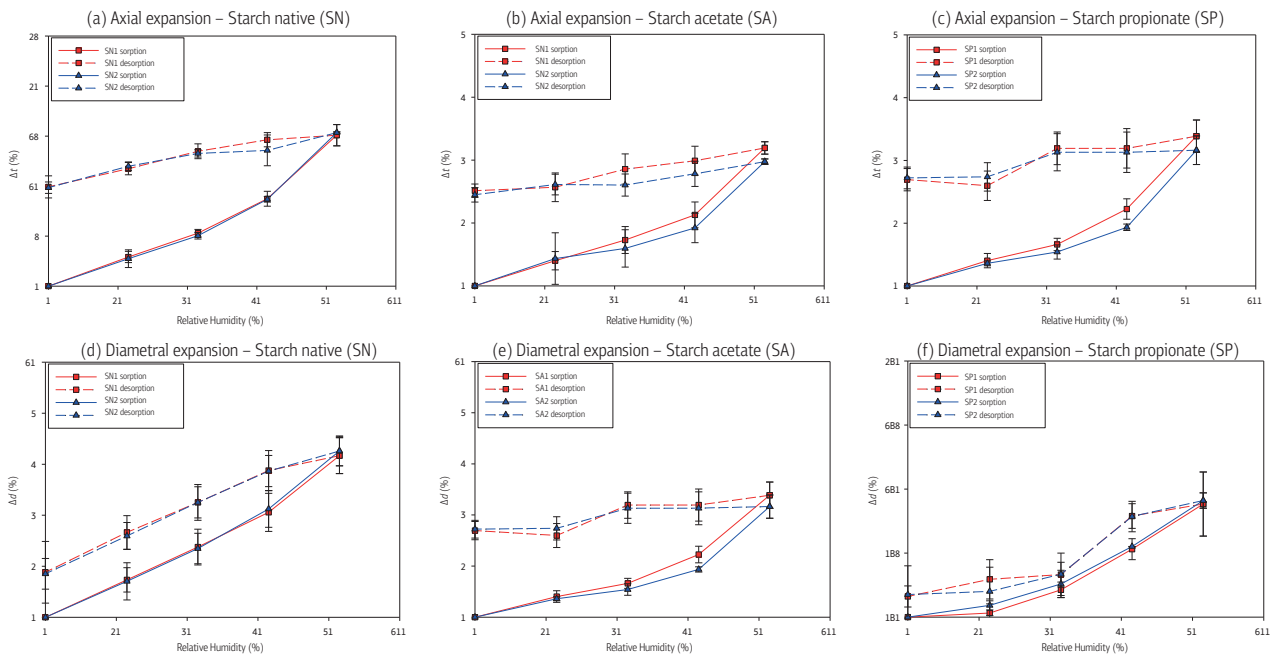


**Figure 3.** Axial ( $\Delta t$ ) (a-c) and diametral ( $\Delta d$ ) (d-f) expansion of native starch (SN), starch acetate (SA), and starch propionate (SP) tablets compressed at 120 (SN1, SA1, SP1) and at 174 (SN2, SA2, SP2) MPa.

SEM microphotographs

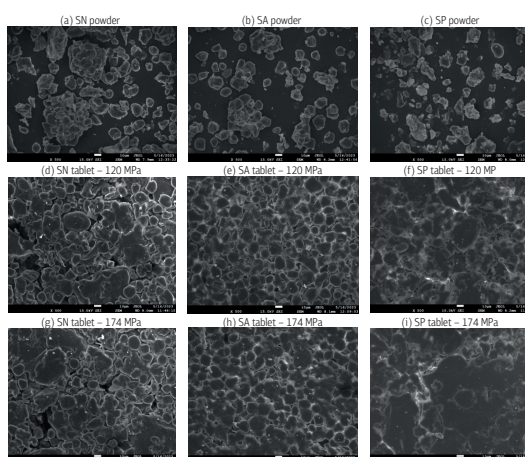


**Figure 4.** SEM microphotographs of SN, SA, and SP powders (a-c) and surfaces of corresponding tablets compressed at 120 (d-f) and 174 MPa (g-i).

sure 174 MPa (comparing blue and red lines in Fig. 2b-c under SVS and in Fig. 2e-f under DVS conditions).

- Axial and diametral expansion of the tablets followed the same order as moisture sorption (Fig. 3) i.e., SN >> SP > SA. Interestingly, it was not affected by the compression pressure.
- DVS results showed low moisture sorption for all starch tablets (Fig. 2d-f, left axis), implying that in-line RH monitoring during tablet formulation is not mandatory. Greater moisture sorption is observed for starch powders (Fig. 2d-f, right axis).
- SP tablets have higher Wc and lower yield pressure (Table 1) indicating ability to deform, develop contact areas and absorb compaction work, thus increasing bonding. This is also demonstrated by the higher tensile strength (TS) of SP tablets compared to SN and SA.
- The greater plasticity of SP (Table 1 Fig. 4), is manifested by the surface of compressed tablet showing extensive integration with fewer boundaries compared to tablets of the other starches.
- The higher plasticity of SP also explains the significantly lower diametral expansion of these tablets (Fig. 3f), compared to SA tablets (Fig. 3e).

- Compression pressure impacted on the sorption of SP and SA (Fig. 2b,c) but not on SN tablets (Fig. 2a). Higher sorption is manifested by tablets compressed at the high pres-

- SP tablets showed longer air permeation times (Table 1) of the air travelling towards the tablet surface due to plastic deformation reducing surface porosity compared to other starch tablets.
- Greater hysteresis is noticed for the SP tablets during SVS (Fig. 2c, arrow) and DVS (Fig. 2f, arrow) sorption/desorption, compared to SA tablets (Figs. 2b and 2e, respectively), signifying vapor entrapment in the tablet structure.
- TS values of tablets exposed to different RH under SVS conditions (Table 2) were only significantly different when comparing strength values obtained at 23 % RH with values obtained at 83% RH.

## References

1. N. Sakhnini, N. Al-Zoubi, G.H. Al-Obaidi, A. Ardakani, Sustained release matrix tablets prepared from cospray dried mixtures with starch hydrophobic esters. *Die Pharmazie*, 70(2015):177-182.
2. N. Al-Zoubi, A. Ardakani, F. Odeh, N. Sakhnini, I. Partheniadis, I. Nikolakakis, Mechanical properties of starch esters at particle and compact level - Comparisons and exploration of the applicability of Hiestand's equation to predict tablet strength. *Eur J Pharm Sci*,147(2020):105292.
3. I. Partheniadis, D. Kopanelou, M. Gamlen & I. Nikolakakis, Monitoring the weight and dimensional expansion of pyridostigmine bromide tablets under dynamic vapor sorption and impact of deliquescence on tablet strength and drug release. *Int J Pharm*, 609(2021):121150.

## Fabricating hybrid particles for possible nose-to-brain delivery of ropinirole

Elmina-Marina Saitani<sup>1</sup>, Natassa Pippa<sup>1</sup>, Paraskevi Papakyriakopoulou<sup>1</sup>, Stergios Pispas<sup>2</sup>, Georgia Valsami<sup>1</sup>

<sup>1</sup>Department of Pharmaceutical Technology, Faculty of Pharmacy, Panepistimioupolis Zografou 15771, National and Kapodistrian University of Athens, Athens, Greece

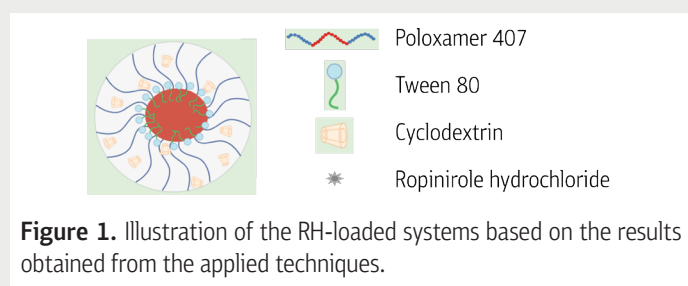
<sup>2</sup>Theoretical and Physical Chemistry Institute, National Hellenic Research Foundation, 48 Vassileos Constantinou Avenue, 11635 Athens, Greece

CONTACT INFO: elminasait@pharm.uoa.gr, valsami@pharm.uoa.gr

### Introduction

Ropinirole hydrochloride (RH) is a non-ergolinic dopamine agonist, used for Parkinson's disease. However, oral administration of RH has limitations, mainly due to the poor systemic bioavailability caused by the extensive hepatic first pass metabolism and the low access to the brain due to the Blood-Brain Barrier (BBB). One promising approach to overcome these issues is the nose-to-brain transport route of administration, bypassing the BBB and permitting direct brain targeting and rapid onset of action.

**Objective:** This study aims to design and develop hybrid systems composed of Poloxamer 407 (P407), non-ionic surfactant (Tween 80), and cyclodextrins (methyl-β-CD or hydroxy-propyl-β-CD) for possible brain drug targeting after nasal administration of RH.

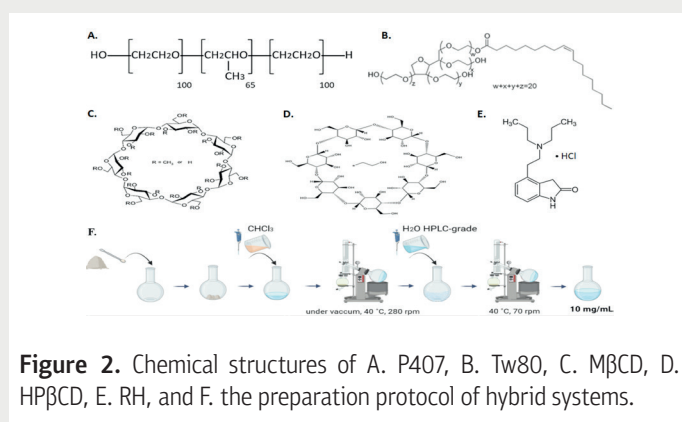


### Methodology

The hybrid systems were formed by the thin-film hydration method.

The systems' physicochemical and morphological characterization was achieved using the following techniques:

- Differential Scanning Calorimetry
- Light Scattering techniques
- Cryogenic Transmission Electron Microscopy
- MTT assay on HEK293 cell lines
- *In vitro* diffusion experiments using Franz cells
- High-Pressure Liquid Chromatography Analysis



### Results

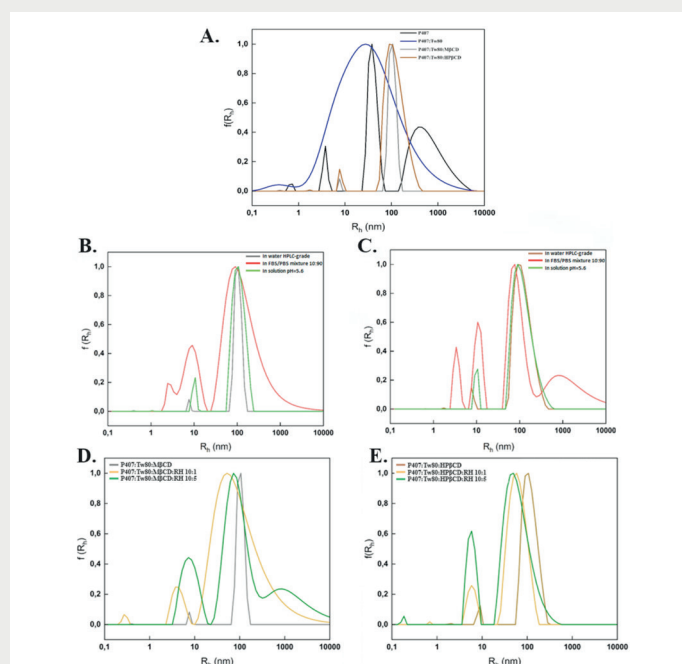


**Figure 3.** A. Size distribution for the P407, P407:Tw80, P407:Tw80:MβCD and P407:Tw80:HPβCD systems; Size distribution in different dispersion media and size distributions for drug-loaded system in weight ratios of 10:1 and 10:5 for P407:Tw80:MβCD (B, D) and P407:Tw80:HPβCD (C, E) systems, respectively.



**Table 1.** The physicochemical properties of the prepared hybrid systems on the day of their preparation.

Colloidal dispersions	w/w	R <sub>h</sub> (Cumulant) (nm) <sup>1</sup>	PDI <sup>2</sup>	Number of peaks	R <sub>h</sub> (Contin) (nm) <sup>3</sup>	Weight of peak (%)	z-potential (mV)
P407	-	97	0.4 <sub>9</sub>	3	1) 4 2) 39 3) 598	1) 6% 2) 38% 3) 55%	-20.5±6.0
P407:Tw80	70:30	18	0.5 <sub>2</sub>	1	29	100%	-6.1±2.0
(P407:Tw80):MβCD	80:20	106	0.3 <sub>2</sub>	2	1) 8 2) 104	1) 3% 2) 97%	-12.9±12.0
(P407:Tw80):HPβCD	80:20	100	0.3 <sub>0</sub>	2	1) 9 2) 114	1) 3% 2) 97%	-6.9±8.4

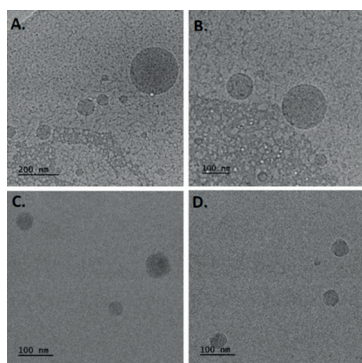


**Figure 4.** Cryo-TEM micrographs of hybrid P407:Tw80:MβCD (A, B) and P407:Tw80:HPβCD (C, D) systems.

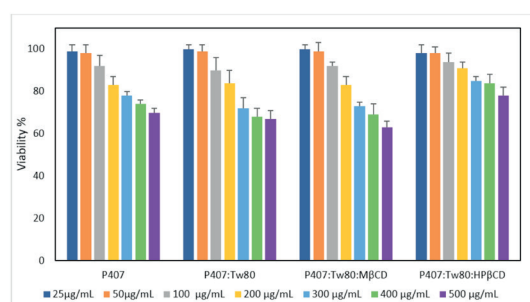


**Figure 4.** Cryo-TEM micrographs of hybrid P407:Tw80:MβCD (A, B) and P407:Tw80:HPβCD (C, D) systems.

- The development of strong interactions between polymer, surfactant, and CD may be associated with the formation of an inclusion complex.
- The ternary systems exhibit stability when exposed to simulated nasal cavity conditions, whereas the PEO chains partially impart biological stability to the composed structures in serum media (Figure 3).

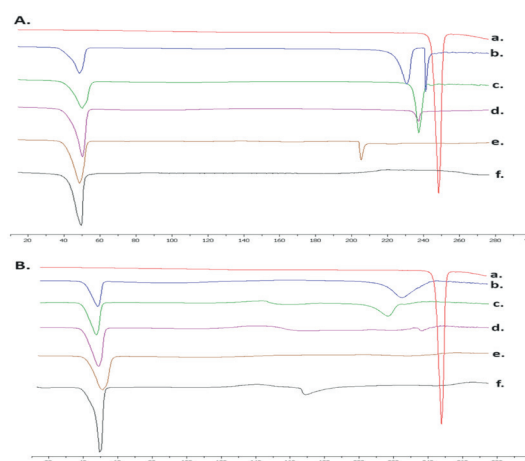


**Figure 6.** DSC thermograms. The heating curves of a. RH, RH-loaded ternary systems [(P407:Tw80:MβCD):RH (A) and (P407:Tw80:HPβCD):RH (B)] in different weight ratios b. 10:10, c. 10:5, d. 10:1, e. 10:0.5 and f. 10:0.1.

- The structures visualized in cryo-TEM images had spherical configurations (Figure 4).
- The prepared systems exhibit no cytotoxicity at low concentrations. As the dose was increased, a correlation between dose and cytotoxicity was observed on HEK293 cell lines, with the degree of cytotoxicity varying based on the materials' composition (Figure 5).
- The most optimum weight ratios for the incorporation of RH were 10:1 and 10:5, as they demonstrated superior cooperativity between the materials and the highest incorporation of RH (Figure 6).
- The addition of RH to the systems in different concentrations influenced the particle size distribution, potentially due to different interactions and self-assembly behaviors among the components (Figures 3 and 6).

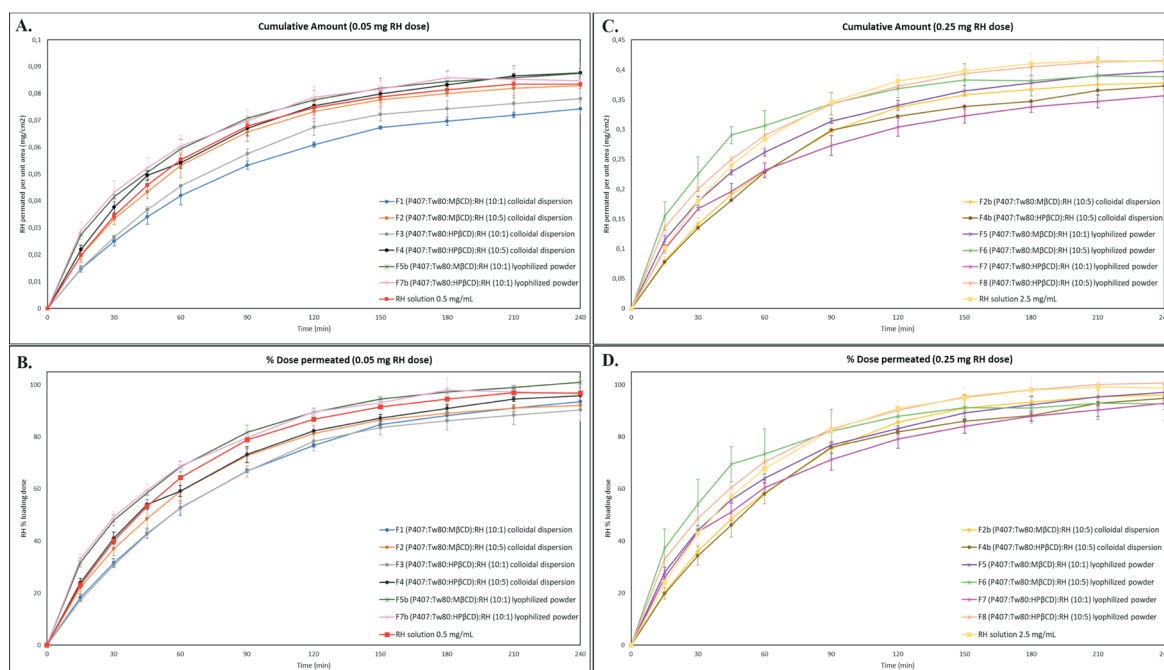


**Figure 7.** Permeation profiles, through regenerated cellulose membranes, for the colloidal dispersions and lyophilized powders of RH-loaded P407 ternary systems in comparison to the RH solutions (0.5 and 2.5 mg/mL). The results are expressed as (A, C) quantity permeated per unit area (mean  $\pm$  SD,  $n=3$ ) and (B, D) % loading dose permeated for the tested formulation (mean  $\pm$  SD,  $n=3$ ). The data is provided for the following RH doses: 0.05 mg (A, B) and 0.25 mg (C, D), respectively.

- The results of *in vitro* diffusion experiments indicated a drug loading higher than 90% in all cases, with the drug release exhibiting a progressive increase over the duration of the experiment (Figure 7). The lyophilized powders demonstrated increased levels of permeated loaded dose of RH from the beginning of the experiment until 90 min compared to the corresponding colloidal dispersions.

## Conclusions

The extensive physicochemical and morphological characterization of these hybrid systems proved their potential as attractive candidates for drug delivery systems with unique properties. These systems present appealing opportunities for RH nasal delivery and nose-to-brain targeting as depicted

by the beneficial results derived from *in vitro* diffusion experiments. To this end, further studies are ongoing to evaluate the *ex vivo* permeation through rabbit nasal mucosa, as well as the *in vivo* serum and brain pharmacokinetic profiles after nasal administration of the developed formulations.

## References:

- Barcia, E.; *et al.* Nanotechnology-based drug delivery of ropinirole for Parkinson's disease. *Drug delivery* 2017, 24, (1), 1112-1123.
- Aly, A. E.; Waszczak, B. L., Intranasal gene delivery for treating Parkinson's disease: overcoming the blood-brain barrier. *Expert opinion on drug delivery* 2015, 12, (12), 1923-41.

**Acknowledgments:** E.-M. S. would like to acknowledge the Bodossaki Foundation for the PhD scholarship.

## *In vitro* modified-release matrix tablets of omeprazole for paediatric patients

**Garyfallia-Ioanna Sotiropoulou, Angeliki Siamidi, Chrystalla Protopapa, Marilena Vlachou\***

Section of Pharmaceutical Technology, Faculty of Pharmacy, National and Kapodistrian University of Athens, Panepistimiopolis-Zografou, 157 84, Athens, Greece

Presentation by: Garyfallia-Ioanna Sotiropoulou, (+30) 6972345401, ioannasotiropoulou@hotmail.gr

\*Corresponding Author: Marilena Vlachou, (+30) 210 7274674, vlachou@pharm.uoa.gr

### Introduction

Omeprazole is an inhibitor of the enzyme system of hydrogen/potassium adenosine triphosphatase (H<sup>+</sup>/K<sup>+</sup>-ATPase), which leads to the inhibition of gastric acid secretion [1]. Because of its mechanism of action, it is indicated for gastroesophageal diseases [1]. Concerning the paediatric population, omeprazole is also prescribed for this group, but the safety profile is not as well established as for adults [2]. The usual doses of omeprazole, in commercial formulations, are 20 and 40 mg [1]. However, due to the particular needs of children and the risk of long-term adverse effects [3], the daily dose could be lower and personalized for each patient.

The aim of this project was to prepare modified-release tablets of omeprazole for paediatric patients and study its dissolution profile.

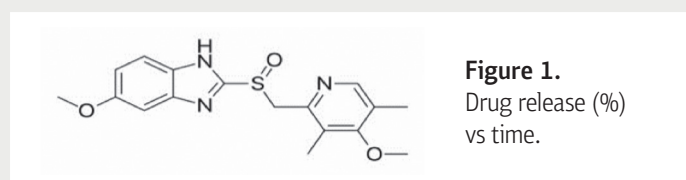


**Figure 1.**  
Drug release (%)  
vs time.

### Methodology

Three tablets were prepared using **Omeprazole**, as the active substance, Chitosan, Sodium Alginate (Medium viscosity), Lactose monohydrate and Magnesium Stearate, as excipients, under direct compression conditions. A USP apparatus II was used for the dissolution experiments, which were conducted at pH=6.8 for 150 min. Samples were analyzed, using UV-Vis spectrophotometry (LLG-uniSPEC 2 Spectrophotometer), at  $\lambda_{\max}$ =301 nm.

### Results

**Figure 2** (%) Drug release from Formulation 1 tablets, vs time.

The results indicate a modified drug release from **Formulation 1**. It has shown an approximately 55% drug release at t=30 min. and a plateau from t=90 min. to t= 150 min. The maximum drug release is approximately 75%, which

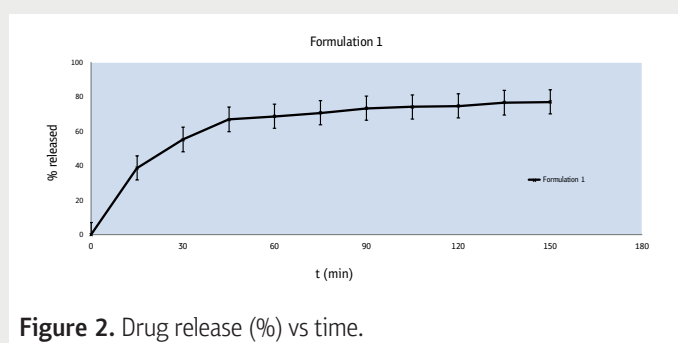


**Figure 2.** Drug release (%) vs time.

**Table 1.** Tablet formulation

Formulation	Formulation 1 (mg/tablet)
Omeprazole	5
Chitosan	1
Sodium Alginate (Medium viscosity)	3.3
Lactose monohydrate	10.5
Magnesium Stearate	0.2
Total	20

indicates the suitability of the **Formulation 1** for the sought delivery profile. Further studies, with coated tablets, are planned to be conducted, at pH=6.8, aiming at augmenting the drug's release in the small intestine simulated environment, and also at pH=4.5, which simulates the gastric fed-state conditions, in order to reduce omeprazole's release under these conditions.

### References

- Al-Badr, A. A. Omeprazole. Profiles of Drug Substances, Excipients and Related Methodology 2010, 35, 151–262.
- Alosaily, Y.A.; Alfallaj, J.M.; Alabduljabbar, J.S.; Alfahaid, E.F.; Alfayez, O.M.; Elrasheed, M. Appropriateness of proton pump inhibitors use in noncritically ill hospitalized children in a tertiary hospital in Saudi Arabia, Saudi Pharmaceutical Journal 2023, 31(9), 101723.
- Pasman, E.A.; Ong, B.; Witmer, C.P.; Nylund C.M. Proton Pump Inhibitors in Children: the Good, the Bad, and the Ugly. Current Allergy and Asthma Reports 2020, 20(39), 1-8.

## Προϋποθέσεις πλαστικοποιητικής δράσης της σορβιτόλης κατά τη θερμοεξώθηση Kollidon® SR διαφορετικού βαθμού ενυδάτωσης

Μιλτιάδης Τόσκας, Ιωάννης Παρθενιάδης, Ιωάννης Νικολακάκης

Laboratory of Pharmaceutical Technology, School of Pharmacy, Faculty of Health Sciences, Aristotle University of Thessaloniki, 54124 Greece.

Email: toskasmi@pharm.auth.gr (M.T.), ioanpart@pharm.auth.gr (I.P.) and yannikos@pharm.auth.gr (I.N.)

### Εισαγωγή

Η σορβιτόλη έχει πλαστικοποιητική δράση και λόγω της χαμηλής θερμοκρασίας τήξης, της βιο-αποικοδόμησης και ως μη-τερηδογόνος προσφέρεται για τη θερμοεξώθηση φαρμάκων. Κατά τη θερμοεξώθηση μειγμάτων με άμυλο παρουσίασε αντι-πλαστικοποιητική δράση σε χαμηλές συγκεντρώσεις με πιθανές συνέπειες στην απελευθέρωση φαρμάκων<sup>[1]</sup>. Το Kollidon® SR είναι θερμοπλαστικό πολυμερές με ανεξάρτητη του pH παρατεταμένη απελευθέρωση φαρμάκου καθώς και με ανασταλτική δράση στην κρυστάλλωση φαρμάκων διατηρώντας υπερκορεσμό. Όμως, εμφανίζει υγροσκοπικότητα και διαφορετική ενυδάτωση σε σχετικά υψηλή σχετική υγρασία<sup>[2]</sup>. Καθότι το νερό είναι επίσης πλαστικοποιητής ο σκοπός της παρούσας εργασίας ήταν να διερευνηθεί η πλαστικοποιητική δράση διαφορετικών συγκεντρώσεων σορβιτόλης στη θερμοεξώθηση Kollidon® SR διαφορετικού βαθμού ενυδάτωσης.

### Πειραματικό

Υλικά: Πολυμερές Kollidon® SR, BASF, Ludwigshafen, Germany) μετά από έκθεση σε συνθήκες χαμηλής (42%) ή υψηλής (75%) σχετικής υγρασίας (RH); πλαστικοποιητής σορβιτόλη (Karion®, Merck, Darmstadt, Germany).

Παραγωγή Θερμοεξωθήματος: Εργαστηριακός μονοκόχλιος

εξωθητής διάταξης (Microtruder RCP-0250, Randcastle, N.J., USA) διάμετρος κοχλία 6.35 mm, μήκος/διάμετρο 24:1, 40 rpm.

### Χαρακτηρισμός σκληρότητας, τραχύτητας και μορφολογίας επιφάνειας

Νανο-διείσδυση: Shimadzu HV-2. Εκτελούνται διαδοχικοί κύκλοι φόρτισης-αποφόρτισης σε διαφορετικά σημεία της επιφάνειας. Το δείγμα (μικροκυλίνδρος 2 mm x 2 mm), στερεώθηκε με kit EroFix (Bruker), λειάνθηκε (SiC 120, 400, 800, 1000 και 2400 mesh) και γυαλίστηκε. Ασκήθηκε δύναμη 98 mN για 30 sec χρησιμοποιώντας διαμαντένια πυραμιδοειδή ακίδα (Vickers 136 μοιρών). Βάθος, διείσδυσης 2 mm, χρόνος χαλάρωσης 20 sec. Παρατήρηση αποτυπωμάτων με μικροσκόπιο Leica 4000M (μέση τιμή από τουλάχιστον 5 μετρήσεις).

Ηλεκτρονική μικροσκοπία σάρωσης SEM: 20 kV, JSM 840A, Jeol, Τόκυο, Ιαπωνία

Στερεά κατάσταση – Διαφορική Θερμιδομετρία Σάρωσης (DSC): DSC 204 F1 Phoenix (NETZSCH, Selb, Γερμανία. 5-10 mg σε δισκάκι αλουμινίου με οπή, εύρος θερμοκρασιών -10 έως 140 °C/ρυθμός 10 °C/min) σε ατμόσφαιρα αερίου αζώτου. Η ψύξη των δειγμάτων πριν το 2ο κύκλου θέρμανσης γινόταν με υγρό N<sub>2</sub> σε -10 °C.

**Πίνακας 1.** Συνθήκες θερμοεξώθησης μειγμάτων Kollidon/σορβιτόλης (KN πολυμερές χαμηλής και KW υψηλής ενυδάτωσης).

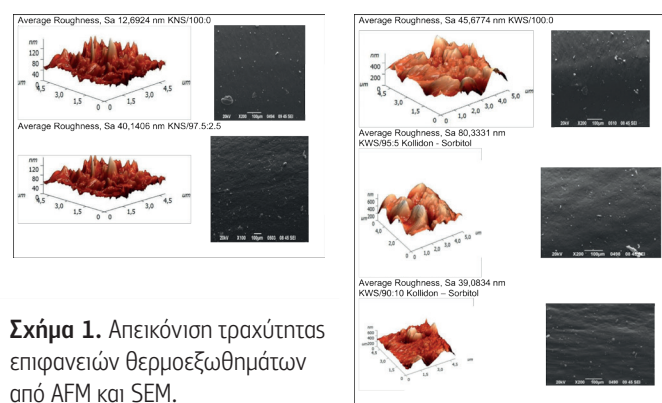
Μείγμα εξώθησης Kollidon:Σορβιτόλη	Θερμοκρασίες ζωνών (°C)				Πίεση στο σωλήνα εξώθησης (MPa)
	T1	T2	T3	T4	
KNS/100:0	80	110	115	113	2.07 - 1.38
KNS/97.5:2.5	80	110	115	113	2.41 - 1.03
KNS/95:5	85	115	120	118	2.07 - 1.38
KNS/90:10	85	115	120	118	2.07 - 1.38
KWS/100:0	90	125	135	138	2.41 - 2.07
KWS/97.5:2.5	85	115	125	123	2.41 - 2.07
KWS/95:5	80	110	120	118	2.41 - 1.72
KWS/90:10	80	110	120	118	2.07 - 1.72

**Διακιοποίηση:** Εργαστηριακή ημι-αυτόματη έκκεντρα δισκιοποιητική μηχανή Gamlen® D-series (Gamlen Tableting Ltd, Nottingham, UK) με δυνατότητα καταγραφής των προφίλ δύναμης/συμπίεσης.

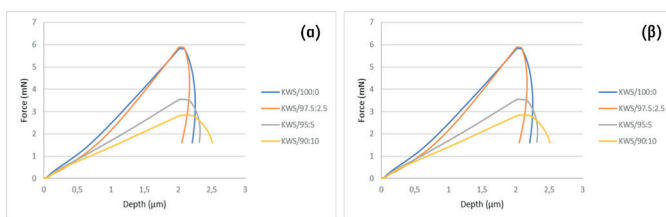
## Αποτελέσματα

**Πίνακας 2.** Θερμοκρασία υαλώδους μετάπτωσης μειγμάτων.

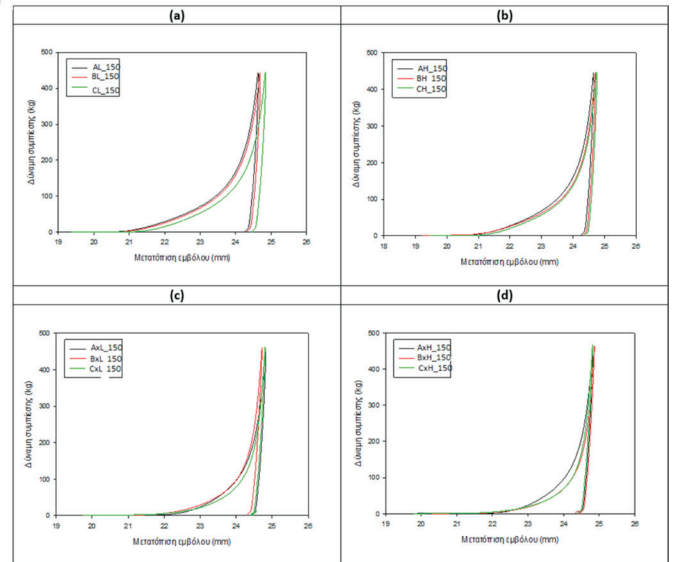
Μείγμα εξώθησης Kollidon:Σορβιτόλη	Θερμοκρασία υαλώδους μετάπτωσης, Tg (°C)		
	Φυσικό μείγμα	Εξωθημένο μείγμα	Predicted (Gordon-Taylor)
Sorbitol	-5.3	n.a.	n.a.
KNS/100:0	35.5	33.2	n.a.
KWS/100:0	34.6	33.6	n.a.
KNS/97.5:2.5	36.7	31.9	32.3
KWS/97.5:2.5	35.2	33.4	32.7
KNS/95:5	35.4	33.7	31.3
KWS/95:5	33.7	34.0	31.7
KNS/90:10	35.5	33.1	29.4
KWS/90:10	34.6	35.2	29.9



**Σχήμα 1.** Απεικόνιση τραχύτητας επιφανειών θερμοεξωθημάτων από AFM και SEM.



**Σχήμα 2.** Καταγραφή μεταβολής βάθους διείσδυσης με ασκούμενη δύναμη κατά τη νανο-διείσδυση για χαμηλής (α) και υψηλής (β) ενυδάτωσης εξωθήματα.



**Σχήμα 3.** Διαγράμματα δύναμης – μετατόπισης θερμοεξωθημένων μειγμάτων Kollidon® SR με σορβιτόλη. (α) και (c) προφίλ φυσικών μειγμάτων και εξωθημάτων με χαμηλό ποσοστό ενυδάτωσης κι αντίστοιχα στα (b) και (d) με υψηλό ποσοστό ενυδάτωσης.

## Συζήτηση

Δυσκολότερη εξώθηση εμφάνισαν τα KWS/100:0 και KWS/97.5:2.5 (Πίνακας 1, τελευταία στήλη). Πέραν των μετρήσεων της τραχύτητας (Σχήμα 1), αυτό υποδηλώνει υψηλότερο ιξώδες των αντίστοιχων τμημάτων KWS/100:0 και KWS/97.5:2.5 λόγω δυνάμεων τριβής.

Εκτός των εξωθημάτων KWS/95:5 και KWS/90:10 που η θερμοεξώθηση οδήγησε σε μικρή μείωση του Tg, υπήρξε σημαντική μείωση για εξωθημένα μείγματα KN (Πίνακας 2).

Τα θερμοεξωθήματα KW παρουσιάζουν σημαντικά μεγαλύτερη σκληρότητα από τα KN για επίπεδα σορβιτόλης από 0% έως 5% (Σχήμα 2), ενώ οι τιμές μικροσκληρότητας των εξωθημάτων KN και KW πλησιάζουν στο επίπεδο σορβιτόλης 10% (1.37 και 1.32, αντίστοιχα).

Η απορροφούμενη μηχανική ενέργεια κατά τη συμπίεση (εμβαδό κάτω από την καμπύλη συμπίεσης, Σχήμα 3) είναι σημαντικά χαμηλότερη στα θερμοεξωθήματα το οποίο σχετίζεται με το χαμηλότερο Tg, πιο μαλακή επιφάνεια και λιγότερες διεπιφανειακές τριβές.

## Συμπεράσματα

Η θερμοεξώθηση οδήγησε σε μείωση του Tg, σε σύγκριση με φυσικά μείγματα και ήταν μεγαλύτερη για εξωθήματα με

πολυμερές χαμηλής ενυδάτωσης (KN). Μάλιστα, τα  $T_g$  των εξωθημάτων μειγμάτων KN ήταν πολύ κοντά στις προβλεπόμενες θεωρητικές τιμές που υποδηλώνει ιδανική ανάμειξη των συστατικών στο εξώθημα.

Η σορβιτόλη λειτουργεί σαν πλαστικοποιητής σε όλες τις αναλογίες για μείγματα με πολυμερές χαμηλής ενυδάτωσης KN, αλλά για μείγματα με πολυμερές υψηλής ενυδάτωσης (KW) μόνο σε αναλογίες 5% και 10% ενώ στη χαμηλή αναλογία 2.5% ασκεί ισχυρή αντιπλαστικοποιητική δράση.

Η αντιπλαστικοποιητική δράση της σορβιτόλης είχε σαν αποτέλεσμα αύξηση της επιφανειακής τραχύτητας και της σκληρότητας, αλλά μείωση της χαλάρωσης τάσης.

#### Αναφορές

- [1]. Chamarthy SP, Pina R. Plasticizer concentration and the performance of a diffusion-controlled polymeric drug delivery system. *Colloid Surf A Physicochem Eng Asp*, 2008; 331(1-2): 25-30.
- [2]. Hauschild K, Picker-Freyer KM. Evaluation of tableting and tablet properties of Kollidon SR: the influence of moisture and mixtures with theophylline monohydrate. *Pharm Dev Technol*, 2006; 11(1): 125-140.

## Dual-Responsive DSPC:P(OEGMA<sub>950</sub>-DIPAEMA) nanostructures: Evaluating the design parameters affecting their performance

Efstathia Triantafyllou<sup>1</sup>, Dimitrios Selianitis<sup>2</sup>, Maria Gazouli<sup>3</sup>, Natassa Pippa<sup>1</sup>, Georgia Valsami<sup>1</sup>, Stergios Pispas<sup>2</sup>

<sup>1</sup>Section of Pharmaceutical Technology, Department of Pharmacy, School of Health Sciences, National and Kapodistrian University of Athens, Panepistimioupolis Zografou, 15771 Athens, Greece;

<sup>2</sup>Theoretical and Physical Chemistry Institute, National Hellenic Research Foundation, 48 Vassileos Constantinou Avenue, 11635 Athens, Greece

<sup>3</sup>Laboratory of Biology, Department of Basic Medical Science, School of Medicine National and Kapodistrian, University of Athens, 11527 Athens, Greece

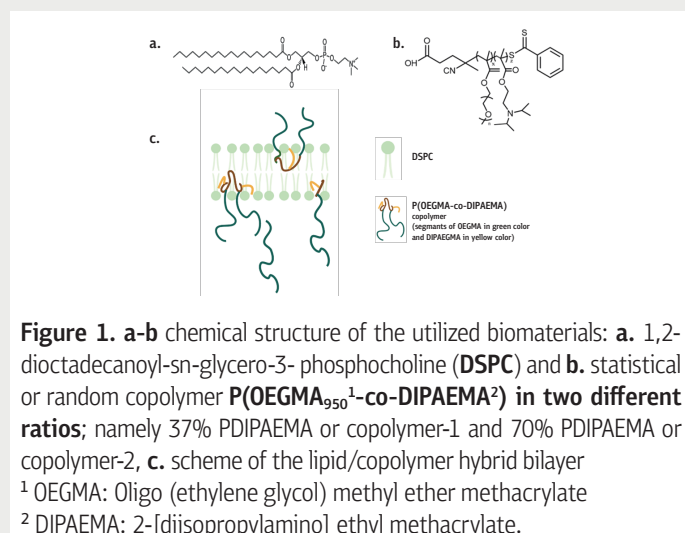
CONTACT INFO: [efstrian@pharm.uoa.gr](mailto:efstrian@pharm.uoa.gr), [natpippa@pharmuoa.gr](mailto:natpippa@pharmuoa.gr)

### Introduction

Hybrid nanoparticles are nanocarriers, composed of **two or more different biomaterials**, which maintain the biophysical properties all of the components. Lipid/polymer nanostructures are among the most promising hybrid nanoparticles, as they combine liposomes' biocompatibility and the physical stability of polymeric nanoparticles. Furthermore, nanoplatfroms that respond to an internal or external stimulus, such as pH or/and heat, can be used for novel treatment due to spatiotemporal release. The **main purpose** of this study is to develop hybrid nanostructures with **stimuli- responsive properties** and investigate the **parameters affecting their behavior** from a biophysical, physicochemical, and toxicological point of view.

### Methodology

- Differential scanning calorimetry
- Dynamic and Static Light Scattering
- Fluorescence spectroscopy
- MTS assay (HEK293 cell lines)



### Preformulation Studies

The preformulation studies demonstrated copolymer's incorporation into the bilayer and a lipid to polymer dependent biophysical behavior (Figure 2). According to these results the location of the copolymer into the bilayer could be as the Figure 1c suggests.

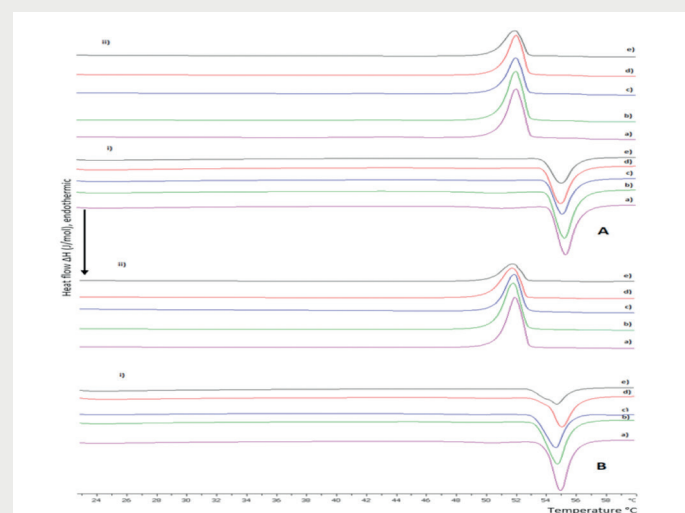


**Figure 2.** Thermotropic behavior of hydrated **A.** DSPC:copolymer-1 and **B.** DSPC:copolymer-2 bilayers in different lipid to polymer ratios: a) 9:1, b) 8:2, c) 7:3, d) 6:4, and e) 5:5 during i) heating and ii) cooling.

### Results

The physicochemical characteristics of the lipid/copolymer nanostructures indicate **appropriate size for drug delivery applications**, polar microenvironment, and a rather loose conformation as described in Table 1, while there **are size fluctuations in different pH and temperature conditions** (Figures 3 and 4). According to MTS assay the nanocarriers are mainly **biocompatible** having a dose dependent cytotoxicity (Figure 5). Generally, the nanostructures utilizing copolymer-2 over 1 are more biocompatible.

**Table 1.** Physicochemical properties of selected lipid/copolymer systems at 25°C and in aqueous dispersion medium.

System	Weight Ratio	I (kHz)	Rh (nm)	PDI	Rg/Rh	I <sub>1</sub> /I <sub>3</sub>
DSPC:1	9:1	4210	62	0,31	1,4	1,65
DSPC:1	7:3	21645	103	0,20	1,3	1,78
DSPC:1	5:5	3023	58	0,31	1,4	1,68
DSPC:2	9:1	1087	58	0.42	-	1.68
DSPC:2	7:3	413	23	0.46	-	1.67
DSPC:2	5:5	499	33	0.27	-	1.58

### Physicochemical behavior in pH and temperature changes

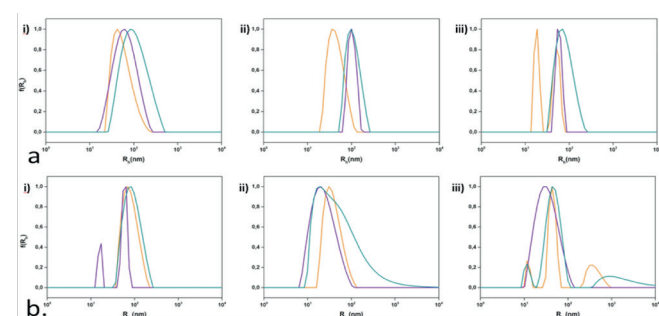


**Figure 3.** Size distribution from DLS for the hybrid systems incorporating (a) DSPC:copolymer-1 and (b) DSPC:copolymer-2 in three different lipid to polymer weight ratios: i) 9:1, ii) 7:3, iii) 5:5, and three different pH media: HCl 0.1N (pH 1.2) (orange color), water for injection (pH 5.5) (purple color), PBS (pH 7.4) (green color).

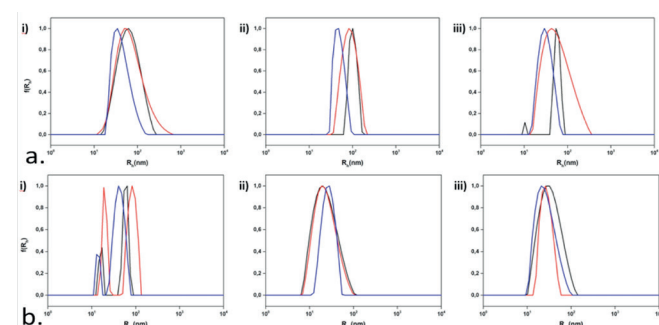


**Figure 4.** Size distribution from DLS for the hybrid systems incorporating (a) DSPC:copolymer-1 and (b) DSPC:copolymer-2 in three different lipid to polymer weight ratios: i) 9:1, ii) 7:3, iii) 5:5, and three different temperatures: 25°C (black color), 37°C (red color), and 60°C (blue color).

### In vitro toxicity

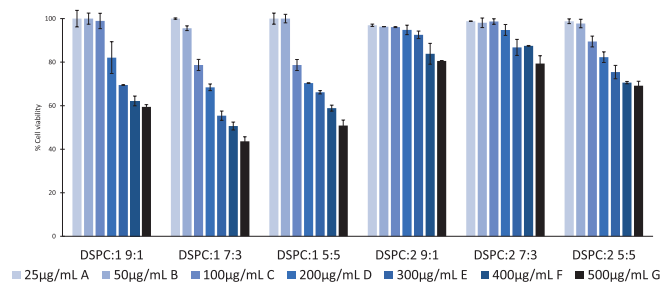


**Figure 5.** Cell viability vs. different concentrations of DSPC hybrid systems incorporating co-polymer: (a) P(OEGMA950-DIPAEMA)-1; or (b) P(OEGMA950-DIPAEMA)-2 at different lipid to polymer weight ratios. The error bars represent the standard deviation.

### Conclusions

**Non-toxic and stimuli-responsive hybrid lipid/copolymer** nanosystems were successfully formed and the main design parameters influencing their performance were identified including:

- copolymer's architecture
- hydrophobic to hydrophilic ratio
- lipid to copolymer ratio.

### References

1. Avanti Polar Lipids. Available online: <https://avantilipids.com/> (accessed 17 June 2022).
2. Triantafyllopoulou E, Selianitis D, Pippa N, Gazouli M, Valsami G, Pispas S. Development of Hybrid DSPC:DOPC:P(OEGMA950-DIPAEMA) Nanostructures: The Random Architecture of Polymeric Guest as a Key Design Parameter. *Polymers*. 2023; 15(9):1989. <https://doi.org/10.3390/polym15091989>

### Acknowledgments

We thank C. Demetzos and his laboratory team for the kind permission to use their lab equipment for the DSC experiments as well as Hector Katifelis for his contribution in the *in vitro* toxicity studies.



## Tablets of Enteric Microencapsulated Oregano Essential Oil Powders -Evaluation and Release

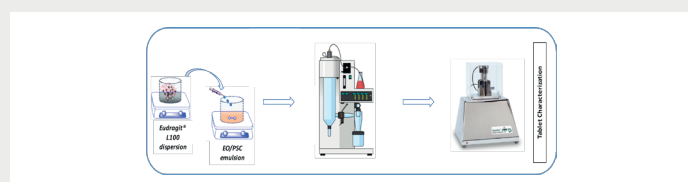
Ioannis Partheniadis, Dimitra Tsalavouti, Anastasia Charisi, Ioannis Nikolakakis

Laboratory of Pharmaceutical Technology, School of Pharmacy, Faculty of Health Sciences, Aristotle University of Thessaloniki, 54124 Greece.

Email: ioanpart@pharm.auth.gr (I.P.), tsalavout@pharm.auth.gr (D.T.), charianast@pharm.auth.gr (A.C.) and yannikos@pharm.auth.gr (I.N.)

### Introduction

Oregano essential oil (EO) of Greek origin with high carvacrol content (86.84%) has been shown to be effective in a microencapsulated with polysaccharides spray-dried solid form against strains of *E. coli*, *Klebsiella sp.*, *S. aureus* and *P. mirabilis*<sup>[1]</sup>. Since its efficiency is associated with action in the intestine, in this work we have prepared tablets of the EO by compressing a spray-dried enteric release powder form in which the EO is microencapsulated in a polysaccharide/ methacrylate wall<sup>[2]</sup>. The polysaccharidic (PSC) part of the wall consisted of Arabic gum, modified starch and maltodextrin, providing emulsion stabilization, environmental protection and prevention of vaporization, of the EO constituents. The methacrylate polymer (PLM) was Eudragit® L100 providing enteric release. Additionally, four different grades of maltodextrins were used differing in their *T<sub>g</sub>* and molecular weight (Mw), and origin (corn or pea).



### Methodology

**Materials:** Oregano essential oil (EO; 85.89% carvacrol) from *Oreganum vulgare* was from Ecopharm (Greece), Arabic gum (AG) from Nexira (France), maltodextrins (MD) (Table 1) and modified food grade starch (Cleargum® CO03, sodium octenyl succinate starch of high and low viscosity respectively) from Roquette (Italy) via Interallis Chemicals, Greece and Eudragit® L100 from Evonik, Darmstadt, Germany via ChemiX SA, Greece.

**Spray-Drying:** The EO/PSC emulsions and Eudragit® L100 dispersion were prepared as described previously<sup>[2]</sup>. PSC emulsions were spray-dried as such to prepare the instant release powders (PSC wall only) or combined with the PLM dispersion in a ratio of 20:80 w/w to prepare the enteric powders (PSC/PLM wall). 100-mL of feed dispersion was

spray-dried (B-191, Büchi, Switzerland) under the conditions: inlet air 145°C, feed rate 3.5 mL/min, air flow 600 mL/min. Yield and oil retention (%) were determined<sup>[1]</sup>.

**Size and shape of particles:** Mean particle diameter and shape (roundness) of particles were analyzed with optical microscopy (Olympus BX41, Japan and video camera Leica DF295, Germany) using image analysis. For the evaluation of the morphology of the particles scanning electron microscopy (SEM) was performed using a microscope equipped with W filament (15 kV, JEOL JSM- 6390LV, Jeol, Tokyo, Japan), EDS and Oxford INCA microanalysis system.

**ATR-FTIR Spectroscopy:** FTIR spectra were obtained using a Shimadzu FT-IR-Prestige-21 spectrometer and software (Shimadzu Corporation, IR Solution 1.3) attached to an ATR system (Specac, Kent, UK) equipped with a diamond/ZnSe crystal.

**Thermal characterization:** Thermogravimetric analysis (TGA) (TGA-50, Shimadzu, Japan) was performed to investigate oil leakage from the particles.

**Compression:** Powder samples (100 mg) were compressed at 80, 125 and 174 MPa on a tablet press (Model GTP-1, Gamlen Tableting Ltd, Nottingham, UK) fitted with 6-mm flat-faced punches at 10 mm/min. The work of compression (Wc) was computed from the area under the compression curve from the recorded force/displacement (f/d) profiles.

### Results

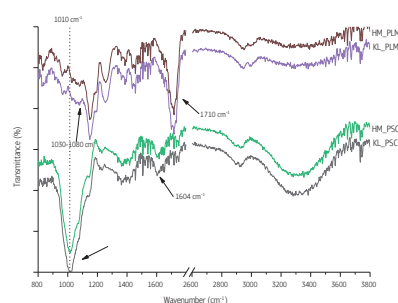


**Figure 1.** ATR-FTIR spectra of PSC only and PSC/PLM wall material spray-dried powders of the HM and KL maltodextrins.

**Table 1.** Weight loss on drying (LOD%) of solvent processed GRI/LEU feeds and corresponding HME extrudates, together with solvent residues in extrudates (mean values  $\pm$ SD, n=3).

SD product	Yield (%)	MC (%)	Recovery of EO (%)	Particle size distribution ( $\mu$ m)				%Oil Leakage*
				d <sub>10</sub>	d <sub>50</sub>	d <sub>90</sub>	Span	
KL_PSC	44.6	6.3 $\pm$ 0.04	76.0	1.27	4.19	8.15	1.64	0.106
LM_PSC	36.9	8.1 $\pm$ 0.07	73.6	1.46	4.33	13.22	2.72	0.935
MM_PSC	47.1	9.5 $\pm$ 0.08	80.0	1.23	5.58	12.75	2.06	2.886
HM_PSC	41.2	9.1 $\pm$ 0.06	74.5	1.91	6.95	15.92	2.02	2.958
KL_PLM	74.1	2.8 $\pm$ 0.06	74.4	2.24	7.43	15.16	1.74	0.226
LM_PLM	69.5	3.6 $\pm$ 0.06	73.0	1.31	4.17	14.91	3.26	0.199
MM_PLM	69.6	4.3 $\pm$ 0.06	76.0	1.98	5.31	14.57	2.37	0.006
HM_PLM	56.0	4.9 $\pm$ 0.15	72.5	1.84	5.57	12.71	1.95	0.643

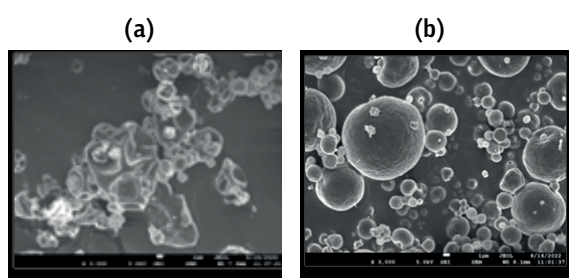


**Figure 2.** SEM microphotographs of KL\_PSC (a) and KL\_PLM (b) spray-dried particles.

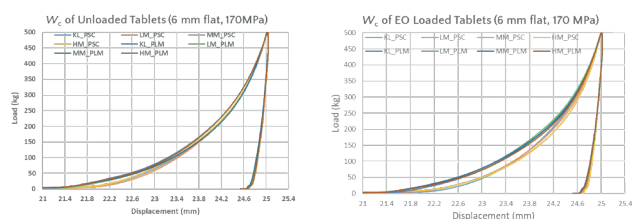


**Figure 3.** F/d profiles from the compression of the placebo and EO-loaded spray-dried powders. Areas under the curve correspond to the work of compression.

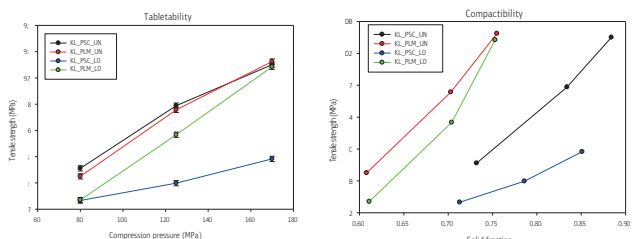


**Figure 4.** Tableability and compactibility profiles for the KL\_PSC and KL\_PLM placebo and EO-loaded products.

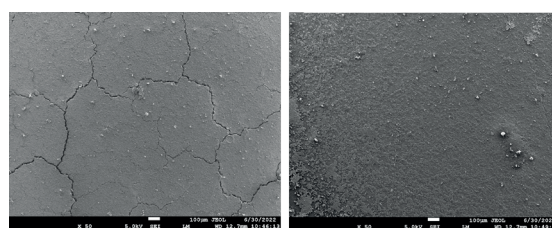


**Figure 5.** SEM microphotographs of tablet surface of KL\_PSC (left) and KL\_PLM (right) spray-dried products.

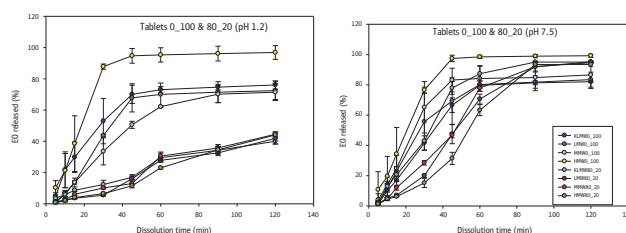


**Figure 6.** *In-vitro* release profiles of tablets of spray-dried products at gastric (pH 1.2) and enteric (pH 7.5) simulated fluids.

**Table 2.** Weight loss on drying (LOD%) of solvent processed GRI/LEU feeds and corresponding HME extrudates, together with solvent residues in extrudates (mean values  $\pm$ SD, n=3).

Wall material	Code	MC (%)	$\rho_s$ (g/cc)
Gum Arabic	GA	9.7 $\pm$ 0.21	1.414
MD Kleptose® Pea high Mw	KL	3.7 $\pm$ 0.10	1.412
MD Corn low Mw	LM	4.4 $\pm$ 0.03	1.424
MD Corn medium Mw	MM	4.5 $\pm$ 0.02	1.407
MD Corn high Mw	HM	5.6 $\pm$ 0.03	1.258
Modified starch	MS	5.6 $\pm$ 0.02	1.479
Eudragit® L100	PLM	2.6 $\pm$ 0.01	1.303

## Discussion & Conclusions

- PSC products gave lower yield due to the softer wall promoting adherence to drying chamber's wall. They also had > 2x %MC than PLM due to their higher hydrophilicity. Median diameters were between 4 and 8  $\mu\text{m}$  as expected for small bench-type spray driers[2] (Table 2).
- Regarding % oil leakage (Table 2, last column), Kleptose® maltodextrin products showed lower loss in both PSC and PSC/PLM products, providing sufficient protection and robust microencapsulation of the EO. In all cases, the polymer offers significant protection of the EO ingredients.
- ATR-FTIR spectroscopy (Fig. 1) revealed interactions between PLM and PSC that could be related to the favorable binding of the polymer with the PSC leading to spherical SD particles with coherent wall, retaining spherical shape and smooth surface during spray drying (Fig. 2).
- There was no obvious effect of MD type on the work of compression (Fig. 3). The higher Wc of PLM tablets is attributed to the PLM presence forming a plastically deforming particle surface. The increase of Wc due to PLM is more profound in the EO loaded tablets.
- From Fig. 4 increasing compression pressure increases tablet strength. Except of sample KL\_PSC\_LO, all others could form tablets at 125 MPa which is near the industri-

ally applied pressure. The curves for unloaded powders are convex but for the EO loaded they are concave implying differences in the compaction mechanism.

- The presence of plastically deforming under compression Eudragit in samples KL-PLM resulted in homogeneous tablet surface without boundaries (Fig. 5). Higher deformation resulted in greater bonding area and higher tablet strength.
- In gastric pH SDP tablets of microencapsulated EO in PSC wall gave complete release after about 60 min., whereas in PLM wall suppressed the release to 40% after 120 min (Fig. 6). In enteric pH the release was completed after about 90 min for all products.
- Rapid and enteric release tablets of EO oregano were developed by encapsulating the EO in emulsions stabilized either with PSC or a combination of PSC/PLM.

## References

1. Partheniadis I, Vergkizi S, Lazari D, Reppas C, Nikolakakis I. Formulation, characterization, and antimicrobial activity of tablets of essential oil prepared by compression of spray-dried powder. *J Drug Del Sci Tec*, 2019; 50: 226-236.
2. Partheniadis I, Zarafidou E, Litinas KE, Nikolakakis I. Enteric Release Essential Oil Prepared by Co-Spray Drying Methacrylate/ Polysaccharides—Influence of Starch Type. *Pharmaceutics*, 2020; 12(6): 571.

## PARTICLE SIZE DISTRIBUTION AND MORPHOLOGY OF UMECLINIDIUM Br API AND VILANDEROL TRIFENATATE API IN ANORO® DRY POWDER INHALER (DPI) USING SEM AND EDX

Stefani Fertaki<sup>a,b</sup>, Christos Kontoyannis<sup>a,b</sup> \*

<sup>a</sup>Department of Pharmacy, University of Patras, GR-26504 Rio Achaïas, Greece

<sup>b</sup>Institute of Chemical Engineering Sciences, Foundation of Research and Technology- Hellas (ICE-HT/FORTH), GR-26504 Platani Achaïas, Greece

\*Corresponding Author: Christos Kontoyannis, 2610962328, kontoyan@upatras.gr

### Introduction

Dry powder inhalers (DPIs) contain a powder formulation, which consists of an ordered mixture of micronized drug and larger carrier lactose particles that are required to improve powder flow properties. The patient's inhalation through the device is used to disperse the powder and to ensure that some of the dose is carried into the lungs [1]. The particle size of active pharmaceutical ingredients (APIs) is normally up to 5  $\mu\text{m}$ , but the size of the carrier particles (usually lactose or glucose) can range from approximately 20 to 65  $\mu\text{m}$  [2]. Identification of the particle size and morphology of such small API particles in usually significantly low content in the simultaneous presence of large carrier lactose particles though, is considered a challenging task. The commonly used analytical techniques such as optical microscopy and/or laser diffraction cannot be applied in the DPIs due to the very low API particle size in the presence of the large carrier particles that cannot be successfully distinguished.

### Scope of the Study

In the current work Anoro® DPI was studied. Each inhaler contains two double-foil blister strips of powder formulation. Each dose contains umeclidinium 62.5 mg in one blister and vilanterol 25 mg in another blister and it is used to treat chronic obstructive pulmonary diseases. The purpose of this work thus, was to identify, discriminate and measure the PSD of the two different APIs in Anoro® DPI along with visual observation of their morphology.

### Methodology

Scanning electron microscope (SEM), which provides information for particles even at nanoscale, coupled with Energy Dispersive X-Ray Spectroscopy (EDX) was used based on the ability of EDX to identify different unique atoms that each of the components contains (Br for umeclidinium identification and Cl for vilanterol identification).

Zeiss SUPRA 35VP SEM operating at 15 kV coupled with EDX (Energy Dispersive X-Ray Spectroscopy) Quanta 200 (Bruker AXS) at resolution of 133 eV. A few milligrams of the sample were placed in SEM holder. Approx. 5 small areas of the sample were scanned for 15-30 min.

### Results

EDX was adjusted to search for Bromide which is present only in Umeclidinium Bromide API or Chloride for Vilanterol. This resulted in visualized score maps with red pixels where the intense bright red pixels corresponded to Bromide or Chloride presence respectively while the dark red pixels corresponded to either Lactose or Magnesium Stearate presence (Fig.1-2). Each red spot was then re-focused using higher magnification and scanned using EDX to verify Bromide presence by its peak as in Fig.3 and check its morphology. The same procedure was repeated until at least 50 API particles were identified. Each API particle was finally calculated using Image J software (Fig.4). The mean diameter of umeclidinium was calculated at approx. 2.91  $\mu\text{m}$  while in vilanterol blister the respective diameter was approx. 2.09  $\mu\text{m}$  along with their d10, d50 and d90 values (Table I).

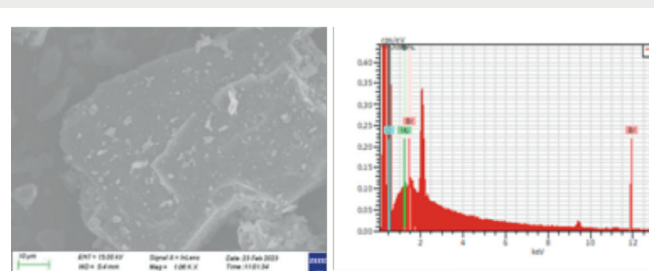


**Figure 1.** SEM image of Anoro® Reference product (blister strips of Umeclidinium bromide blend) at 1.06KX Magnification (left image) and EDX microanalysis (right image).



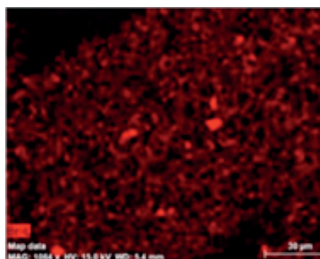


Figure 2. Visualized maps using EDX microanalysis.

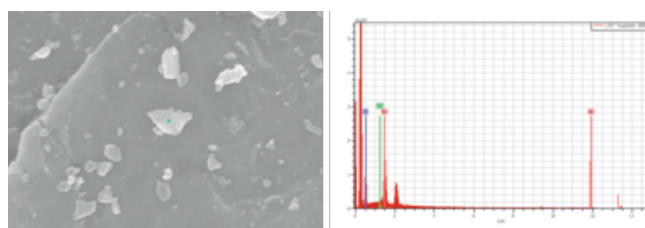


Figure 3. EDX microanalysis of first red spot of Fig.2 .

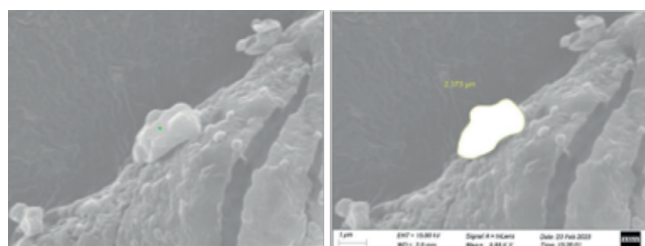


Figure 4. Images of Anoro® Reference product (blister strips of Umeclidinium bromide blend) Lot: GU2P in original mode (left) and after Image Analysis method (right) using 12.54KX magnification.



Table 1. Particle size measurements of Umeclidinium bromide and Vilanterol particles measured from Anoro® Reference resulting from the calculated area of each particle.

Umeclidinium Br			
D(0.1)	D(0.5)	D(0.9)	Mean Diameter
2.75 μm	4.60 μm	7.30 μm	2.91 μm
Vilanterol Trifenatate			
D(0.1)	D(0.5)	D(0.9)	Mean Diameter
1.91 μm	2.80 μm	4.30 μm	2.09 μm

## References

- [1] S.P. Newman, AEROSOLS, Encyclopedia of Respiratory Medicine, 2006.
- [2] Beth L. Laube, Myrna B. Dolovich, Aerosols and Aerosol Drug Delivery Systems, Middleton's Allergy (Eighth Edition), 2014.

## GREEN SYNTHESIS AND CHARACTERIZATION OF COPPER OXIDE NANOPARTICLES FOR TOPICAL APPLICATION

Chrysi Chaikali<sup>1</sup>, Paraskevi Lampropoulou<sup>2</sup>, Dimitris Papoulis<sup>2</sup>, Konstantinos Avgoustakis<sup>1</sup>, Fotini Lamari<sup>1</sup>,  
Sophia Hatziantoniou<sup>1\*</sup>

<sup>1</sup>Department of Pharmacy, University of Patras, Patras GR-26504, Greece

<sup>2</sup>Department of Geology, University of Patras, Patras GR-26504, Greece

e-mail: sohatzi@upatras.gr

### Introduction:

Green synthesis methods involving natural plant extracts and juices have gained interest because of their eco-friendly nature and potential uses in nanoparticle synthesis. Copper oxide nanoparticles (CuONPs) have found applications in a wide variety of fields, including pharmaceuticals and cosmetics, due to their unique properties such as antibacterial and anti-inflammatory effects. **In this study**, we report a green and sustainable method for CuONPs synthesis using natural reducing agents. Juices from Pomegranate (*Punica granatum*) and black chokeberry (*Aronia melanocarpa*) and extracts from rockrose (*cistus ladanifer*), sea buckthorn (*Elaeagnus rhamnoides*, syn. *Hippophae rhamnoides*), and dittany (*Origanum dictamnus*), were used as reducing agents for the synthesis of CuONPs. Conventional CuONPs were also prepared using chemical reducing agents (ascorbic acid or NaBH<sub>4</sub>) and served as control. The synthesis method was optimized regulating the experimental conditions such as temperature, pH and volume ratio of reactants. The synthesis of CuONPs was monitored using UV-Vis spectroscopy. The physicochemical characteristics of the CuONPs (size and ζ-potential distribution) was estimated using Dynamic Light Scattering (DLS) and Electrophoretic Light Scattering (ELS) respectively. Their crystallinity was characterized using X-Ray Diffraction (XRD). The physicochemical stability of the CuONPs aqueous distributions was evaluated by storing them under several conditions and monitoring their physicochemical characteristics weekly for 30 days.

### Methodology

The synthesis of CuONPs was achieved using CuCl<sub>2</sub>·2H<sub>2</sub>O solutions (1mM) and pomegranate juice or a solution of chokeberry juice, buckthorn, dittany and rockrose. CuONPs

were, also, synthesized using conventional reducing agents (ascorbic acid or NaBH<sub>4</sub> for comparison). The CuONPs were synthesized under light at 60°C-80°C and pH was adjusted at 12 using NaOH solution (10N). The reaction time was 60 seconds and after its completion the solution was centrifuged in 12.000 rpm for 15 minutes. The sediment was collected and dispersed in deionized water and the procedure was repeated 3-4 times. The sediment was left in a laboratory oven to dry for 24 hours and then was stored for further analysis.

The formation of the CuONPs monitored using UV/Vis spectrophotometry (UV-1800 UV-vis spectrophotometer, SHIMADZU, Kyoto, Japan).

The mean size (average hydrodynamic diameter) and zeta-potential of CuONPs was monitored by Dynamic Light Scattering (DLS) and Electrophoretic Light Scattering (ELS) respectively (Zetasizer, Nano ZS, Malvern Panalytical, Malvern, UK). The samples were diluted in WFI (sample/WFI 1:6 v/v) and measurements for each sample were repeated three times at 25°C. TEM analysis revealed the morphology of CuONPs, deriving from different reducing agents. The crystalline nature of the nanoparticles was determined by X-Ray Diffraction (XRD, Bruker D8 Advance Diffractometer, Berlin, Germany) and SAED patterns from TEM.

The stability of CuONPs was assessed for a period of 30 days by monitoring their mean size and zeta-potential at predetermined time intervals (1, 8, 15, 22, 30 days after preparation).

### Results

#### Nanoparticle synthesis monitored by UV/Vis spectroscopy

The UV/Visible spectroscopy results indicated the presence of surface plasmon resonance peaks, at about 400nm which are characteristic of metallic nanoparticles of Cu<sub>2</sub>O (Fig 1).

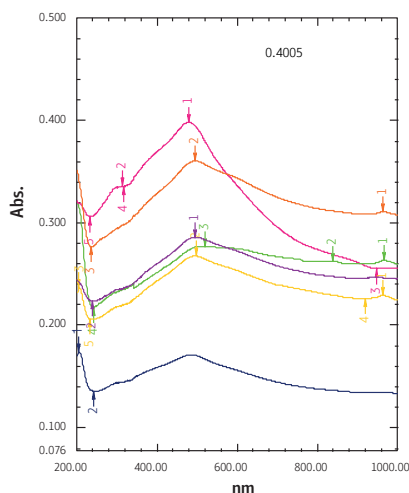


Figure 1. UV/Vis spectrum of the CuONPs with different reducing agents.

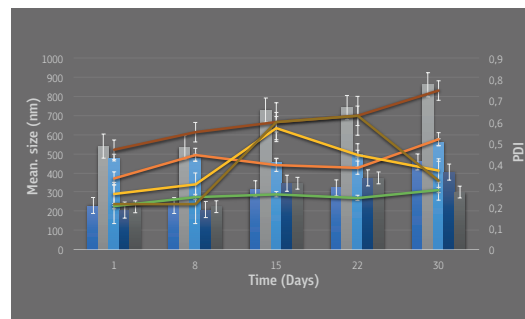


Figure 2. Monitoring of size distribution of CuONPs for 30 days. CuONPs using pomegranate juice (■), chokeberry juice (■), buckthorn (■), dittany (■) and rockrose (■).

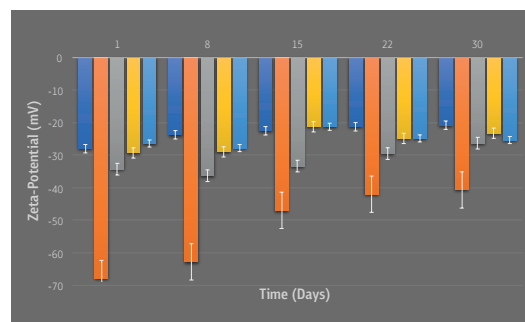


Figure 3. Monitoring of zeta-potential distribution of CuONPs for 30 days. CuONPs using pomegranate juice (■), chokeberry juice (■), buckthorn (■), dittany (■) and rockrose (■).

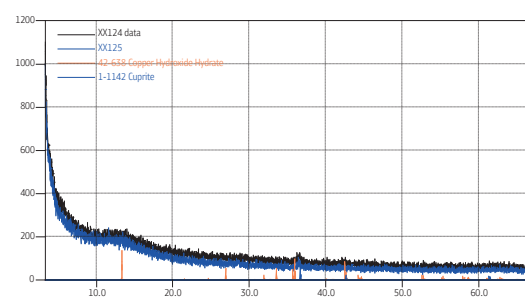


Figure 4. XRD spectrum of CuONPs.

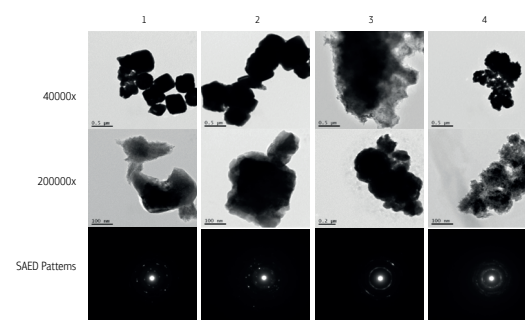


Figure 5. TEM images and SAED Patterns of the CuONPs obtained by pomegranate juice

### Impact of the reducing agent on the physicochemical characteristics of CuONPs

According to Table 1, particles with smaller size and better zeta-potential value were obtained from the reaction using dittany as reducing agent.

Table1: Physicochemical properties of CuONPs.

Reducing agent	Mean size (nm)	Pdl	ζ-potential (mV)
pomegranate juice	230 ± 23,48	0,334 ± 0,04	-28 ± 0,6
chokeberry juice	540 ± 26,05	0,261 ± 0,04	-67,9 ± 2,22
buckthorn	480 ± 5,1	0,204 ± 0,04	-34,3 ± 0,1
dittany	206 ± 6,39	0,469 ± 0,2	-29,3 ± 2,42
rockrose	223 ± 4,04	0,213 ± 0,01	-26,4 ± 0,65
NaBH4	320 ± 17,32	0,250 ± 0,035	-23,3 ± 1,61

### Stability study of CuONPs

The size and zeta-potential distribution of the CuONPs which were obtained from reaction of different reducing agents was monitored for 30 days. All the CuONPs were stable during the 30 days time period, except from the CuONPs which were produced using chokeberry juice (Fig 2, 3).

### Crystallinity of CuONPs

The XRD results showed the presence of Cu<sub>2</sub>O in the CuONPs which were obtained by the reactions of different reducing agents (Fig 4).

### Morphology of CuONPs

The TEM images revealed the morphological differences between the CuONPs which are obtained in different reaction conditions using pomegranate juice. The SAED patterns of the CuONPs are also shown, which reveal the distance between the diffraction centers and prove the crystal structure of the synthesized CuONPs (Fig. 5).

### Conclusions

Our results suggest that pomegranate juice, chokeberry juice, buckthorn, dittany and rockrose are promising candidates for

the green synthesis of CuONPs suitable for topical applications in pharmaceuticals and cosmetics.

### References

1. Miu, B. A., & Dinischiotu, A. (2022). *Molecules* (Basel, Switzerland), 27(19), 6472.
2. Siakavella, I. K., Lamari, F., Papoulis, D., Orkoulas, M., Gkolfi, P., Lykouras, M., Avgoustakis, K., & Hatziantoniou, S. (2020). *Pharmaceutics*, 12(12), 1244.
3. Chakraborty, N., Banerjee, J., Chakraborty, P., Banerjee, A., Chanda, S., Ray, K., Acharya, K., & Joy Sarkar. (2022). *Green Chemistry Letters and Reviews*, 15(1), 187-215.
4. Khan, I., Saeed, K., Khan, I., (2019), *Arabian Journal of Chemistry*, 12(7), 908-931.



## Πρόδρομα αποτελέσματα τυχαίοποιημένης, ελεγχόμενης με placebo μελέτης της επίδρασης παραγώγων της καφεΐνης στη μικροτοπογραφία του δέρματος

Μαρία Χρυσογιάννη<sup>α</sup>, Σταματίνα Πιτσάβα<sup>α</sup>, Μιλτιάδης Χαλικιάς<sup>β</sup>, Ελένη Σκαλτσά<sup>γ</sup>, Παναγούλα Παύλου<sup>α,δ</sup>, Φωτεινή Μέλλου<sup>δ</sup>, Σπυρίδων Παπαγεωργίου<sup>α,δ</sup>, Απόστολος Παπαδόπουλος<sup>α,δ</sup>, Ελένη Κίντζιου<sup>α,δ</sup>, Ευστάθιος Ράλλης<sup>δ</sup>, Αθανασία Βαρβαρέσου<sup>α,δ</sup> \*

<sup>α</sup>Εργαστήριο Χημείας-Βιοχημείας-Κοσμητολογίας, Τμήμα Βιοϊατρικών Επιστημών, Πανεπιστήμιο Δυτικής Αττικής 28 Αγίου Σπυρίδωνος, GR-12243

<sup>β</sup>Τμήμα Λογιστικής και Χρηματοοικονομικής Πανεπιστήμιο Δυτικής Αττικής 28 Αγίου Σπυρίδωνος, GR-12243

<sup>γ</sup>Τομέας Φαρμακογνωσίας, Τμήμα Φαρμακευτικής, Εθνικό και Καποδιστριακό Πανεπιστήμιο Αθηνών, Ζωγράφου, GR-15771

<sup>δ</sup>Τομέας Αισθητικής και Κοσμητολογίας, Τμήμα Βιοϊατρικών Επιστημών, Πανεπιστήμιο Δυτικής Αττικής 28 Αγίου Σπυρίδωνος, GR-12243

\*Υπεύθυνος αλληλογραφίας: Αθανασία Βαρβαρέσου, [anarvares@uniwa.gr](mailto:anarvares@uniwa.gr)

### Εισαγωγή

Το αλκαλοειδές καφεΐνη, χρησιμοποιείται στα καλλυντικά με ισχυρισμούς: αντι-γήρανσης, μείωσης της κυτταρίτιδας και του τοπικού πάχους και εξάλειψης των μαύρων κύκλων και του οιδήματος στην περιοχή κάτω από τα μάτια. Εκτός από την ελεύθερη μορφή της σε σκόνη, χρησιμοποιούνται και οι ενθυλακωμένες της μορφές, τόσο σε λιποσώματα όσο και σε κυκλοδεξτρίνες. Το κίτρινο αλκαλοειδές, βερβερίνη έχει αντιοξειδωτικές, αντιφλεγμονώδεις και αντιμικροβιακές ιδιότητες, ενώ έχουν αναφερθεί και αντιγηραντικές ιδιότητες.

Το αλκαλοειδές, πιπερίνη, φαίνεται να αυξάνει την ενδοδερμική μεταφορά των ενεργών συστατικών. Τα κόκκινα φύκη, λόγω των εξαιρετικά πλούσιων βιοδραστικών συστατικών τους – μεταξύ των οποίων και αλκαλοειδή- παρουσιάζουν ποικίλους λειτουργικούς ρόλους κατά την ανάπτυξη νέων, «πράσινων», καινοτόμων καλλυντικών προϊόντων.

Αν και η λιπολυτική δράση της καφεΐνης έχει μελετηθεί αρκετά, οι σχετικές με την επίδρασή της στη μικροτοπογραφία και την ελαστικότητα του δέρματος ιδιότητες της δεν έχουν εκτενώς διερευνηθεί. Αναπτύξαμε τις παρακάτω Συνθέσεις:

Σύνθεση 1: ο/w γαλάκτωμα, ως placebo.

Σύνθεση 2: Η σύνθεση του placebo όπου ενσωματώθηκαν ενεργά συστατικά που περιέχουν λιποσωμική καφεΐνη, βερβερίνη, πιπερίνη και εκχύλισμα κόκκινων φυκών.

Σύνθεση 3: Η σύνθεση του placebo όπου ενσωματώθηκαν ενεργά συστατικά που περιέχουν καφεΐνη σε κυκλοδεξτρίνη, βερβερίνη, πιπερίνη και εκχύλισμα κόκκινων φυκών.

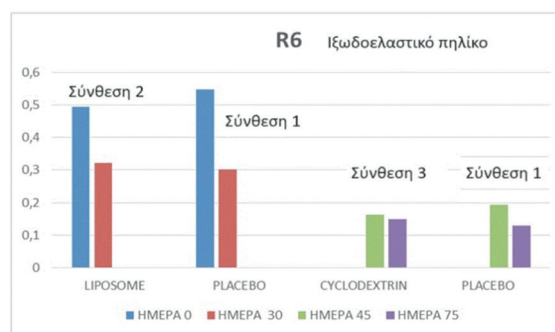
### Μέθοδοι

Διεξήχθη κλινική μελέτη-αξιολόγηση 75 ημερών, της επίδρασης των παραπάνω συνθέσεων στην ελαστικότητα του

δέρματος (Cutometer® dual MPA 580, Courage and Khazaka, Cologne, Germany) και στη μικροτοπογραφία του δέρματος υγιών εθελοντών με βιοφυσικές μετρήσεις καθώς και με αυτοαξιολόγηση.

Η μελέτη ήταν τυχαίοποιημένη, ελεγχόμενη με placebo, στην οποία συμμετείχαν 20 υγιείς γυναίκες ηλικίας 35-60 ετών.

Κατά τις πρώτες 30 ημέρες (Φάση 1), το μισό πρόσωπο υποβλήθηκε σε θεραπεία με placebo (1) και το άλλο μισό με το λιποσωμικό προϊόν καφεΐνης (2). Ακολούθησε ένα διάλειμμα 15 ημερών με το placebo (Φάση 0) να εφαρμόζεται σε όλο το πρόσωπο, ώστε τα αποτελέσματα της επόμενης φάσης (Φάση 2) να μην επηρεαστούν από την επίδραση της Σύνθεσης 2. Για τις επόμενες 30 ημέρες, το μισό πρόσωπο υποβλήθηκε σε θεραπεία με placebo (1) και το άλλο μισό με το προϊόν καφεΐνης σε κυκλοδεξτρίνη (3). Τα προϊόντα εφαρμόζονταν δύο



Φάση 1  
Σύνθεση 1 p=0.004 HM0-30  
Σύνθεση 2 p=0.02 HM0-30  
Φάση 2  
Σύνθεση 3 p=0.46 HM 45-75  
Σύνθεση 1 p=0.004 HM45-HM75

**Διάγραμμα 1.** Μεταβολή του παράγοντα R6 για τις Συνθέσεις 1, 2, 3 κατά τη διάρκεια του πειράματος.

**Πίνακας 1.** Οι συνθέσεις αποδείχθηκαν σταθερές στη δοκιμασία της επιταχυνόμενης γήρανσης και στην αποτελεσματικότητα του συστήματος συντήρησης (ΕΦ). Φυσικοχημική σταθερότητα -Επιταχυνόμενη γήρανση Σύνθεση 2- λιποσωμακική καφεΐνη (Ενδεικτικά).

Κύκλος	°C	pH	Χρώμα	Οσμή	Αίσθηση	Ιξώδες	Διαχωρισμός φάσεων	Αποτέλεσμα παρατήρησης
1ος	4	5,5	NCC	N	P	VN	NS	ΑΠΟΔΕΚΤΟ
	25	5,5	NCC	N	P	VN	NS	ΑΠΟΔΕΚΤΟ
	45	5,45	NCC	N	P	VN	NS	ΑΠΟΔΕΚΤΟ
2ος	4	5,5	NCC	N	P	VN	NS	ΑΠΟΔΕΚΤΟ
	25	5,5	NCC	N	P	VN	NS	ΑΠΟΔΕΚΤΟ
	45	5,45	NCC	N	P	VN	NS	ΑΠΟΔΕΚΤΟ
3ος	4	5,48	NCC	N	P	VN	NS	ΑΠΟΔΕΚΤΟ
	25	5,47	NCC	N	P	VN	NS	ΑΠΟΔΕΚΤΟ
	45	5,44	NCC	N	P	VN	NS	ΑΠΟΔΕΚΤΟ
4ος	4	5,48	NCC	N	P	VN	NS	ΑΠΟΔΕΚΤΟ
	25	5,46	NCC	N	P	VN	NS	ΑΠΟΔΕΚΤΟ
	45	5,44	NCC	N	P	VN	NS	ΑΠΟΔΕΚΤΟ
5ος	4	5,48	NCC	N	P	VN	NS	ΑΠΟΔΕΚΤΟ
	25	5,46	NCC	N	P	VN	NS	ΑΠΟΔΕΚΤΟ
	45	5,44	NCC	N	P	VN	NS	ΑΠΟΔΕΚΤΟ
6ος	4	5,47	NCC	N	P	VN	NS	ΑΠΟΔΕΚΤΟ
	25	5,46	NCC	N	P	VN	NS	ΑΠΟΔΕΚΤΟ
	45	5,43	NCC	N	P	VN	NS	ΑΠΟΔΕΚΤΟ
7ος	4	5,45	NCC	N	P	VN	NS	ΑΠΟΔΕΚΤΟ
	25	5,44	NCC	N	P	VN	NS	ΑΠΟΔΕΚΤΟ
	45	5,42	NCC	N	P	VN	NS	ΑΠΟΔΕΚΤΟ
8ος	4	5,43	NCC	N	P	VN	NS	ΑΠΟΔΕΚΤΟ
	25	5,42	NCC	N	P	VN	NS	ΑΠΟΔΕΚΤΟ
	45	5,40	NCC	N	P	VN	NS	ΑΠΟΔΕΚΤΟ
χρώμα	NCC: χωρίς αλλαγή χρώματος		αίσθηση		P: ευχάριστη αίσθηση, εύκολη επάλειψη			
	SCC: ελαφρώς αλλαγή στο χρώμα				U: δυσάρεστη αίσθηση, κολλώδης, σχετικά δύσκολη επάλειψη			
	CCC: αλλαγή στο χρώμα				VU: πολύ δυσάρεστη αίσθηση, πολύ κολλώδης, δύσκολη επάλειψη			
οσμή	N: φυσιολογική		Διαχωρισμός Φάσεων		NS: χωρίς διαχωρισμό φάσεων			
	M: ελαφρώς αλλοιωμένη				PS: διαχωρισμός φάσεων			
	IM: υπερβολικά αλλοιωμένη							

φορές την ημέρα. Τις ημέρες 0, 30 (Φάση 1: 0-30), 45 (Φάση 0: 31-45) και 75 (Φάση 2: 45-75) έγιναν οι οργανολογικές μετρήσεις της ελαστικότητας του δέρματος και τις ημέρες 30 και 75 οι δοκιμασίες αυτο-αξιολόγησης.

Τα αποτελέσματα εξετάστηκαν με παραμετρικές και μη παραμετρικές στατιστικές δοκιμασίες (*paired samples t-tests* και *Wilcoxon tests*).

#### Αποτελέσματα-Συζήτηση:

Οι συνθέσεις αποδείχθηκαν σταθερές στη δοκιμασία της επιταχυνόμενης γήρανσης και στη δοκιμασία του συστήματος συντήρησης-δοκιμασία πρόκλησης (Πίνακες 1, 2).

**Ελαστικότητα:** Παράγοντας R6 -Ιξωδοελαστικό ηλικίο: R6=U<sub>v</sub>/U<sub>e</sub> Ο παράγοντας R6, όπως φαίνεται στο Διάγραμμα 1, μειώθηκε και στις δύο φάσεις του πειράματος. Ειδικότερα,

**Πίνακας 2:** Αποτελεσματικότητα συστήματος συντήρησης : Σύνθεση 2- λιποσωμακή καφεΐνη (Ενδεικτικά)

	Κριτήρια	Μονάδες	Μέτρηση	Μέθοδος
Ολική μεσόφιλη χλωρίδα/total viable count	<100 cfu/gr (A)	cfu/g	<10	ISO 21149:2017
	<1000 cfu/gr (B)			
Ζύμες/Yeasts	<100 cfu/gr (A)	cfu/g	<100	ISO 16212:2017
	<1000 cfu/gr (B)			
Μύκητες/Moulds	<100 cfu/gr (A)	cfu/g	<100	ISO 16212:2017
	<1000 cfu/gr (B)			
<i>Escherichia coli</i>	ΑΠΟΥΣΙΑ	cfu/g	ΔΑ	ISO 21150:2015
<i>Staphylococcus aureus</i>	ΑΠΟΥΣΙΑ	cfu/g	ΔΑ	ISO 22718:2015
<i>Pseudomonas aeruginosa</i>	ΑΠΟΥΣΙΑ	cfu/g	ΔΑ	ISO 22717:2015

ΔΑ= Δεν ανιχνεύθηκε, Ανεπιθύμητες ενέργειες : Δεν αναφέρθηκαν

στην πρώτη φάση μειώθηκε κατά 53,1% (P=.02) για τη Σύνθεση 2 και κατά 80,8% (P=.004) για τη Σύνθεση 1.

Στη δεύτερη φάση του πειράματος, ο παράγοντας R6 μειώθηκε κατά 9,4% (P=.46) για τη Σύνθεση 3 και κατά 49,9% (P=.004) για τη Σύνθεση 1.

Σε όλες τις παραπάνω περιπτώσεις, η μείωση του παράγοντα R6 υποδεικνύει αύξηση της ελαστικότητας του δέρματος, άρα και αποτελεσματικότητα των Συνθέσεων. Στατιστικώς σημαντικά αποτελέσματα παρουσιάζουν οι Συνθέσεις 1 και 3 καθώς ισχύει ότι P<0.05.

Πρόδρομα αποτελέσματα αυτο-αξιολόγησης εθελοντών οδήγησαν στο συμπέρασμα ότι το σύμπλοκο καφεΐνης-κυκλοδεξτρίνης (Σύνθεση 3) έχει μεγαλύτερη αποτελεσματικότητα από την λιποσωμακή καφεΐνη (Σύνθεση 2).

Η όποια διαφορά μεταξύ της αυτο-αξιολόγησης και των βιοφυσικών μετρήσεων ίσως να πρέπει να αποδοθεί στην

καλύτερη υφή της σύνθεσης καφεΐνη σε κυκλοδεξτρίνη (Σύνθεση 3), και η οποία μπορεί να επηρέασε την αυτο-αξιολόγηση.

Ανεπιθύμητες ενέργειες από την εφαρμογή των Συνθέσεων δεν αναφέρθηκαν.

### Βιβλιογραφία

- Luiz, H., Pinho, J. O., & Gaspar, M. M. (2023). Advancing Medicine with Lipid-Based Nanosystems—The Successful Case of Liposomes. *Biomedicine*, 11(2), 435. <https://doi.org/10.3390/biomedicine11020435>
- Χρυσογιάννη Μ. Ανάπτυξη και Μελέτη Σταθερότητας καλλυντικών προϊόντων με αλκαλοειδή <https://polynoe.lib.uniwa.gr/xmlui/handle/11400/4068>

### Ευχαριστίες

Βιομηχανία Πλαστικών ΑΒΕΕ, Θεσσαλονίκη.

## Experimental gingivitis in mice

Papantonaki A.I.<sup>1\*</sup>, Moustaka E.<sup>1</sup>, Petsiou A.<sup>1</sup>, Valakosta M.<sup>1</sup>, Almpani C.<sup>1</sup>, Loumou P.<sup>1</sup>, Georgakopoulou E.<sup>1</sup>, Damoulis P.<sup>1</sup>, Sfniadakis I.<sup>2</sup>, Anastassopoulou J.<sup>1</sup>, Vitsos A.<sup>1</sup>, Mossialos D.<sup>3</sup>, Rallis M.<sup>1</sup>

<sup>1</sup>Section of Pharmaceutical Technology, Department of Pharmacy, School of Health Sciences, National and Kapodistrian University of Athens,

<sup>2</sup>Athens Naval Hospital, Pathologoanatomic Laboratory, <sup>3</sup>Department of Biochemistry & Biotechnology, University of Thessaly

\* Corresponding Author: Anastasia-loanna Papantonaki, [tpapantonaki@gmail.com](mailto:tpapantonaki@gmail.com)

### Introduction

Periodontitis results in the destruction of gingival tissue and alveolar bone. Its primary etiological factor is biofilm dysbiosis, resulted from bacterial accumulation.<sup>1</sup> Diabetes Mellitus is a major risk factor for periodontal disease.<sup>2</sup> Experimental animal models enable the study of its pathogenesis and the test of new treatments. The aim of this study was to develop a simplified and efficient model of gingivitis induction in both normal and diabetic mice, mimicking the pathogenesis in humans.

### Methodology

#### Animals

52 hairless male mice type SKH-hr2 were divided into 4 groups:

- non-diabetic mice without ligation (controls)
- diabetic mice without ligation
- non-diabetic mice with ligation
- diabetic mice with ligation

#### Induction of type 1 Diabetes Mellitus

Two consecutive daily intraperitoneal injections of 100 mg/kg streptozotocin (STZ).

The obtained glucose levels were 500-600 mg/dl.

#### Induction of gingivitis

Ligation of the left maxillary incisor with the use of dental floss.<sup>3,4</sup>

#### Evaluation

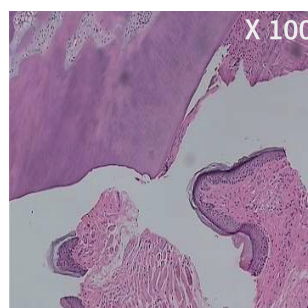
1. Clinical assessment (scoring system)

	Scoring system
0	Normal
1	Erythema
2	Erythema, oedema
3	Erythema, oedema, bleeding on probing

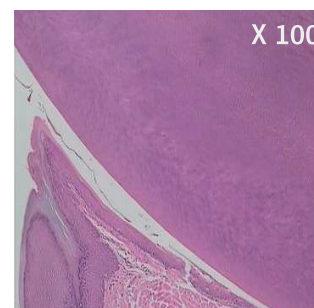
2. Histopathological analysis
3. Photo-documentation
4. Periodontal Transepidermal Water Loss (TEWL)
5. Periodontal pH
6. Body weight
7. Blood glucose

### RESULTS- DISCUSSION

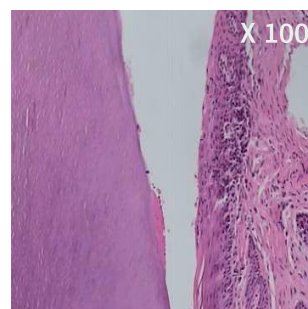
#### Histopathological analysis of the periodontium



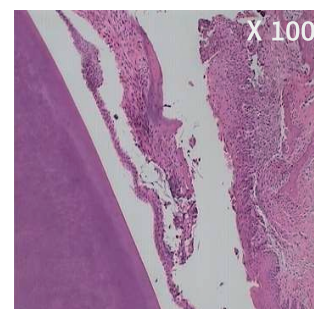
Non-diabetic mice without ligation: no inflammation



Diabetic mice without ligation: no inflammation



Non-diabetic mice with ligation: severe inflammation (aggregation of neutrophils and lymphocytes)

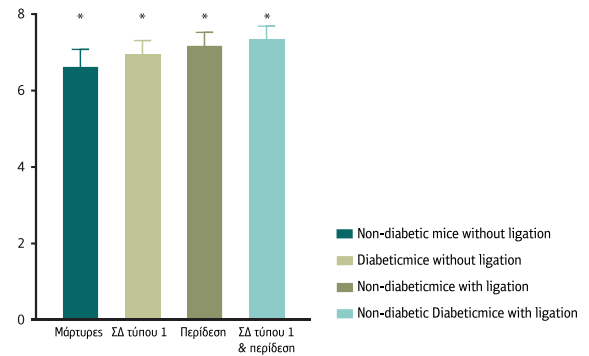


Diabetic mice with ligation: severe inflammation (aggregation of neutrophils and lymphocytes)

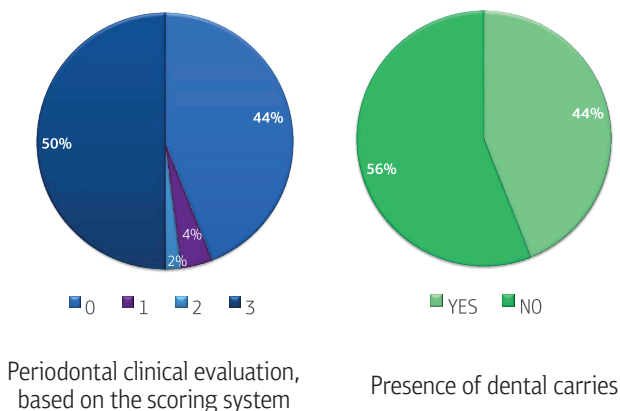
### Photo-documentation



### pH of the periodontium



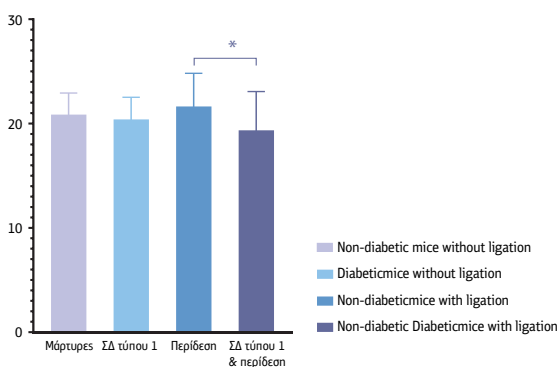
### Clinical evaluation



### Conclusions

- Ligation of the maxillary incisors provided a successful and easy method for the induction of gingivitis in mice, which does not require any specialized equipment or surgical procedure.
- Both normal and diabetic mice that received ligation developed periodontal disease. Both could be employed as gingivitis models.
- Ligation resulted in inflammation, erythema, oedema and hemorrhage. An abundance of neutrophils and lymphocytes was histologically identified in the periodontal tissue.
- Dental caries were obtained. This model could also be used for experimental induction of dental caries.

### Transepidermal water loss of the periodontium



### References

1. Gasner, N.S.; Schure, R.S. Periodontal Disease. 2023.
2. Preshaw, P.M.; Alba, A.L.; Herrera, D.; Jepsen, S.; Konstantinidis, A.; Makrilakis, K.; Taylor, R. Periodontitis and diabetes: a two-way relationship. *Diabetologia*. 2012, 55(1):21-31.
3. Chipashvili, O.; Bor B. Ligature-induced periodontitis mouse model protocol for studying Saccharibacteria. *STAR Protoc*. 2022, 8;3(1):101167.
4. Li, D.; Feng, Y.; Tang, H.; Huang, L.; Tong, Z.; Hu, C.; Chen, X.; Tan, J. A Simplified and Effective Method for Generation of Experimental Murine Periodontitis Model. *Front Bioeng Biotechnol*. 2020, 25;8:444.

## Healing potential of the Marine Polysaccharides Carrageenan and Ulvan on second degree burns

Statha D.<sup>1\*</sup>, Papaioannou A.<sup>1</sup>, Kikionis S.<sup>2</sup>, Kostaki M.<sup>1</sup>, Sfiniadakis I.<sup>3</sup>, Vitsos A.<sup>1</sup>, Anastassopoulou J.<sup>1</sup>, Ioannou E.<sup>2</sup>, Roussis V.<sup>2</sup>, Rallis M.<sup>1</sup>

<sup>1</sup>Section of Pharmaceutical Technology, Department of Pharmacy, School of Health Sciences, National and Kapodistrian University of Athens

<sup>2</sup>Section of Pharmacognosy and Chemistry of Natural Products, Department of Pharmacy, School of Health Sciences, National and Kapodistrian University of Athens, 3Athens Naval Hospital, Pathoanatomic Laboratory

\*Corresponding Author: Statha D., demetrastatha@gmail.com

### Introduction

Burn healing is an ongoing scientific challenge and up to date there are no effective treatments.

Marine polysaccharides, especially ulvans and carrageenans, have shown antibacterial, anti-inflammatory and immunoregulatory properties 1,2, while few different studies have reported their beneficial effect on wounds' treatment 3-5. In order to optimize the treatment of burn wounds with carrageenan and ulvan, gels with different doses of the polysaccharides were tested *in vivo*.

### Materials & Methods

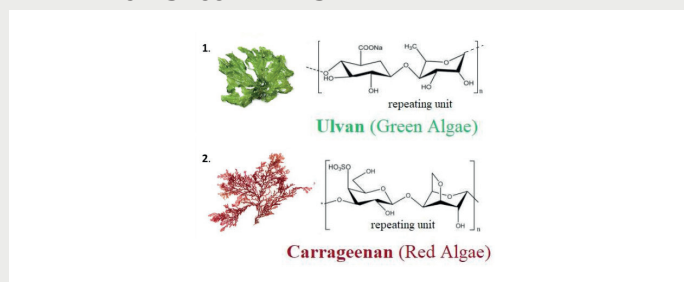
#### ANIMALS

Hairless female mice type SKH-hr2 Protocol Number: 775329/09-08-22

#### BURNS

Metal stamp heated to  $69 \pm 2^\circ\text{C}$  2nd degree burn

#### MARINE POLYSACCHARIDES



#### TREATMENTS

- Control
- Mice with 4% polyacrylamide, C13-14 isoparaffin and laureth-7 (Vehicle)
- Mice with 1,5% w/w Ulvan gel
- Mice with 5% w/w Ulvan gel
- Mice with 10% w/w Ulvan gel
- Mice with 1,5% w/w Carrageenan gel
- Mice with 5% w/w Carrageenan gel
- Mice with 10% w/w Carrageenan gel

7. Mice with 5% w/w Carrageenan gel

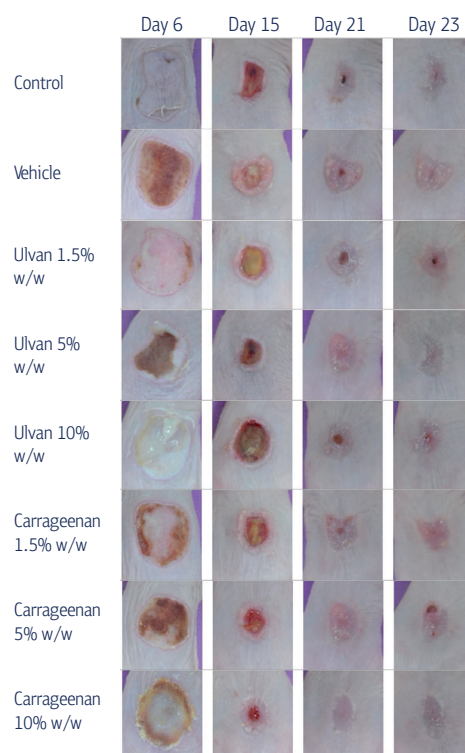
8. Mice with 10% w/w Carrageenan gel n=7 per treatment

### VALUATION

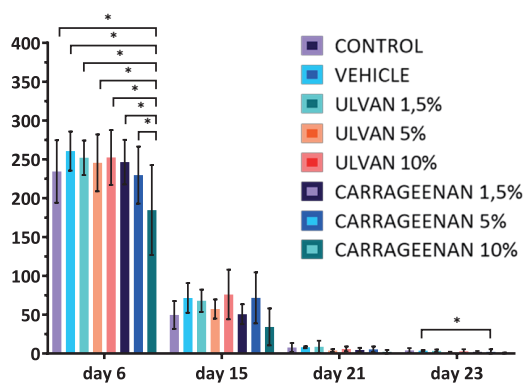
- Clinical Assessment- Photodocumentation
- Histopathological Evaluation
- Transepidermal Water Loss - Sebum
- Hydration
- Skin Thickness
- Antera 3D
- Fourier-transform infrared spectroscopy

### Results - Discussion

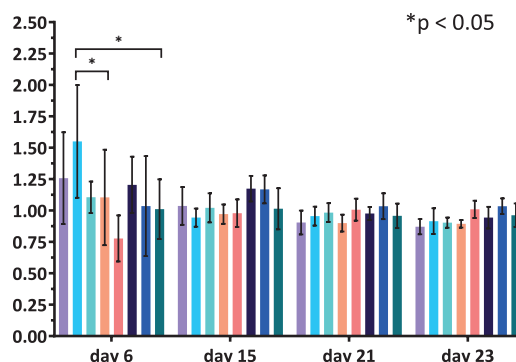
#### TRANSEPIDERMAL WATER LOSS OF THE PERIODONTIUM



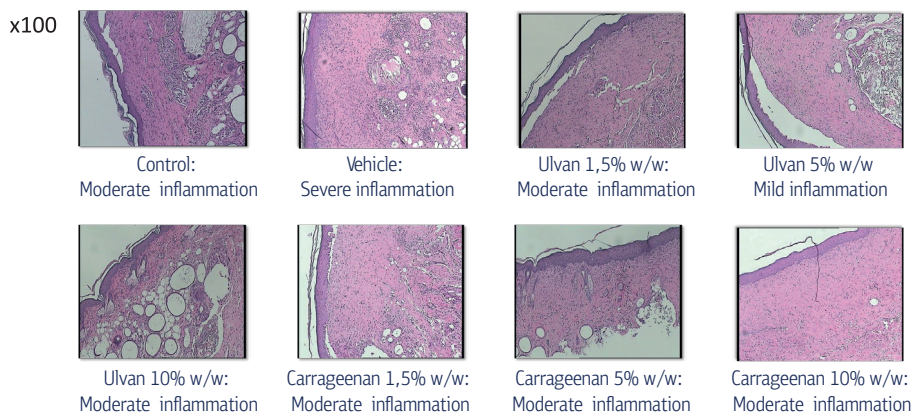
BURN WOUND AREA (mm<sup>2</sup>)



HEMOGLOBIN LEVELS



### HISTOPATHOLOGICAL OBSERVATIONS



### Conclusions

- Clinical and histopathological assessment and reduction rate of the burn wound area showed that the 10% w/w carrageenan gel significantly enhanced burn healing especially at the early stages.
- At the later stages of burn healing, the 5%w/w ulvan gel showed a significant effect.
- The gelling agent (polyacrylamide, C13-14 isoparaffin and laureth-7) exhibited moderate topical toxicity.

### References

1. Wan, M. *et al.* Biomaterials from the sea: Future building blocks for biomedical applications. *Bioact. Mater.* 6, 4255–4285 (2021).

2. Iliou, K., Kikionis, S., Ioannou, E. & Roussis, V. Marine Biopolymers as Bioactive Functional Ingredients of Electrospun Nanofibrous Scaffolds for Biomedical Applications. *Mar. Drugs* 20, 314 (2022).

3. Jaiswal, L., Shankar, S. & Rhim, J.-W. Carrageenan-based functional hydrogel film reinforced with sulfur nanoparticles and grapefruit seed extract for wound healing application. *Carbohydr. Polym.* 224, 115191 (2019).

4. Khaliq, T. *et al.* Self-crosslinked chitosan/κ-carrageenan-based biomimetic membranes to combat diabetic burn wound infections. *Int. J. Biol. Macromol.* 197, 157–168 (2022).

5. Sulastri, E., Zubair, M. S., Lesmana, R., Mohammed, A. F. A. & Wathoni, N. Development and Characterization of Ulvan Polysaccharides-Based Hydrogel Films for Potential Wound Dressing Applications. *Drug Des. Devel. Ther.* 15, 4213–4226 (2021).

## Τα φαρμακεία της Προσφυγικής Κοκκινιάς

### Γρηγόρης Αγκυραλίδης

Φαρμακοποιός M.Sc., E-mail: [Gregorios.agyralides@googlemail.com](mailto:Gregorios.agyralides@googlemail.com)

#### Εισαγωγή

Ως Κοκκινιά αναφέρεται η περιοχή η οποία είναι γνωστή σήμερα ως Νίκαια και ανήκει στο Δήμο Νίκαιας- Αγίου Ιωάννη Ρέντη. Στην περιοχή αυτή εγκαταστάθηκαν κυρίως πρόσφυγες οι οποίοι κατέφθασαν στο λιμάνι του Πειραιά μετά τη Μικρασιατική καταστροφή, τον Σεπτέμβριο του 1922.

Η οργάνωση, η στέγαση, η σίτιση και η προσαρμογή στη νέα κατάσταση ήταν οι βασικές προτεραιότητες. Παράλληλα, οργανώθηκε και αναπτύχθηκε η κοινωνική, οικονομική και επαγγελματική ζωή. Αυτό περιλάμβανε και την ίδρυση και λειτουργία φαρμακείων.

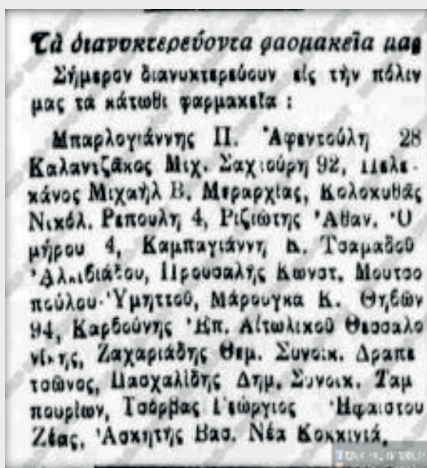
#### Υλικό-Μέθοδος

Αναζητήθηκαν στη βιβλιογραφία πληροφορίες σχετικά με τα φαρμακεία της προσφυγικής Κοκκινιάς, τους φαρμακοποιούς που τα διατηρούσαν, τον επιστημονικό, θεσμικό και κοινωνικό τους ρόλο, κατά το χρονικό διάστημα από το 1922 μέχρι και την περίοδο του Μεσοπολέμου.

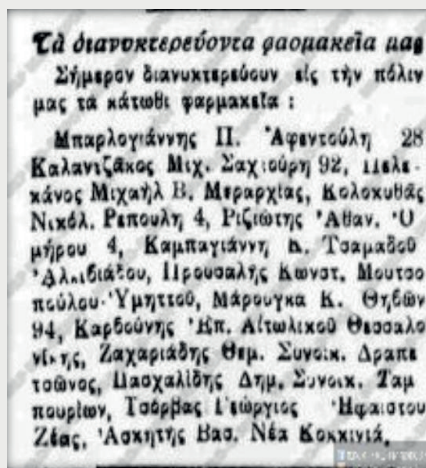
#### Αποτελέσματα

Κατά την εξεταζόμενη περίοδο, στην Κοκκινιά λειτούργησαν τα φαρμακεία των Χαρ. Αλβανίδη (λεωφ. Κορδελιού), Βασ. Ασκητή, Σπυρ. Βλασιάδη (οδός 22α), Ε. Βλουμίδη, Σπ. Βολο-

νάκη (Σάρδεων 32), Κιμ. Γκιουλιστιάνη (οδός 8), Ι. Διαμαντίδη (με την επωνυμία «Εθνικόν», Ζωοδόχου Πηγής 54), Θ. Ιωαννίδη (οδός Αγίων Αναργύρων), Χαρ. Λεοντιάδη, Μαυρομάτη, Κ. Μαρούγκα (Θηβών 94), Μπεναρδή, Παν. Προυσαλή, Κ. Προυσάλογου (οδός Εχειδιών και Μυκάλης), Σ. Τοπαλιάν και Ε. Χατζόπουλου (Μοργκεντάου 7). Συνέβαλαν σημαντικά στη διατήρηση της υγείας και στην αντιμετώπιση των ασθενειών του πληθυσμού, που μαστίζονταν από τη φυματίωση και τις γαστρεντερικές διαταραχές, ενώ στον παιδιατρικό πληθυσμό εμφάνιζαν έξαρση τα τραχώματα και ο δάγκειος πυρετός, καθώς τα παιδιά φοιτούσαν σε σχολεία με πολυμελείς αίθουσες με ανεπαρκή υγιεινή και με έλλειψη καθαρού αέρα. Παράλληλα παρείχαν πρωτοβάθμια περίθαλψη και πρώτες βοήθειες. Έντονη ήταν η δραστηριοποίηση των φαρμακοποιών σε τοπικούς συλλόγους και φορείς όπως η πρώτη κοινότητα προσφύγων Νέας Κοκκινιάς (Λεοντιάδης), ο Εθνικός Σύλλογος Κοκκινιάς (Ασκητής), ο Σύνδεσμος Παλαιάς και Νέας Κοκκινιάς (Διαμαντίδης) καθώς και ο Ποδοσφαιρικός Όμιλος «Άρης» Νέας Κοκκινιάς. Πέρα από θέματα όπως η εξασφάλιση αδειών και η ανέγερση φαρμακείων, οι σύλλογοι αυτοί ασχολήθηκαν ενεργά με την αποκατάσταση των προσφύγων, την κοινοτική οργάνωση, τη διευθέτηση των τοπικών υποθέσεων, την αλληλοβοήθεια αλλά και θέματα όπως η παροχή πιστοποιητικών



**Εικόνα 1.** Έτος 1934: Διανυκτερεύοντα φαρμακεία στην ευρύτερη περιοχή Πειραιά και στη Νέα Κοκκινιά



**Εικόνα 2.** Έτος 1936: Διανυκτερεύοντα φαρμακεία στην ευρύτερη περιοχή Πειραιά και στη Νέα Κοκκινιά



**Εικόνα 3.** Έτος 1937: Διανυκτερεύοντα φαρμακεία στην ευρύτερη περιοχή Πειραιά και στη Νέα Κοκκινιά



απορίας και η διευκόλυνση των τουρκόφωνων προσφύγων μέσω μετάφρασης (Γκιουλιστάνης). Επίσης η Εταιρεία Φίλων του Λαού Κοκκινιάς διευκόλυνε άπορους ασθενείς να προμηθεύονται φάρμακα. Οι δράσεις αυτές προσέφεραν στον προσφυγικό πληθυσμό της Κοκκινιάς φαρμακευτική περίθαλψη, αλλά και συνεισέφεραν στην αυτό-οργάνωσή του με σκοπό την αποκατάσταση και την κοινωνική του ένταξη.

### Βιβλιογραφία

- Γιώργος Αγκυραλίδης. Η Προσφυγόπολη Νίκαια – Νέα Κοκκινιά. Οσελότος. Αθήνα 2022.
- Κυριακή Παπαθανασοπούλου. Προσφυγική εγκατάσταση στη Νίκαια. Σύλλογοι, Ταυτότητες, Μνήμη. Εκδόσεις Ασίην. Αθήνα 2023.
- Η ιστορία των φαρμακείων στον Πειραιά. MLP-BLOG-G-PSOT. 24 Ιουλίου 2014. <https://mlp-blo-g-spot.blogspot.com/2014/07/FarmakeiaPirea.html>. Προσπελάστηκε: 21 Νοεμβρίου 2023.

## Η ιστορία του ελληνικού φαρμακείου από την ίδρυση του ελληνικού κράτους

**Πανταζόγλου Ευαγγελία, Χατζηπαύλου Δήμητρα**

Φαρμακευτική Σχολή, Αριστοτέλειο Πανεπιστήμιο Θεσσαλονίκης, Εθνικής Αμύνης 39, Θεσσαλονίκη, Ελλάδα

pantazog@pharm.auth.gr, hadjirav@pharm.auth.gr

### Εισαγωγή

• Αντικείμενο αυτής της εργασίας αποτελεί η παρουσίαση της ιστορικής εξέλιξης του ελληνικού φαρμακείου μετά την ίδρυση του ελληνικού κράτους. Ο πρωταρχικός ρόλος του φαρμακοποιού στην εξυπηρέτηση του κοινωνικού συνόλου αλλά και του φαρμακείου ως χώρου συνάθροισης και κοινωνικής συζήτησης, καθιστούν το ελληνικό φαρμακείο ένα σημαντικό στοιχείο της ελληνικής κληρονομιάς και άσκησης της πρωτοβάθμιας φροντίδας υγείας διαχρονικά.

### Μεθοδολογία

• Στην προσέγγιση του θέματος για τη συλλογή δεδομένων χρησιμοποιήθηκαν βιβλιογραφικές πηγές από την Εθνική Βιβλιοθήκη, το Υπουργείο Υγείας και Πρόνοιας, το Μορφωτικό

Ίδρυμα της Εθνικής Τράπεζας της Ελλάδας, από το Φαρμακευτικό Μουσείο Θεσσαλονίκης, από τον Πανελλήνιο Φαρμακευτικό Σύλλογο, σε συνεργασία με τους κατά τόπους συλλόγους και από τις βιβλιοθήκες των ελληνικών πανεπιστημίων. Φαρμακευτικές περιοδικές εκδόσεις έδωσαν στοιχεία για την καθημερινότητα των φαρμακείων. Η καταγραφή των φαρμακείων γίνεται με βάση την ενσωμάτωση τους στο ελληνικό κράτος. **Κατά την Περίοδο της Ελληνικής Επανάστασης 1823-1831** εντοπίζεται η λειτουργία φαρμακείων στο Μεσολόγγι, στο Ναύπλιο, στην Πάτρα, στην Ερμούπολη Σύρου, στην Ύδρα και στον Πόρο. Αξίζει να σημειωθεί ότι οι φαρμακοποιοί συνεισέφεραν σημαντικά στην Επανάσταση, τόσο σε **επιστημονικό επίπεδο αλλά και σε αγωνιστικό**



1. Το πρώτο φαρμακείο στο Ναύπλιο (Φωτογραφία από Πελοπόννησιακό Λαογραφικό Ίδρυμα, 1960)



2. Εικόνα από το εσωτερικό του φαρμακείου Κωβαίου στη Σύρο



3. Φωτογραφία από το Φαρμακείο Ραφαλιά στην Ύδρα (περίπου 1890, από τον ιστότοπο του φαρμακείου)



4. Εσωτερικό φαρμακείου (αρχές 20ού αιώνα) του Σταμάτιου Κρίνου (πηγή Τα Αθηναικά)



5. Άποψη του φαρμακείου Γερολυμάτου την εποχή που στεγαζόταν στην οδό Αθήνας



6. Φωτογραφία από το φαρμακείο Μπακάκου από τον ιστότοπο του φαρμακείου



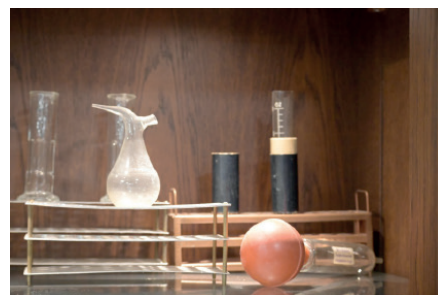
7. Διαφήμιση στη “Νέα Αλήθεια” του 1910



8. Το Φαρμακείο Ζωγράφου όταν η οδός Μοναστηρίου ονομαζόταν Εγνατία



9. Το φαρμακείο του Νίκου Γαβριήλ Πεντζίκη, στην οδό Εγνατία, που ήταν στέκι λογοτεχνών και ζωγράφων. Στην είσοδο διακρίνεται ο φαρμακοποιός λογοτέχνης και ζωγράφος (με το παλτό) μαζί με το συγγραφέα Ηλία Πετρόπουλο



7, 8. Αντικείμενα που χρησιμοποιήθηκαν στο φαρμακείο, όπως καταγράφηκαν και φυλάσσονται στο Φαρμακευτικό Μουσείο Θεσσαλονίκης

Μετά τη δολοφονία του Καποδίστρια στο Ναύπλιο και τον εμφύλιο πόλεμο οι Μεγάλες Δυνάμεις επενέβησαν και όρισαν Βασιλιά της Ελλάδας τον Όθωνα με μεταφορά της πρωτεύουσας στην **Αθήνα** το 1834. Στην Αθήνα ιδρύθηκαν πολλά φαρμακεία που έμειναν γνωστά μέχρι σήμερα. Το 1836 ο **Σταμάτιος Κρίνος**, ένας από τους καθηγητές του Πανεπιστημίου Αθηνών ίδρυσε φαρμακείο στην Αθήνα. Επίσης το 1860 ξεκινάει και η ιστορία του φαρμακείου του **Γερολυμάτου**. Σημείο αναφοράς αποτέλεσε και το φαρμακείο του **Μπακάκου** (1917).

- Στη **Θεσσαλονίκη**, αν και αυτή δεν είχε ενσωματωθεί ακόμα στο ελληνικό κράτος επίσημα μέχρι το 1912, υπήρχε Ελληνικό Φαρμακείο από το 1887. Αυτή τη χρονιά ιδρύθηκε φαρμακείο και φαρμακαποθήκη στη διασταύρωση των οδών Εγνατία και Αγίας Σοφίας από τον Γαβριήλ Πεντζίκη.

Τη λειτουργία του φαρμακείου συνέχισε ο υιός του, Νίκος Γ. Πεντζίκης, και το φαρμακείο συνεχίζει τη λειτουργία του στις μέρες μας.

- Από τα πιο γνωστά φαρμακεία της Θεσσαλονίκης ήταν το φαρμακείο Ζωγράφου. Ο Ζωγράφος φοίτησε στην Κωνσταντινούπολη και μετά εγκαταστάθηκε στη Θεσσαλονίκη και ίδρυσε το φαρμακείο «Ιπποκράτης» στην οδό Εγνατίας (1891). Αξίζει να σημειωθεί ότι σε αυτό το φαρμακείο αλλά και σε άλλα, τον καιρό του αγώνα γινόταν και συναντήσεις αγωνιστών και τύχαιναν περίθαλψης τραυματίες πατριώτες

### Συμπεράσματα

Κατά τα πρώτα έτη της ίδρυσης του Ελληνικού Κράτους η ίδρυση φαρμακείων δεν απαιτούσε ιδιαίτερες προϋποθέσεις. Από το 1834 όμως εκδόθηκαν Βασιλικά Διατάγματα και

περιορισμοί για την άσκηση του φαρμακευτικού επαγγέλματος και ανάλογα και με την εκάστοτε περίοδο στο φαρμακευτικό τομέα ελήφθησαν διάφορα νομοθετικά μέτρα που διαμόρφωσαν το πλαίσιο λειτουργίας τους. Χαρακτηριστικό της νομοθεσίας της λειτουργίας των φαρμακείων και της άσκησης του επαγγέλματος του φαρμακοποιού στην Ελλάδα είναι η μη κωδικοποιημένη της μορφή. Βλέπουμε δηλαδή ότι οι διάφορες διατάξεις είναι διάσπαρτες σε διάφορα νομοθετήματα σε βάθος χρόνου μέχρι και σήμερα.

#### **Βιβλιογραφικές αναφορές**

1. Ελένη Σκαλτσά: Ιστορία της Φαρμακευτικής, Αθήνα 2015

2. Εμμανουήλ Ι. Εμμανουήλ: Ιστορία της Φαρμακευτικής, Αθήνα 1948
3. Κωστόπουρος Θ.: Βονιφάτιος Βοναφίν, Ανάπλι 1979,σελ.48,59
4. Κρίνος Δ: Η Αληθινή Ερμούπολις επαγωγικώς ...Μια άλλη γνωριμία με τη Σύρα, εκδ.Ακτίνα-Ν.Ψιλόπουλος 2005,
5. Παυλίδου Αντιγόνη : Τα φαρμακεία των Αθηνών, Αθήνα 2022

#### **Ευχαριστίες**

Οι συγγραφείς ευχαριστούν ιδιαίτερα το Φαρμακευτικό Μουσείο Θεσσαλονίκης, τον Πανελλήνιο Φαρμακευτικό Σύλλογο και τους κατά τόπους Φαρμακευτικούς Συλλόγους για την υποστήριξη και βοήθεια.

## Ο ρόλος του φαρμακοποιού στη διαχείριση του καρκινικού πόνου

Ευάγγελος Αλιφέρης, Σταματία Γκαράνη – Παπαδάτου

Πανεπιστήμιο Δυτικής Αττικής, Τμήμα Πολιτικών Δημόσιας Υγείας, Λεωφόρος Αλεξάνδρας 196, 11521 Αθήνα, email: ealiferis@yahoo.gr

### Εισαγωγή

Ο καρκίνος εξακολουθεί να αποτελεί μία από τις πρώτες αιτίες θανάτου απαριθμώντας περίπου 10 εκατομμύρια θανάτους το 2020 με ένα από τα μεγάλα προβλήματα στις περιπτώσεις καρκίνου να είναι η αποτελεσματική διαχείριση του καρκινικού πόνου.

### Στόχος

Η πολυπλοκότητα των σημερινών επιδημιολογικών και φαρμακολογικών δεδομένων στη θεραπεία ογκολογικών ασθενών, απαιτεί ευρεία συνεργασία μεταξύ των κλάδων προς όφελος του ασθενούς και προς όφελος της Δημόσιας Υγείας. Σκοπός αυτής της μελέτης είναι να διερευνήσει, να εντοπίσει και να περιγράψει πώς οι Φαρμακοποιοί ειδικότερα μπορούν να συμβάλουν στην αποτελεσματικότερη διαχείριση του καρκινικού πόνου, δεδομένου ότι είναι πιο εύκολα προσβάσιμοι από τους ασθενείς και τις περισσότερες φορές σε άμεση συνεργασία με ιατρικό και νοσηλευτικό προσωπικό. Η μελέτη διερευνά τις τρέχουσες τάσεις και τη σημασία του ρόλου του φαρμακοποιού στη διαχείριση των οπιοειδών, στην εκπαίδευση, την εξατομικευμένη φροντίδα, τα φάρμακα εκτός ενδείξεων και τις νέες τεχνολογίες.

### Μεθοδολογία

Έγινε αναζήτηση στη βάση δεδομένων PubMed. Μελέτες που δημοσιεύθηκαν μεταξύ 2000 και 2022 συμπεριλήφθηκαν χρησιμοποιώντας τις ακόλουθες λέξεις-κλειδιά: φαρμακοποιός, ανακούφιση από τον πόνο, παρηγορητική φροντίδα, διαχείριση πόνου, καρκίνος, προχωρημένο και τελικό στάδιο, νέες τεχνολογίες, off label. Η γλώσσα αναζήτησης και η γλώσσα των πηγών καθορίστηκαν στα αγγλικά.

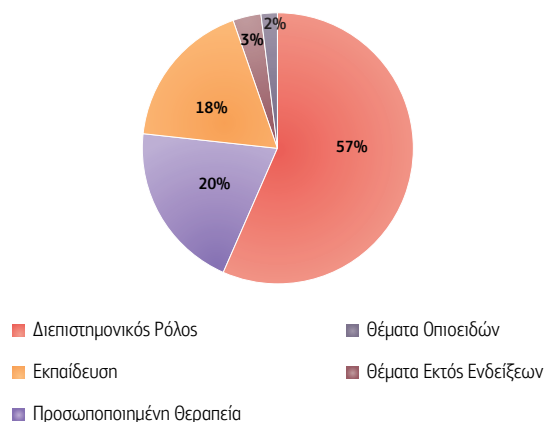
### Αποτελέσματα

Η πλειονότητα των μελετών που διερευνήθηκαν δίνουν έμφαση στον διεπιστημονικό και ηγετικό ρόλο των φαρμακοποιών στην προσπάθεια καλύτερης διαχείρισης του καρκινικού πόνου και παροχής καλύτερης ποιότητας παρηγορητικής φροντίδας. Σύμφωνα με αυτές τις μελέτες, πρέπει να αναπτυχθούν

πολιτικές στις οποίες ο φαρμακοποιός θα πρέπει να είναι αναπόσπαστο μέλος της διεπιστημονικής ομάδας

Πολλές μελέτες επισήμαναν επίσης ότι οι φαρμακοποιοί πρέπει να αναπτύξουν έναν ιδιαίτερο ρόλο μέσω της εκπαίδευσης στα θέματα των οπιοειδών και της παροχής φαρμάκων στους ασθενείς. Τέλος, λίγες μελέτες έθιξαν την ανάγκη των φαρμακοποιών να υιοθετήσουν νέες τεχνολογίες και να αξιοποιήσουν περαιτέρω τις δυνατότητες εξατομικευμένων θεραπειών που φαίνεται να είναι η κυρίαρχη τάση για το μέλλον.

Κατηγοριοποίηση των Άρθρων



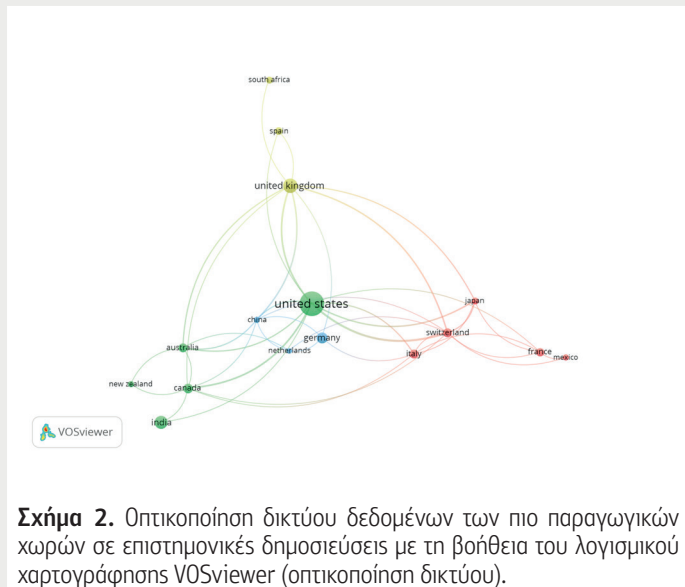
### Συμπεράσματα

Αυτή η μελέτη επιβεβαιώνει τη σημασία του ρόλου του φαρμακοποιού στη διαχείριση του καρκίνου του πόνου. Ο αυξανόμενος αριθμός σχετικών δημοσιεύσεων αποκαλύπτει μεγαλύτερη ευαισθητοποίηση της επιστημονικής κοινότητας προς αυτή την κατεύθυνση σε σχέση με έναν πληθυσμό που μεγαλώνει ηλικιακά και έχει μεγαλύτερη και μάλιστα χρόνια ανάγκη για ανακούφιση από τον πόνο. Αποδεικνύεται ότι ο ειδικός ρόλος των φαρμακοποιών υιοθετείται όλο και περισσότερο σε κλινικές και ξενώνας. Απαιτείται πρόσθετη έρευνα προκειμένου να βελτιστοποιηθούν οι τρόποι και να αναπτυχθούν πολιτικές που θα επιτρέψουν στους φαρμακοποιούς να γίνουν αναπόσπαστο μέρος της όλης διαδικασίας.

## Βιβλιογραφία

1. Jul;23(7):1123-1142. doi: 10.1016/j.jpain.2022.02.002. Epub 2022 Feb 10. PMID:Van Beek, K., Siouta, N., Preston, N., Hasselaar, J., Hughes, S., & Payne, S. *et al.* (2016). To what degree is palliative care integrated in guidelines and pathways for adult cancer patients in Europe: a systematic literature review. *BMC Palliative Care*, 15(1). doi: 10.1186/s12904-016-0100-0
2. Tricco AC, Lillie E, Zarin W, O'Brien KK, Colquhoun H, Levac D, Moher D, Peters MDJ, Horsley T, Weeks L, Hempel S, Akl EA, Chang C, McGowan J, Stewart L, Hartling L, Aldcroft A, Wilson MG, Garritty C, Lewin S, Godfrey CM, Macdonald MT, Langlois EV, Soares-Weiser K, Moriarty J, Clifford T, Tunçalp Ö, Straus SE. PRISMA Extension for Scoping Reviews (PRISMA-ScR): Checklist and Explanation. *Ann Intern Med*. 2018 Oct 2;169(7):467-473. doi: 10.7326/M18-0850. Epub 2018 Sep 4. PMID: 30178033.
3. Maleki S, Alexander M, Fua T, Liu C, Rischin D, Lingaratnam S. A systematic review of the impact of outpatient clinical pharmacy services on medication-related outcomes in patients receiving anticancer therapies. *J Oncol Pharm Pract*. 2019 Jan;25(1):130-139. doi: 10.1177/1078155218783814. Epub 2018 Jun 25. PMID: 29938594. Oliveira CS, Silva MP, Miranda ÍKSPB, Calumby RT, de Araújo-Calumby RF. Impact of clinical pharmacy in oncology and hematology centers: A systematic review. *J Oncol Pharm Pract*. 2021 Apr;27(3):679-692. doi: 10.1177/1078155220976801. Epub 2020 Dec 10. PMID: 33302824.
4. Shrestha S, Kc B, Blebil AQ, Teoh SL. Pharmacist Involvement in Cancer Pain Management: A Systematic Review and Meta-Analysis. *J Pain*. 2022 35151871.





**Σχήμα 2.** Οπτικοποίηση δικτύου δεδομένων των πιο παραγωγικών χωρών σε επιστημονικές δημοσιεύσεις με τη βοήθεια του λογισμικού χαρτογράφησης VOSviewer (οπτικοποίηση δικτύου).

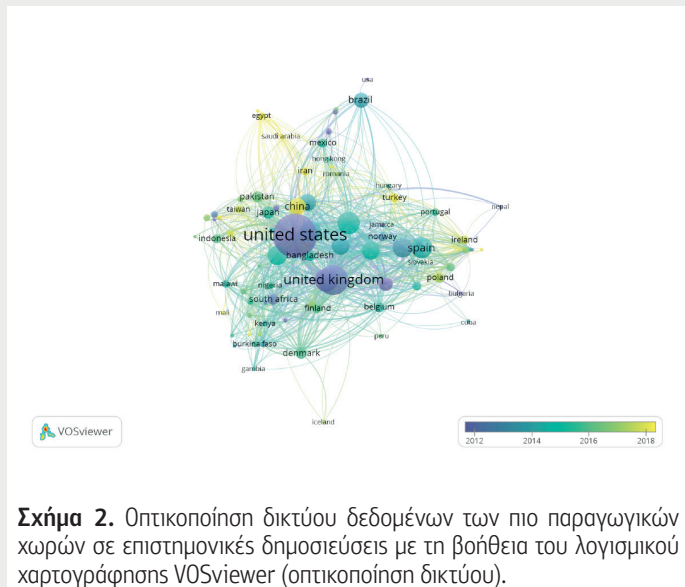
επιστήμη της διατροφής και το καθημερινό διαιτολόγιο του ανθρώπου.

#### Αναφορές:

- Παπανικολάου Ζ., Γούλας Α., (2023). Διερεύνηση εξαγωγικών δραστηριοτήτων σε τρόφιμα που προέρχονται από τα δάση. 21ο Πανελλήνιο Δασολογικό Συνέδριο. Λουτρά Αιδηψού, 22-25 Οκτωβρίου
- Fish, G., & Lord, D. (2023). Nutritional Marketing. In Nutrition Science, Marketing Nutrition, Health Claims, and Public Policy (pp. 135-152). Academic Press.
- Masten Rutar, J., Jagodic Hudobivnik, M., Nečemer, M., Vogel Mikuš, K., Arčon, I., & Ogrinc, N. (2022). Nutritional quality and safety of the spirulina dietary supplements sold on the Slovenian market. Foods, 11(6), 849.







**Σχήμα 2.** Οπτικοποίηση δικτύου δεδομένων των πιο παραγωγικών χωρών σε επιστημονικές δημοσιεύσεις με τη βοήθεια του λογισμικού χαρτογράφησης VOSviewer (οπτικοποίηση δικτύου).

#### Αναφορές:

- Παπανικολάου Ζ., Γούλας Α., (2023). Διερεύνηση εξαγωγικών δραστηριοτήτων σε τρόφιμα που προέρχονται από τα δάση. 21ο Πανελλήνιο Δασολογικό Συνέδριο. Λουτρά Αιδηψού, 22-25 Οκτωβρίου
- Outerbridge, C. A., & Owens, T. J. (2023). Nutritional management of skin diseases. *Applied Veterinary Clinical Nutrition*, 345-383.
- Ζγουνδ, S. E. H., Shakhshir, M., Abushanab, A. S., Koni, A., Shahwan, M., Jairoun, A. A., & Al-Jabi, S. W. (2023). Bibliometric mapping of the landscape and structure of nutrition and depression research: visualization analysis. *Journal of Health, Population and Nutrition*, 42(1), 1-13.
- Dent, E., Wright, O. R., Woo, J., & Hoogendijk, E. O. (2023). Malnutrition in older adults. *The Lancet*.

## Οι αγώνες δρόμου και οι συμμετέχοντες ως εξειδικευμένες αγορές για τα τοπικά αγροδιατροφικά προϊόντα

**Ζαχαρίας Παπανικολάου<sup>1\*</sup>, Απόστολος Γούλας<sup>2</sup>**

<sup>1</sup> Δημοκρίτειο Πανεπιστήμιο Θράκης, Τμήμα Αγροτικής Ανάπτυξης, Ορεσιτιάδα, Ελλάδα

<sup>2</sup> Δημοκρίτειο Πανεπιστήμιο Θράκης, Τμήμα Αγροτικής Ανάπτυξης, Ορεσιτιάδα, Ελλάδα

\*Υπεύθυνος συγγραφέας: Παπανικολάου Ζαχαρίας, 6978060873, zpapanik@agro.duth.gr

### Εισαγωγή

Τα τελευταία χρόνια οι αγώνες δρόμου και οι αθλητικές διοργανώσεις μαζικού χαρακτήρα γνωρίζουν μεγάλη ανάπτυξη παγκοσμίως αλλά και στη χώρα μας. Πολλοί ερευνητές έχουν μελετήσει και παρουσιάσει τη συμβολή των αγώνων δρόμου στην τοπική οικονομία και ανάπτυξη των περιοχών που διοργανώνουν και φιλοξενούν τέτοιου είδους αθλητικές διοργανώσεις. Σύμφωνα με τους Γούλα Α., Παππά Μ., και Θεοδοσίου Γ., (2017). Τα νέα μοντέλα ανάπτυξης τις τελευταίες δεκαετίες έχουν γίνει ο πυρήνας μιας μεγάλης προσπάθειας για βιωσιμότητα και οικονομική ανάπτυξη. Είναι επίσης κρίσιμο για τα νέα μοντέλα να εφαρμόσουν την κοινωνική πτυχή καθώς και την οικονομική πτυχή. Αυτό μπορεί να επιτευχθεί θεωρώντας ως κρίσιμα εργαλεία για την ανάπτυξη, τον πολιτισμό και την αθλητική δραστηριότητα, σε συνδυασμό με την ιστορική μνήμη των διάφορων αριών.

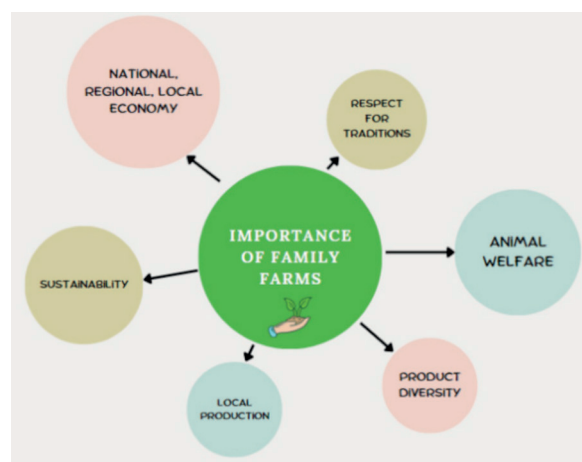
### Εργαλεία αστικής ανάπτυξης

Επιπλέον, αυτό είναι αρκετά γνωστό σε προγράμματα αστικής ανάπλασης στις μεγάλες ευρωπαϊκές πόλεις. Αυτός είναι ένας από τους κύριους λόγους για τον πολιτισμό σε συνδυασμό με τις τοπικές αθλητικές εκδηλώσεις και δραστηριότητες να θεωρούνται εργαλεία αστικής ανάπτυξης. Παράλληλα, μελετώντας το προφίλ των ανθρώπων που συμμετέχουν στους αγώνες δρόμου παρατηρεί κανείς ότι τρέφονται υγιεινά και προσέχουν τη διατροφή τους, ενώ είναι διατεθειμένοι να ξοδέψουν περισσότερα για να αποκτήσουν αγροδιατροφικά προϊόντα υψηλής διατροφικής αξίας, παραδοσιακά και γευστικά. Η σημασία της ποιότητας των προϊόντων έχει δημιουργήσει μια παγκόσμια τάση στη διατροφή, βοηθώντας στη δημιουργία μιας εξαιρετικά ανταγωνιστικής αγοράς τροφίμων. Η πτυχή της ποιότητας και του τόπου παραγωγής είναι ένα μοναδικό πλεονέκτημα για τη διατήρηση της παγκόσμιας ανταγωνιστικότητας.

### Προέλευση των τροφίμων

Οι καταναλωτές, τα τελευταία χρόνια, ενδιαφέρονται όλο και

περισσότερο για την προέλευση των τροφίμων όχι μόνο για λόγους υγείας αλλά και για εσωτερική ανάγκη να ικανοποιήσουν την έλλειψη «πρωτότυπων» και «παραδοσιακών» γεύσεων και γεύσεων της καθημερινότητάς τους (Θεοδοσίου Γ., Γούλας Α., και Duquenne M. N., 2017) και δευτερευόντως για την υποστήριξη της προστασίας του περιβάλλοντος και της διατήρησης της βιοποικιλότητας στον τόπο παραγωγής. Η παγκόσμια τάση που έχει επικρατήσει γύρω από την τυποποίηση των αγροτικών προϊόντων έχει δημιουργήσει μια εναλλακτική τάση αποτίμησης και κατανάλωσης τυπικών προϊόντων μιας περιοχής. Σε αυτά τα τυπικά προϊόντα, η κοινωνική συμμετοχή και η ποιότητά τους θεωρείται ότι ενισχύουν την οικονομική δραστηριότητα και μπορούν να αποτελέσουν ανταγωνιστικό πλεονέκτημα στις εγχώριες και διεθνείς αγορές (Goodman 2003; Bowen and Mutersbaugh, 2014).



**Σχήμα 1.** Η σημαντικότητα των τοπικών προϊόντων ((Source: processing according to FAO, accessed 10 February 2023).

### Αναφορές:

- Bowen S., and Mutersbaugh T., (2014), 'Local or localized? Exploring the contributions of Franco-Mediterranean agrifood

theory to alternative food research', Agriculture and Human Values, Vol. 31(2), pp. 201-213.

- Goulas A., Pappa M., and Theodossiou G., (2017), 'A novel local development model paradigm: The case of Ippokratios race', 3rd Conference Changing Cities: Landscape & Socio – economic dimensions, Syros Greece.
- Theodossiou G., Goulas A., and Duquenne M.N., (2017), 'Defining factors of consuming local nutritional products: New consuming behaviours', European Regional Science Association (ERSA) 2017 – 29 August – 1 September 2017, Groningen, The Netherlands.
- Hardy, I. G. N. W., Mahayasa, I. N. W., Arsa, I. G. B. A., Fanggidae, L. W., & Tualaka, T. M. C. Consumer preferences on the kiosk model of dryland agricultural products in east Nusa Tenggara.
- Mao, Y., & Wang, S. (2023). Recent developments in radio frequency drying for food and agricultural products using a multi-stage strategy: A review. Critical Reviews in Food Science and Nutrition, 63(16), 2654-2671.

## Ο ρόλος του φαρμακοποιού στην σύγχρονη δομή της φαρμακοβιομηχανίας

Γεώργιος Τσιούμας<sup>a\*</sup>, Αλεξάνδρα Μαυρομάτη<sup>b</sup>, Μαργαρίτα Νταντάμη<sup>b</sup>, Κατερίνα Παπαταξιάρχου<sup>a</sup>

<sup>a</sup>Clinical Operations, Ιατρικό Τμήμα, Elpen Pharmaceutical Co. Inc.

<sup>b</sup>Φαρμακευτική Σχολή Επιστημών Υγείας, Εθνικό και Καποδιστριακό Πανεπιστήμιο Αθηνών

\*Corresponding Author: Γεώργιος Τσιούμας, +30 6980017384, [gtsioumas@elpen.gr](mailto:gtsioumas@elpen.gr)

### Σκοπός

Ο ρόλος του φαρμακοποιού στην σύγχρονη δομή της φαρμακοβιομηχανίας είναι ομοιογενής σε παγκόσμιο επίπεδο. Πιθανόν να ποικίλει ανάλογα με τον τίτλο εργασίας, την περιγραφή καθηκόντων και την ευθύνη θέσης. Οι φαρμακοποιοί βάσει του γνωστικού επιστημονικού αντικειμένου τους επιτελούν κρίσιμους και εξειδικευμένους ρόλους σε διάφορα λειτουργικά τμήματα της φαρμακευτικής βιομηχανίας.

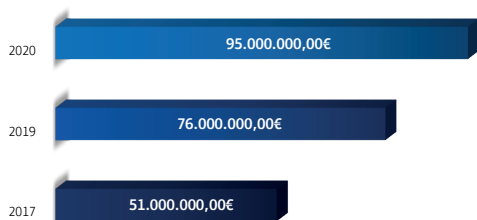
### Υλικά και Μέθοδοι

Μέσω βιβλιογραφικής αναζήτησης και επισκόπησης αναδύθηκαν ορισμένοι από τους βασικούς ρόλους, τις αρμοδιότητες και τους κλάδους εξειδίκευσης των φαρμακοποιών στην φαρμακευτική βιομηχανία.

### Αποτελέσματα

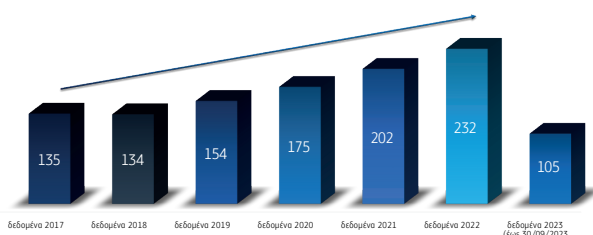
Ακολουθούν 12 κύριοι τομείς δράσης των φαρμακοποιών στην σύγχρονη φαρμακοβιομηχανία: **1. Έρευνα και Ανάπτυξη (E&A) – Research & Development (R&D):** έρευνα, ανακάλυψη, σύνθεση και ανάπτυξη νέων φαρμάκων, προκλινικές δοκιμές. [Διάγραμμα 1] **2. Σύνθεση προϊόντος – Product Formulation:** διαμόρφωση νέων φαρμακευτικών προϊόντων, ανάπτυξη της σύνθεσης, των μορφών δόσολογίας και των συστημάτων χορήγησης. **3. Παραγωγή – Production & Manufacturing:** ευθύνη για την επίβλεψη των διαδικασιών παραγωγής φαρμακευτικών προϊόντων. [Διάγραμμα 2] **4. Ποιοτικός έλεγχος και διασφάλιση ποιότητας – Quality Control/Quality Assurance:** ποιοτικός έλεγχος και διασφάλιση ότι τα φαρμακευτικά προϊόντα

Δαπάνη της φαρμακευτικής βιομηχανίας για E&A



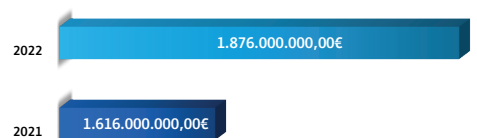
**Διάγραμμα 1.** Δαπάνη φαρμακευτικής βιομηχανίας για τα έτη 2017, 2019 και 2020 στην Έρευνα και Ανάπτυξη.

Συνολικός αριθμός κλινικών μελετών στην Ελλάδα



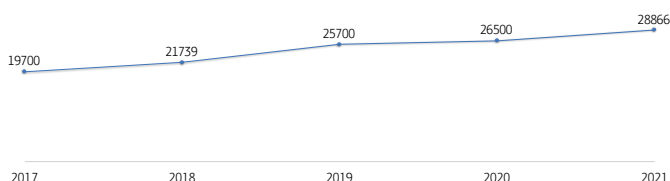
**Διάγραμμα 3.** Συνολικός αριθμός κλινικών μελετών στην Ελλάδα από το έτος 2017 έως 30/09/2023.

Παραγωγή φαρμάκου στην Ελλάδα σε αξία (ex-factory)



**Διάγραμμα 2.** Παραγωγή φαρμάκου στην Ελλάδα για τα έτη 2021 και 2022 σε αξία ex-factory.

Αριθμός απασχολούμενων στον κλάδο του φαρμάκου



**Διάγραμμα 4.** Η συνολική απασχόληση στον κλάδο φαρμάκου για τα έτη 2017, 2018, 2019, 2020 και 2021.

πληρούν καθορισμένα πρότυπα ποιότητας, επίβλεψη στις διαδικασίες παραγωγής, Ορθές Πρακτικές Παραγωγής (GMP, Good Manufacturing Practice). **5. Ρυθμιστικά θέματα – Regulatory Affairs:** διασφάλιση ότι τα φαρμακευτικά προϊόντα πληρούν όλες τις κανονιστικές απαιτήσεις και τα πρότυπα ποιότητας, προετοιμασίας και ρυθμιστικές υποβολές στις υγειονομικές αρχές (π.χ. ΕΟΦ). **6. Κλινική Έρευνα – Clinical Research:** διασφάλιση της διεξαγωγής κλινικών δοκιμών και μελετών σύμφωνα με τις κανονιστικές απαιτήσεις και την Ορθή Κλινική Πρακτική (GCP, Good Clinical Practice), παρακολούθηση και αξιολόγηση της ασφάλειας και της αποτελεσματικότητας των υπό έρευνα φαρμάκων. [Διάγραμμα 3] **7. Φαρμακοεπαγρύπνηση και ασφάλεια φαρμάκων – Pharmacovigilance & Drug Safety:** παρακολούθηση και αναφορά ανεπιθύμητων ενεργειών και παρενεργειών που σχετίζονται με φαρμακευτικά προϊόντα. **8. Πρόσβαση αγοράς/Οικονομικά της υγείας – Market Access & Health Economics:** αξιολόγηση της οικονομικής και κλινικής αξίας των φαρμακευτικών προϊόντων με σκοπό την πρόσβαση/διείσδυση στην αγορά με ταυτόχρονη στρατηγική τιμολόγησης. **9. Ιατρικές Υποθέσεις – Medical Affairs:** παρέχεται ιατρική και επιστημονική γνώση για τα φαρμακευτικά σκευάσματα προς τους επαγγελματίες υγείας και τους ασθενείς. **10. Πληροφορίες και εκπαίδευση για τα φάρμακα – Drug Information & Education:** παροχή εκπαιδευτικού υλικού και πληροφοριών για τα φάρμακα σε επαγγελματίες υγείας, ασθενείς και καταναλωτές διασφαλίζοντας την κατάλληλη και ασφαλή χρήση τους. **11. Πωλήσεις και μάρκετινγκ – Pharma Sales & Marketing:** αναπτύσσεται στρατηγική προώθησης των φαρμακευτικών σκευασμάτων με ταυτόχρονη εκπαίδευση των επαγγελματιών υγείας. **12. Pharmacy Benefits Management (PBM):** διαχείριση των συνταγογραφούμενων φαρμάκων σε σχέση

με τις ασφαλιστικές εταιρείες και κρατικούς φορείς, με βελτιστοποίηση των συνταγών φαρμάκων και έλεγχο του κόστους.

### Συμπεράσματα

Οι φαρμακοποιοί στις φαρμακευτικές εταιρείες αξιοποιούν τις επιστημονικές γνώσεις και την εξειδίκευσή τους με κρίσιμους ρόλους για τη διασφάλιση της ανάπτυξης, της ασφάλειας, της αποτελεσματικότητας, της παραγωγής και της διάθεσης των φαρμακευτικών σκευασμάτων με τελικό στόχο, το όφελος του ασθενούς. Η φαρμακοβιομηχανία στην Ελλάδα είναι ένας από τους στυλοβάτες της Ελληνικής Οικονομίας συμβάλλοντας στο ΑΕΠ €6,2 δισεκατομμύρια (3,3% του ΑΕΠ) το 2021, ενώ το ίδιο έτος απασχολούσε περίπου 28.900 προσωπικό. Συνεπώς, τόσο η παραγωγή και η διάθεση των φαρμάκων εντός του ελλαδικού χώρου αλλά και το εξαγωγικό εμπόριο των φαρμακευτικών προϊόντων (4,7% του συνόλου των ελληνικών εξαγωγών όλων των αγαθών για το 2022) καθιστούν την φαρμακοβιομηχανία για τον ελληνικό χώρο έναν από τους πιο ελκυστικούς τομείς απασχόλησης.

### Βιβλιογραφία

1. Career Opportunities for the Pharm. D. in Industrial Clinical Research and Drug Development, <https://doi.org/10.3109/10601338409027321>
2. Pharmacists in industry, [https://doi.org/10.1016/S0160-3450\(16\)31297-1](https://doi.org/10.1016/S0160-3450(16)31297-1)
3. The role of a pharmacist as a medical information specialist in the pharmaceutical industry <https://doi.org/10.1016/j.cptl.2019.11.005>
4. European Industrial Pharmacists Group <https://eipg.eu/>
5. How-to-become-industrial-pharmacist, <https://uk.indeed.com/career-advice/finding-a-job/how-to-become-industrial-pharmacist>
6. Η Φαρμακευτική αγορά στην Ελλάδα, ΓΕΓΟΝΟΤΑ & ΣΤΟΙΧΕΙΑ 2022 (ΣΦΕΕ), <https://www.sfee.gr/category/typos/facts-figures/>
7. <https://www.eof.gr/web/guest/ct-list>

**ΕΡΓΑΣΙΕΣ ΜΕΤΑΠΤΥΧΙΑΚΩΝ ΚΑΙ ΔΙΔΑΚΤΟΡΙΚΩΝ ΦΟΙΤΗΤΩΝ**

- 1 **Αναγνώστου Μαρία, Τόμου Αικατερίνη-Μιχαέλα, Vanti Gioulia, Μυλωνάκη Εμμανουέλα, Κρίγκας Νικόλαος, Καριώτη Αναστασία, Bilia Anna-Rita, Σκαλτσά Ελένη**  
"Chemical composition of *Stachys parolinii* extract and its formulation for cutaneous use"
- 2 **Καλλιμάνης Παναγιώτης, Μαγιάτης Προκόπιος, Παναγιωτοπούλου Αγγελική, Χίνου Ιωάννα**  
"Extraction Optimization of betulinic acid through different herbal preparations from *Rosmarinus officinalis* L. by <sup>1</sup>H- $\eta$ NMR"
- 3 **Καλλιμάνης Παναγιώτης, Προδρομίδης Σεραφείμ, Μαγιάτης Προκόπιος**  
"Onychomycosis due to *Candida albicans* successfully treated topically with an herbal formulation: A case report"
- 4 **Καρδάση Ζωή, Ντίνα Ευαnthία, Αληγιάννης Νεκτάριος,, Κουρουνάκη Αγγελική**  
"Medicinal properties of six Balkan plants traditionally used for the treatment of skin diseases from ethnobotany to scientific evidence"
- 5 **Τόμου Αικατερίνη-Μιχαέλα, Σκαλτσά Ελένη**  
"Τσάι του βουνού: Ανεξάντλητη πηγή βιοδραστικών συστατικών"
- 6 **Θεοφίλη Μαρία- Ιλεάνα, Βασδαγιάννη Ελένη, Καραλής Ευάγγελος**  
"Simulated dosing regimens of monoclonal antibodies and classical treatments for migraine"
- 7 **Κυρίτση Αικατερίνη, Τάγκα Άννα, Στρατηγός Αλέξανδρος, Καραλής Ευάγγελος**  
"A clinical study of allergic contact dermatitis in polysensitized and monosensitized patients: Machine learning and classic methods"
- 8 **Κυρίτση Αικατερίνη, Τάγκα Άννα, Στρατηγός Αλέξανδρος, Καραλής Ευάγγελος**  
"Contact allergy to preservatives in a patient cohort with occupational contact dermatitis: Machine learning analysis of patch test data"
- 9 **Παπαδάκη Κέλλυ, Καραλής Ευάγγελος**  
"Prolonged Infusion of Antibiotics in Critically Ill Patients: Dosage Regimens Based on Simulations for Meropenem and Tobramycin"
- 10 **Τσιπλακώβα Αναστασία, Δαμησανονίτς Ivana, Stefanονίτς Nikola, Τοσίτς Tatjana, Catić-Đorđević Aleksandra, Καραλής Ευάγγελος**  
"Machine Learning and Modeling Approaches for the Analysis of Antiepileptic Plasma Levels"
- 11 **Λυκούρας Μιχαήλ, Όρκουλα Μαλβίνα, Κοντογιάννης Χρήστος**  
"Προσδιορισμός του μεγέθους των σωματιδίων των δραστικών ουσιών στην κρέμα Trivocort® με τη χρήση φασματοσκοπίας Micro-raman"
- 12 **Μουίκης Ανδρέας, Ασπιώτη Ιωάννα, Παπαιωάννου Λυγερή, Γαζούλη Μαρία, Δήμας Κωνσταντίνος, Αυγουστάκης Κωνσταντίνος**  
"Development of novel PLGA Nanospheres Co-Loaded with paclitaxel and losartan for the treatment of highly desmoplastic tumors"
- 13 **Νικολόπουλος Αναστάσιος, Λαγοπάτη Νεφέλη, Πίππα Νατάσσα, Καραλής Ευάγγελος**  
"Data mining in the design and development of liposomal anticancer drugs"

- |    |  |
|----|--|
| 14 | <b>Παπακυριακοπούλου Παρασκευή, Μπαλάφας Ευάγγελος, Gaia Colombo, Ρέκκας Μ. Δημήτριος, Κωστομπτσόπουλος Νικόλαος, Βαλσαμή Γεωργία</b><br>"Nose to brain delivery of donepezil nasal films"   |
| 15 | <b>Παρθενιάδης Ιωάννης, Νικολακάκης Ιωάννης</b><br>"A modified solvent processed feed HME process for the preparation of drug/amino acid CAMS"   |
| 16 | <b>Παρθενιάδης Ιωάννης, Αθανασίου Αλεξάνδρ, Νικολακάκης Ιωάννης</b><br>"Peppermint Oil Spray Dried Powders - Encapsulating Wall Composition, Particulate Characteristics and Powder Cohesiveness"  |
| 17 | <b>Παρθενιάδης Ιωάννης, Σταθάκης Γεώργιος, Νικολακάκης Ιωάννης</b><br>"Static And Dynamic Vapor Sorption of Hydrophobic Starch Ester Powders and Corresponding Tablets"  |
| 18 | <b>Σαϊτάνη Ελμίνα-Μαρίνα, Πίππα Νατάσσα, Παπακυριακοπούλου Παρασκευή, Πίσπας Στέργιος, Βαλσαμή Γεωργία</b><br>"Fabricating hybrid particles for possible nose-to-brain delivery of ropinirole"   |
| 19 | <b>Σωτηροπούλου Γαρυφαλλιά-Ιωάννα, Σιαμίδα Αγγελική, Πρωτόπαππα Χρυστάλλα, Βλάχου Μαριλένα</b><br>"In vitro modified-release matrix tablets of omeprazole for paediatric patients"   |
| 20 | <b>Τόσκας Μιλτιάδης, Παρθενιάδης Ιωάννης, Νικολακάκης Ιωάννης</b><br>"Επίδραση του βαθμού ενυδάτωσης Kollidon® SR στην πλαστικοποιητική δράση της σορβιτόλης κατά την εξώθηση διμερών μειγμάτων τους"  |
| 21 | <b>Τριανταφυλλοπούλου Ευσταθία, Σελιανίτης Δημήτριος, Πίππα Νατάσσα, Γαζούλη Μαρία, Βαλσαμή Γεωργία, Πίσπας Γεώργιος</b><br>"Dual responsive DSPPC:P(OEGMA 950 DIPAEMA) nanostructures: Evaluating the design parameters affecting their performance"  |
| 22 | <b>Τσαλαβούτη Δήμητρα, Παρθενιάδης Ιωάννης, Χαρίση Αναστασία, Νικολακάκης Ιωάννης</b><br>"Tablets of Enteric Microencapsulated Oregano Essential Oil Powders Evaluation and Release"   |
| 23 | <b>Φερτάκη Στεφανία, Κοντογιάννης Χρήστος</b><br>"Particle size distribution and morphology of umeclidinium Br API and vilanderol trifenate API in anoro® dry powder inhaler (DPI) using sem and edx"  |
| 24 | <b>Χαϊκάλη Χρυσή, Λαμπροπούλου Παρασκευή, Παπούλης Δημήτρης, Αυγουστάκης Κωνσταντίνος, Λάμαρη Φωτεινή, Χατζηαντωνίου Σοφία</b><br>"Green synthesis and characterization of copper oxide nanoparticles for topical application"   |
| 25 | <b>Βαρβαρέσου Αθανασία, Χρυσογιάννη Μαρία, Πιτσάβα Σταματίνα, Χαλικιάς Μιλτιάδης, Παύλου Παναγούλα, Μέλλου Φωτεινή, Παπαγεωργίου Σπυρίδων, Παπαδόπουλος Απόστολος, Κίντζιου Ελένη, Ράλλης Ευστάθιος</b><br>"Πρόδρομα αποτελέσματα τυχαίοποιημένα, ελεγχόμενα με placebo μελέτης της επίδρασης της επίδρασης παράγωγων της καφεΐνης στη μικροτοπογραφία του δέρματος" |
| 26 | <b>Παπαντωνάκη Αναστασία Ιωάννα, Μουστακά Ειρήνη, Πέτσιου Αντιγόνη, Βαλακώστα Μυρσίνη, Αλμπάνη Χαρά, Λούμου Παναγιώτα, Γεωργακοπούλου Ελένη, Δαμουλής Πέτρος, Σφηνιαδάκης Ιωάννης, Αναστασοπούλου Ιωάννα, Βίτσος Ανδρέας, Μόσσιαλος Δημήτρης, Ράλλης Μιχαήλ</b><br>"Experimental gingivitis in mice"   |



- |    |   |
|----|---|
| 27 | <b>Σταθά Δήμητρα, Παπαϊωάννου Ασημίνα, Κικιώνης Στέφανος, Κωστάκη Μαρία Σφηνιαδάκης Ιωάννης, Βίτσος Ανδρέας, Αναστασοπούλου Ιωάννα, Ιωάννου Ευσταθία, Ρούσσης Βασίλειος, Ράλλης Μιχαήλ</b><br>"Healing potential of the Marine Polysaccharides Carrageenan and Ulvanon second degree burns" |
| 28 | <b>Αγκυραλίδης Γρηγόρης</b><br>"Τα φαρμακεία της προσφυγικής Κοκκινιάς"   |
| 29 | <b>Πανταζόγλου Ευαγγελία, Χατζηπαύλου Δήμητρα</b><br>"Η ιστορία του ελληνικού φαρμακείου από την ίδρυση του ελληνικού κράτους"  |
| 30 | <b>Αλιφέρης Ευάγγελος, Γκαράνη – Παπαδάτου Σταματία</b><br>"Ο ρόλος του φαρμακοποιού στη διαχείριση του καρκινικού πόνου"   |
| 31 | <b>Παπανικολάου Ζαχαρίας, Γούλας Απόστολος</b><br>"Μάρκετινγκ συμπληρωμάτων διατροφής: Μια βιβλιογραφική ανασκόπηση"  |
| 32 | <b>Παπανικολάου Ζαχαρίας, Γούλας Απόστολος</b><br>"Διαχείριση του υποσιτισμού και συμπληρώματα διατροφής. Μία βιβλιομετρική ανάλυση"  |
| 33 | <b>Γούλας Απόστολος, Παπανικολάου Ζαχαρίας</b><br>"Οι αγώνες δρόμου και οι συμμετέχοντες ως εξειδικευμένες αγορές για τοπικά αγροδιατροφικά προϊόντα"   |
| 34 | <b>Τσιούμας Γιώργος, Μαυρομάτη Αλεξάνδρα, Νταντάμη Μαργαρίτα, Παπαταξιάρχου Κατερίνα</b><br>"Ο ρόλος του φαρμακοποιού στην σύγχρονη δομή της φαρμακοβιομηχανίας"  |